The role of iRhom2 in the pathogenesis of head and neck squamous cell carcinomas

Matthew Agwae

A Thesis presented for the degree of Doctor of Philosophy

April, 2018

Supervisor: Dr Janet M Risk

Cancer Research Centre

Institute of translational medicine

University of Liverpool

ABSTRACT

It has been proposed that the Notch signalling pathway plays a key role in the pathogenesis of head and neck squamous cell carcinomas (HNSCC). It has also been shown that the sheddase, ADAM17, whose intracellular trafficking and subsequent maturation is dependent on iRhom2, is key in the activation of the Notch pathway at the cell membrane, leading to the release of an intracellular domain for downstream activities. This thesis investigates the levels and distribution of iRhom2 and ADAM17 in HNSCC, and functional changes resulting from up-regulation of iRhom2 in HNSCC cell lines.

Immunoblotting, using protein samples extracted from fresh, snap-frozen tissues (68 HNSCC and 27 paired normal tissues), and probing for iRhom2 identified relatively high expression levels of this protein in 43/68 tumour samples compared to 5/27 normal samples ($p<0.05$). Similar observations were obtained for ADAM17 expression, with high expression in 27/68 tumour samples compared to 4/27 normal samples ($P<0.05$). A positive correlation was observed between levels of expressions of iRhom2 and ADAM17 in these tissues (though not statistically significant), but only iRhom2 expression correlated with patient survival ($p<0.05$). Non-correlation of iRhom2 expression with other clinicopathological features was perhaps due to the relatively small number of samples investigated. Using a different cohort of HNSCC tissues, we also assessed levels of iRhom2 and ADAM17 and their intracellular distribution using tissue microarray (TMA) approach. Western blot results could not be corroborated with this methodology, given that most of the tissues stained

negative for iRhom2, and 76/88 stained “highly positive” for ADAM17, with no observable specificity with ADAM17 staining pattern. Up-regulation of iRhom2 was achieved in the HNSCC cell lines, PE/CA-PJ15 and LIV37K; and in NOK (normal oral keratinocyte) cells and was, followed by shRNA knock-down of RHBDF2 (which codes for iRhom2). No observable differences were observed in the rate of cell replication when comparing wild-type, over-expressing and knock-down clones across each of the cell lines. However, a higher rate of cell migration was demonstrated in association with iRhom2 up-regulation, more in the HNSCC cell lines than the NOK. This higher rate of migration was shown to be reversed by the shRNA knock-down of RHBDF2, demonstrating that it is increased iRhom2 that is causative. Furthermore, a significant increase in the level of expression of mature ADAM17 was observed, following upregulation of iRhom2.

iRhom2 and ADAM17 are both up-regulated in HNSCC, with up-regulation of iRhom2 associated with increased cell migration and decreased patient survival. Further experiments should aim to address whether it is the increased ADAM17 expression / activity and / or Notch activity that is the downstream effector of the observed effects. If will be important to expand the cohort of samples and cell lines used for this study to further validate the present findings, while also optimising some of the aspects that have not achieved significant results.

Statement of Originality

I, Matthew Agwae hereby confirm that the research work that makes up this thesis has been carried out by me, with due reference ascribed to originators in arears where collaboration has been required and reference sought. I hereby attest to having ensured the work presented is original, does not go against the laws of the land and does not break copyright laws.

Matthew Agwae

Collaborations

1. TMA cores utilised for IHC part of this experiment were obtained from Dr Janet M Risk, having been assembled for a thesis work by Dhanda J, with results already published, 2014.
2. Plasmid used for RHBDF2 over-expression was obtained from Dr Janet M Risk, having been assembled by Rehab El Maddani, including the restriction digest for her Masters project.

Publications

1. Upregulation of iRhom2 in head and neck squamous cell carcinoma: analysis of clinical tissues (Awaiting publishing)
2. Role of iRhom2 in the pathogenesis of head and neck squamous cell carcinoma (Awaiting publishing)
3. Review: iRhom2, ADAM17 and Notch signalling in oral cancer (Awaiting publishing)

Conferences and Presentations

1. Oral presentation: Role of iRhom2 in the pathogenesis of head and neck squamous cell carcinoma – International Association of Oral Pathologists (IAOP), Lagos, 2015
2. Oral presentation: Role of iRhom2 in the pathogenesis of head and neck squamous cell carcinoma – National association of oral and maxillofacial surgeons (NAOMS), Enugu, 2016
3. Poster presentation: Role of iRhom2 in the pathogenesis of head and neck squamous cell carcinoma – National Cancer Research Institute (NCRI) conference, Liverpool, 2016
4. Poster presentation: Role of iRhom2 in the pathogenesis of head and neck squamous cell carcinoma – North West Cancer Research (NWCR), Liverpool, 2017

5. Poster presentation: Role of iRhom2 in the pathogenesis of head and neck squamous cell carcinoma – Canadian Cancer Research Association, CCRA, Vancouver, 2017

ACKNOWLEDGEMENT

Very many thanks to my supervisor, Dr Janet M Risk for her unquantifiable role through my PhD. I appreciate all the members of the Janet Risk research team, including those who have moved to other locations; Prof Richard Shaw, James Wilson, Frances Greaney, Laura Cossar, Khaled Ben Salah, Okoturo Eyituoyo, and all the masters and undergraduate team members. Many thanks to all the members of the other head and neck groups at the Cancer research centre. Special thanks also go to Georgina Gill, Ahoud Alotibi, and Jason C. Anyadike for helping out with some of the figures, Fidelia A. Ajibogun, Onome Ebiri, Lola Fagbemi, Dolapo Ajike and Bajela Oluwaseun, for helping with corrections and general editing. Massive thanks to Andrea Varro who made my Liverpool experience an easy one, and all the team members in the PGR office are appreciated massively.

Table of Contents

Table of figures

Abbreviations

ADAM	A disintegrin and metalloproteinase
APS	Ammonium persulphate
AREG	Amphiregulin
Bcl-2	B-cell lymphoma 2
BSA	Bovine Serum Albumin
CAF	Cancer associated fibroblasts
CAM	Cell adhesion molecules
CMVIE	Cytomegalovirus immediate early promoter
DAPI	4'-6-diamino-2-phenylindole
DBD	DNA binding domain
DDR	DNA damage repair
DMSO	dimethylsulphoxide
EBV	Epstein-Barr virus
ECM	Extracellular matrix

ECMV	Encephalomyocarditis virus
ECS	Extracapsular spread
EDTA	Ethylenediamine tetraacetic acid
EGF	Epidermal Growth Factor
EGFR	Epidermal Growth Factor Receptor
ELISA	Enzyme-Linked Immunosorbent Assay
ER	Endoplasmic reticulum
ERAD	ER-associated degradation
FGF	Fibroblast growth factor
FISH	Fluorescence in situ hybridisation
FNAB	Fine needle aspiration biopsy
FOM	Floor of mouth
H&E	Haemotoxylin and Eosin stain
HB-EGF	Heparin-binding EGF
HCL	Hydrochloric acid
HEK	Human embryonic kidney
HIV	Human immunodeficiency virus
HNSCC	Head and neck squamous cell carcinoma
HPV	Human papilloma virus
IARC	International agency for research on cancer
IMP	Intramembrane serine proteases
IRES	Internal ribosomal entry site
iRhom	Inactive rhomboid protein
KD	Knock-down
LPS	Lipopolysaccharide
MAPK	Mitogen-activated protein kinase

MMP	Matrix metalloprotease
mRNA	Messenger RNA
Neo	Neomycin
NEXT	Notch extracellular truncation
NOK	Normal oral keratinocyte
NICD	NOTCH Intracellular Domain
NPT	Neomycin phosphotransferase gene
OSCC	Oesophageal Squamous Cell Carcinoma
PARL	Presenilins-associated-rhomboid-like
PBS	Phosphate Buffered Saline
PCR	Polymerase chain reaction
PVDF	Polyvinylidene fluoride
RIP	Regulated intramembrane proteolysis
RQ	Relative quantification
RT-PCR	Reverse Transcriptase-polymerase chain reaction
SDS	Sodium dodecyl sulphate
SDS-PAGE	SDS-polyacrylamide gel electrophoresis
shRNA	Short hairpin RNA
S.D	Standard deviation
STAT	Signal transducer and activator of transcription
TEMED	*N,N,N,N*-tetramethylethylenediamine
TGF-α	Transforming Growth Factor-α
TMD	Transmembrane domain
TACE	TNF-α converting enzyme
TMA	Tissue microarray
TMH	Transmembrane helix
TNF-α	Tumour necrosis factor-α

TOC	Tylosis with Oesophageal Cancer
Tris	Tris-hydroxymethylaminoethane
UIM	Ubiquitin interacting motif
VEGFR	Vascular endothelial growth factor receptor
WT	Wild Type

CHAPTER1:

INTRODUCTION

1 CHAPTER 1: INTRODUCTION

1.1 Introduction

Current research is preoccupied with the molecular basis of cancer. A high proportion attempting to highlight specific biomarkers, targets for therapy and possible prognostic parameters. This study will investigate the possible role of the rhomboid protein, iRhom2 in the pathogenesis of oral cancers, particularly head and neck squamous cell carcinomas, with a focus on its proposed interaction with the sheddase, ADAM17.

Specific mechanisms have been suggested in an attempt to unravel the remarkably complex process by which normal cells become transformed into cancerous or malignant variants or derivatives. These often focus on activities which result in

alterations in four vital and overlapping cellular events – growth, proliferation, differentiation and cell death. The multistep process of carcinogenesis is proposed to lead to gradual and successive genetic changes ultimately leading to the acquisition of a "growth advantage" for the transformed cancer cells[1]. Eight survival capabilities, described as the hallmarks of cancer are common with virtually all cancer types. These survival capabilities enable cancerous cells adopt a new mechanism which works contrary to the original anticancer defence mechanisms possessed by healthy non-cancerous cells. They have been described as; self-sufficiency in growth signals, insensitivity to anti-growth signals, evasion of apoptosis, limitless replication, sustained angiogenesis, tissue invasion/metastasis, reprogramming of energy metabolism and evading immune destruction[2] (**Figure 1.1**). A sound understanding of the basic hallmarks of cancer is important in the development of effective anticancer therapeutic agents as well as in unmasking potential prognostic biomarkers.

1.2 The hallmarks of cancer

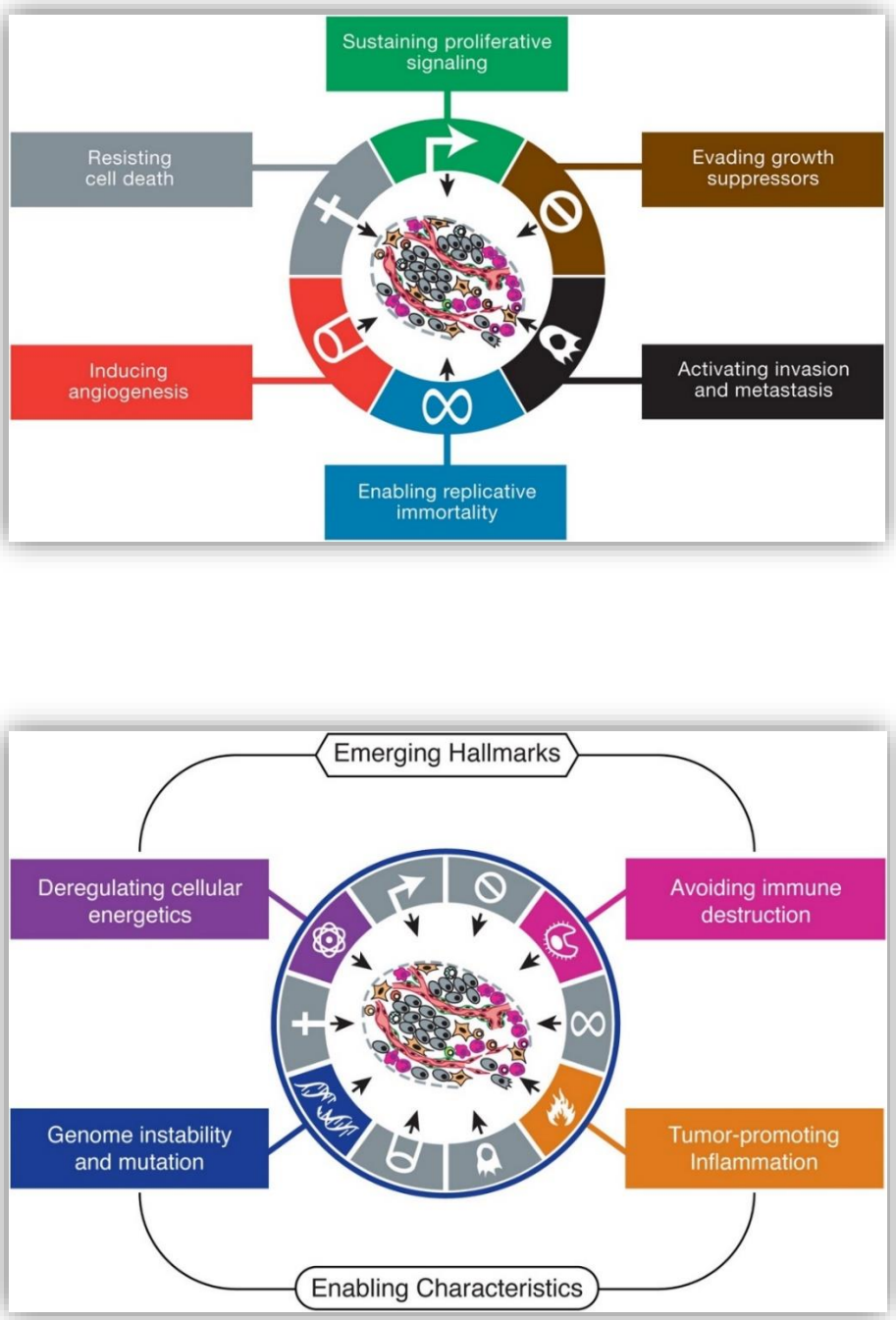

Figure 1.1 Hallmarks of cancer:

Top - Illustration of the initial six hallmark capabilities first proposed. **Bottom** – Latest additional two hallmarks and two enabling characteristics. Adopted from Hanahan et al[2].

1.2.1 Self-sufficiency in growth signal.

For normal active proliferation, healthy cells will generally require the passage and conduction of stimulating signals. For this to happen, specific extracellular signalling molecules are required, in addition to membrane bound or transmembrane receptors[3] (**Figure 1.2**), including adhesion molecules such as integrins and cadherins[4]. Such signalling molecules could be components of the extracellular matrix such as collagen and glycoproteins[5], or soluble growth factors such as bFGF and VEGF[6].

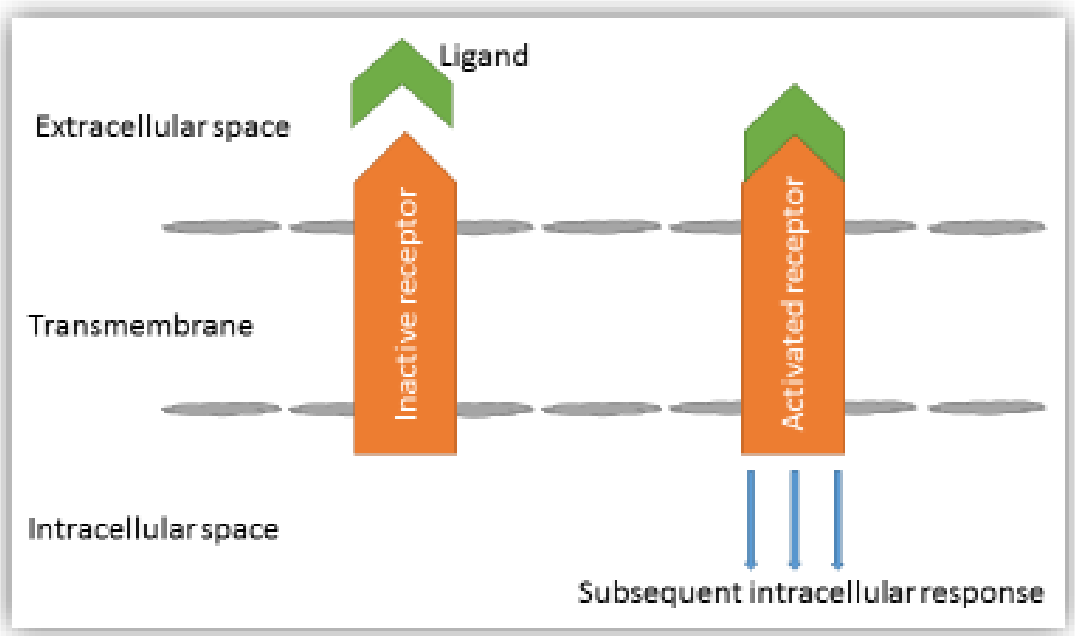

Figure 1.2 Signal passage and conduction:

Illustration of the concept of signal passage and conduction to generate response such as proliferation. It involves the binding of a ligand to membrane bound or transmembrane receptors, leading to conformational changes and the generation of response. Adopted from Lappano et al[7].

These bind as ligands to specific membrane bound receptors for onward transmission of signals intracellularly. An example is illustrated in (**Figure 1.3**), in which the RAS-RAF-MEK1/2 pathway is activated by the binding of ligands which could be soluble growth factors, hormones or other stimuli, with resultant transmission of signals intracellularly, culminating in one form of response or the other such as proliferation or influence on gene expression[8].

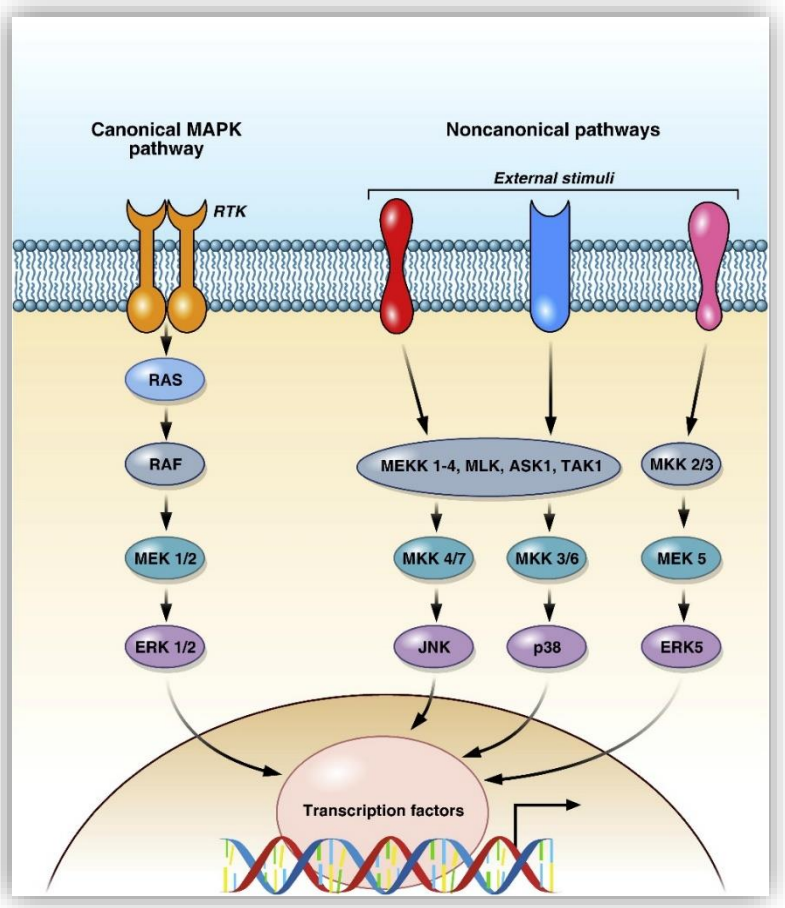

Figure 1.3 MAPK pathway:

An illustration of the MAPK pathway. Adopted from Martineli et al, 2017[8].

It is therefore apparent that normal cells rely on external or exogenous molecules for the maintenance of growth or proliferation. This reliance on exogenous factors is less apparent with tumour cells which are often able to mimic signal transduction in a number of ways and trigger as well as sustain cell proliferation. An example is the case where a HIF-1α dependent autocrine feedback was shown to enhance survival of prostate cancer cells starved of serum[9]. This acquired growth signal autonomy is thought to be modulated by numerous oncogenes which act in favour of tumour proliferation. Equally, the normal tightly regulated growth signal pathway may be deregulated at any of the three distinct phases – the extracellular molecules, the transmembrane receptors, or the intracellular mechanism responsible for translation of signals into action, such as the SOS-Ras-Raf-MAP cascade[10] (**Figure 1.3**). With autocrine stimulation, tumour cells are able to manufacture and respond to growth molecules without dependence on other neighbouring cells for supply. An example is the autocrine stimulation of glioblastomas by PDGF (platelet-derived growth factor)[11]. Deregulation of membrane bound receptors often exists in the form of overexpression of such receptors, thereby making the tumour cells hypersensitive to normal or subnormal levels of growth factors. A notable example is the case of increased expression of EGFR in brain and breast cancer[12,13]. The overexpressed receptors may even signal constitutively without the binding of ligands, further stimulating the proliferation of tumour cells[14,15]. In a more complex manner, still very much less understood, deregulation can occur within the intracellular mechanism responsible for the translocation of signals into action. A notable example is the Ras protein in the SOS-Ras-Raf-MAP cascade, in which the Ras protein is found to be structurally altered in about 25% of cancer cases[16]. This structural alteration leads to

constitutive signalling, even in the absence of stimulations by ligand-receptor complexing[16].

1.2.2 Insensitivity to antigrowth signals.

Similar to the need for growth signals for proliferation, antigrowth signals also exist. These signals work in a coordinated manner for the homeostasis of cells, ensuring a balance in the rate of growth / proliferation. Antigrowth signalling molecules may be in the form of soluble molecules, immobilised components of the ECM, or indeed as cell membrane receptors[17]. Cells do not generally replicate endlessly. They are induced into a temporary G_o phase from an active proliferative phase, or into a more permanent postmitotic/differentiation state[18]. This is mainly via the retinoblastoma protein family[19], and tumour cells have to devise a means of evading this control in order to sustain proliferation. Normally, among other antigrowth factors, TGFβ prevents the phosphorylation of pRb, thereby keeping it in the hypophosphorylated state. In this state, pRb hinders the ability of E2F to promote expression of an array of genes responsible for the progression of cells from the G1 phase into the S phase. Upstream deregulation with TGFβ or its receptors truncates this system, resulting in hyperphosphorylation of the pRb and therefore enhanced E2F function, ultimately leading into cells moving from the G1 phase to the S phase[20] (**Figure 1.4**).

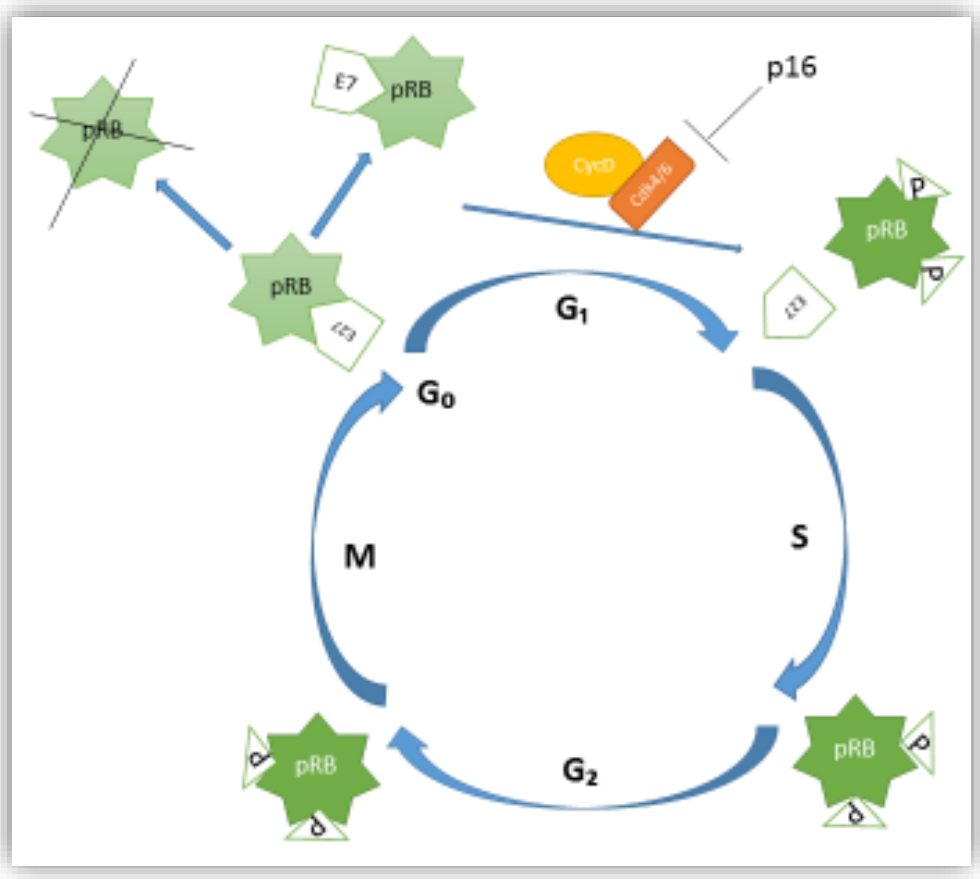

Figure 1.4 The pRB-E2F pathway:

The pRB-E2F pathway is illustrated with E2F shown to be inhibited by the binding of pRB. This occurs in the G_0 and G_1 phase. In proliferating cells however, the Cyc D / Cdk4/4 complex enables the phosphorylation of pRB to release E2F. The released E2F induces genes for S phase. The pRB-E2F complex is disenabled by mutations in the RB gene in cancer.

1.2.3 Evading apoptosis.

The regulated and orchestrated cellular process in both physiological and pathological settings, leading to cell death and phagocytosis of the dead cells is referred to as apoptosis[21-23]. Two groups of key players in the apoptosis pathway include sensors and effectors. The former monitors both intracellular and extracellular environment for abnormalities such as DNA damage / hypoxia and cell attachments, leading to a trigger of programmed cell death that is carried out by "effectors"[24]. There is also directed cell killing via death ligands, for instance, cells expressing Fas or TNF receptors trigger or initiate the process of apoptosis by binding to death ligands and protein cross-linking[25,26].

It is important to note also that cells generally maintain their existence based on vital "cell-matrix" and "cell-cell" interactions which generate signals necessary for normal cell function. This inherent cell-cell / cell-matrix mechanism for supply of signal will have to be compromised for cell death to occur under normal circumstances[27,28]. The mitochondrion is the power house of the cell. It is therefore no surprise that most of the apoptotic signals are targeted at this organelle which, in response, releases the cytochrome C protein to herald cell destruction[29]. This release is governed by the Bcl-2 family, which are either pro- or anti-apoptotic through their stimulation or inhibition of this release of Cytochrome C, respectively[30] (**Figure 1.5**). The effectors of apoptosis are the caspases, which eventually bring about controlled cell death (**Figure 1.6**). They begin this by initiating the execution pathway, triggered by cleavage of caspase-3. The pathway involves the fragmentation of DNA and other

cellular events such as degradation of cytoskeletal and nuclear proteins, and cross linking of proteins.

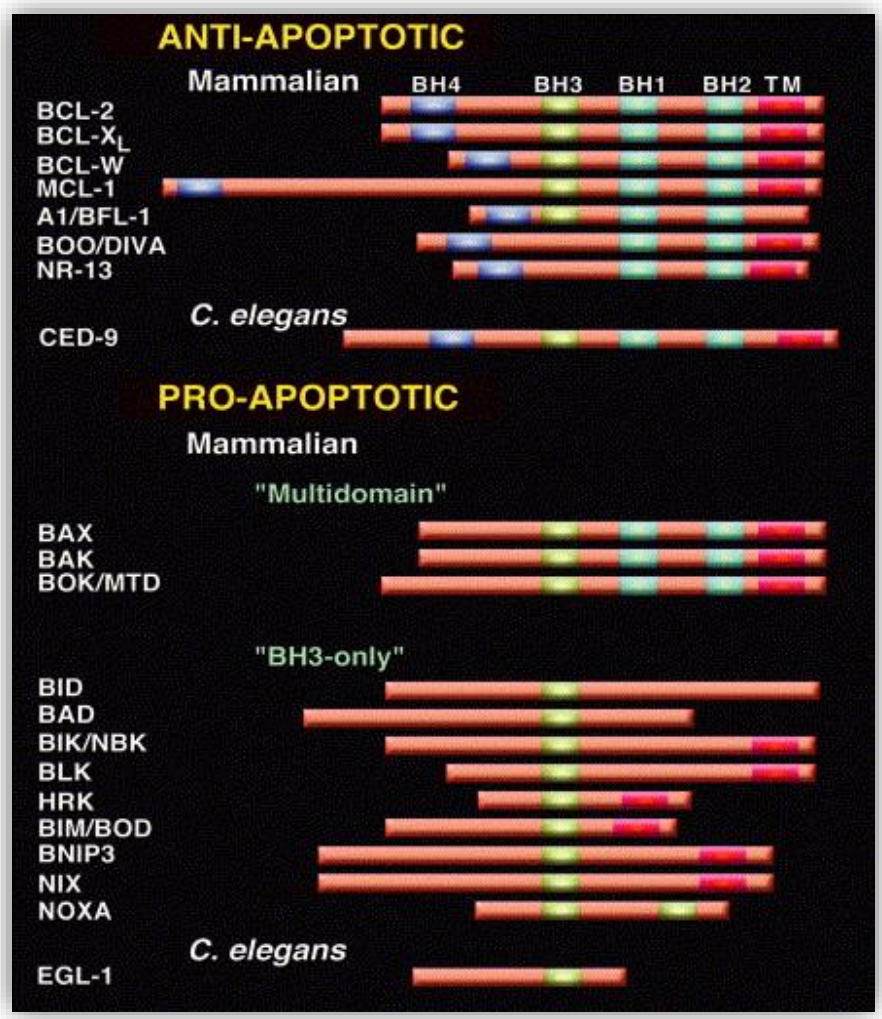

Figure 1.5 Members of the Bcl-2 family:

Members of the Bcl-2 family of proteins grouped into pro- and anti-apoptotic sub-groups. Adopted from L. Scorrano et al.[30]

There is formation of apoptotic bodies and late in the execution pathway, uptake of the apoptotic cells by phagocytic cells following expression of ligands for phagocytic cell receptors[25]. For cancer cells to thrive therefore, they must devise a means of deactivating the apoptotic pathway/machinery. Tumour cells are able to achieve this through a variety of ways, the most common is via p53 mutation, observed in more than 50% of cancer cases[31]. This is no surprise, considering the transcriptional activities of p53 generally lead to the activation / upregulation of downstream target genes such as MDM2 and CDKN1A. These in turn are involved with cellular activities that bring about cell cycle arrest, DNA repair, senescence and programmed cell death. Inactivating mutations in p53 will therefore promote increased proliferation and possibly metastasis[31]. Indeed, tumour cells have been shown to use many different mechanisms to abrogate the apoptotic pathway, including transcriptional / translational and post translational regulation of proteins. Transcriptional / translational approach involves overexpression of anti-apoptotic proteins and the suppression of pro-apoptotic proteins expression, while the pro-translational regulation involves steps such as altering protein function, destruction of pro-apoptotic proteins and stabilizing MCL-1[32]. For instance, it has been demonstrated in lung and colon cancer cell lines that the existence of a false FAS receptor competes with active FAS receptors for the pro-apoptotic FAS ligand, thereby limiting apoptosis[33].

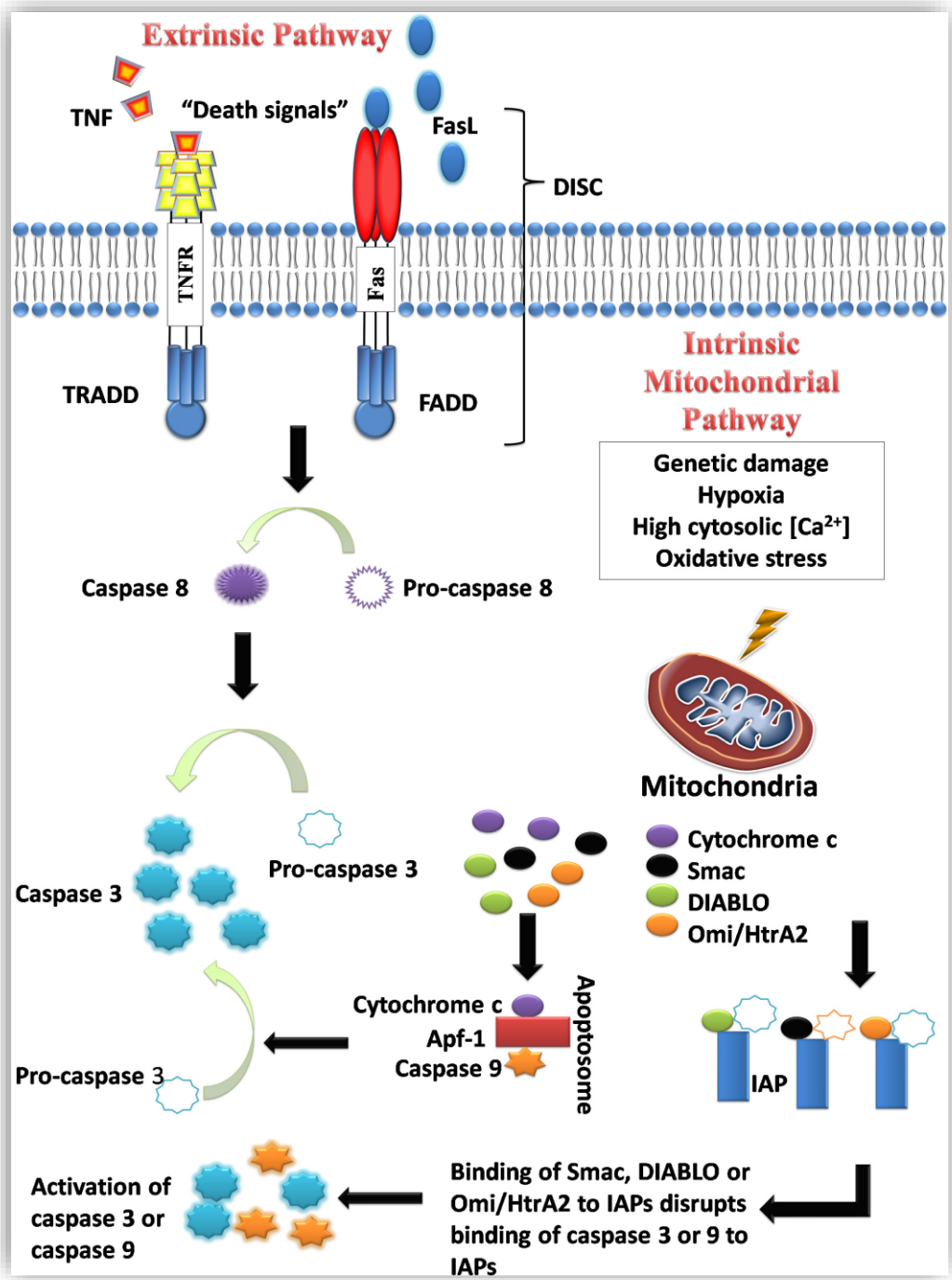

Figure 1.6 intrinsic and extrinsic pathways of apoptosis:

An illustration of both intrinsic and extrinsic pathways of apoptosis[22].

1.2.4 Limitless replicative potential.

It is proposed that there is an inherent mechanism by which normal cells restrict the number of cell divisions they can undertake. For example, cells placed in culture will normally not continue to replicate indefinitely, rather they will achieve a finite number of replications and then reach a state of senescence after a number of duplications[34]. Replication may be pushed further to a stage known as the "crisis point", characterised by massive cell death[35]. It is estimated that 1 in 10^7 of such cell population escape entirely to become immortalised, replicating indefinitely[36]. Tumour masses are thought to comprise of a variety of cell types, including a population of immortalised cells[37,38]. Finite replication found normally with cells may be attributed to progressive loss in telomere with every cycle of cell duplication. With this loss, chromosomes are left unprotected and thus exposed as targets for DNA damage[39,40], and telomere maintenance is observed in malignant cells. This is majorly due to upregulation of the telomerase enzyme. This in turn ensures that the telomere DNA repeats (TTAGGG), are constantly replenished and maintained at the 3′ ends of the chromosomes, following rounds of cell replication[41]. That way, telomere shortening is prevented, cellular replication is maintained and DNA damage prevented.

1.2.5 Sustained angiogenesis.

To thrive, cancer tissues develop angiogenic potentials to ensure effective nutrient and oxygen supply[42,43]. Signals for this are generated by soluble factors and their corresponding endothelial membrane bound receptors, typified by VEGF (vascular endothelial growth factor), which binds to its endothelial membrane bound tyrosine kinase receptors, neuropilin-1/2[44]. Signalling by VEGF (vascular endothelial growth factor) is generally required for both vasculogenesis (formation of new blood vessels from angioblasts during embryogenesis), and angiogenesis (formation of new blood vessels from already existing vasculature)[45,46]. There exist an almost equal number of endogenous inhibitors to angiogenesis as there are stimulators, this therefore suggests the process of vasculogenesis is tightly as well as critically regulated with the balance between both groups of stimulator and inhibitors. Interference with those in support of angiogenesis will therefore inhibit angiogenesis [47]. Thrombospondin-1 is a typical example of a potent angiogenic inhibitors[48]. This member of the thrombospondin family of proteins, synthesised, secreted and functioning in the extracellular matrix, regulates angiogenesis by direct and indirect means[49]. Direct via physical impact on vascular endothelial cells, and indirectly via other angiogenic regulators[49]. Taken together, several investigations point to the fact that angiogenesis or formation of new capillaries is likely to be a prerequisite for the growth of tumours[50], and that tumours are able to switch from a quiescent state of capillary formation to active angiogenesis[51].

1.2.6 Tissue invasion and metastasis.

Invasion and metastasis are both forms of tumour dissemination, and are considered the most deadly acquired capabilities of tumours, as they render the tumours more difficult to manage following spread to other tissues[52]. Tumour metastasis in particular is put as the leading cause of mortality due to cancer[53]. It is the general believe that after tumours have exhausted their initial and primary site, they will tend to spread to neighbouring or distant sites to create additional space. There is however the view that, prior to when crowding becomes an issue, and at the initial stage of tumour establishment and growth, invasion and metastasis or dissemination of tumour cells may still occur[52,54]. Tumour cells invade neighbouring sites but metastasise to farther niches, tumour metastasis is therefore the establishment of secondary tumours at a location entirely different from their primary site[55]. **Table 1.1** highlights the notable differences between invasion and metastasis[56]. They metastasise by first invading the surrounding stroma, then travel through blood or lymphatic vessels before migrating out to form new colonies[57] (**Figure 1.7**).

Table 1.1 Metastasis and invasion

METASTASIS	INVASION
Establishment of distant tumours	Local migration through tissue
Distant travel via conduits	Contiguous tumour
Seeding in ectopic microenvironment	Normal / similar / orthotopic microenvironment

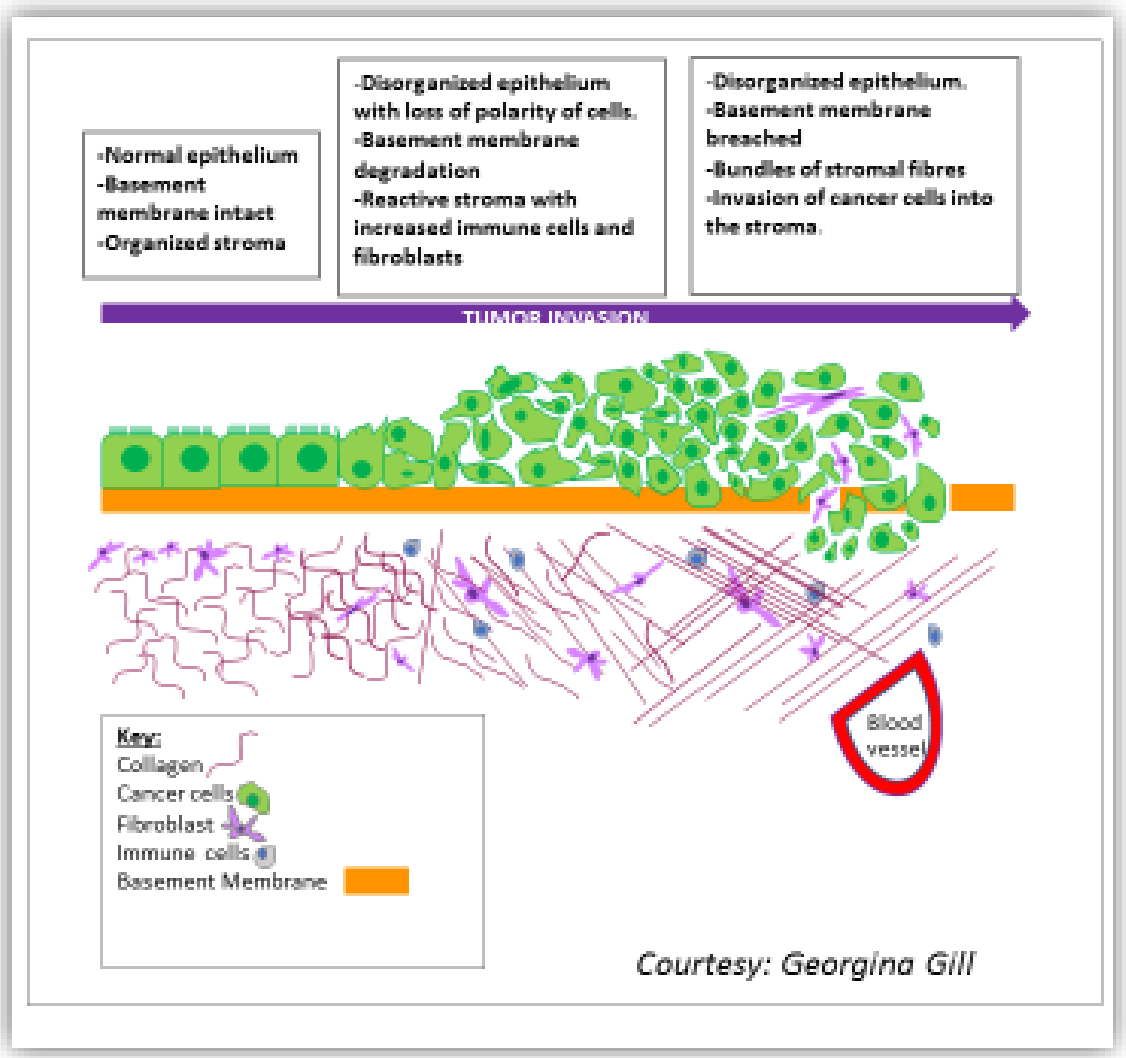

Figure 1.7 Illustration of tumour invasion:

Illustration of tumour invasion, gradually into neighbouring stroma and on to blood vessels for possible distant seeding.

This process of seeding and the conditions of an entirely new environment will generally appear harsh on the seeded cells, but, due to genetic instability and heterogeneity of tumour cells, they are said to be able to generate a subset of cells with a phenotypic characteristic that enables them withstand such otherwise

incompatible and new microenvironment[58]. The acceptability or accommodating nature of the new microenvironment, mostly determined by the nature of its stroma organisation is a huge factor for successful seeding[57].

Expressions of CAM (cell adhesion molecules) members of the immunoglobulin family and cadherins, and integrins by tumour cells has been shown to be an important feature in the survival of metastatic tumours in their new site[59].

1.2.7 Reprogramming energy metabolism

Neoplasm generally entails increased tissue growth and proliferation, thereby increasing the demand on energy metabolism. Under normal physiological conditions, healthy cells are known to, under aerobic conditions, process glucose by converting same into pyruvate. This occurs during glycolysis and takes place largely in the cytosol of cells[60]. The resultant pyruvate is channelled into the mitochondria for onward production of CO_2, with a positive gradient in Oxygen concentration favouring this mitochondria reaction[61]. It is therefore the normal trend to have more pyruvate channelled into the mitochondria for conversion into CO_2, a process known as oxidative phosphorylation, in aerobic conditions. Tumour cells have been shown to possess the ability to act in the contrary, rather favouring reaction in the opposite direction - a condition first described by Warburg and known as aerobic glycolysis[62,63]. Oxidative phosphorylation will usually produce abundant ATP, therefore, a metabolic switch in favour of glycolysis will incur shortage in ATP, put at approximately 18 fold less. To compensate for this reduced efficiency in ATP production, cancer cells

increase uptake of glucose to compensate via increased glycolysis. They achieve this by the upregulation of glucose transporters such as GLUT1[64]. This increased glycolysis adopted by tumour cells has also been demonstrated to be associated with tumour suppressor genes such as p53 as well as oncogenes such as MYC and RAS[65]. With this capability, cancer cells are able to cope in an ensuring hypoxic condition mostly due to excessive demand for oxygen and possible cell / tissue overcrowding. In which case they are able to upregulate enzymes favouring glycolysis such as HIF1α and HIF2α, as well as glucose transporters[66]. It is thought that the increased glycolysis provides essential substrates for the supply of amino acids, necessary for the assembly of new cells and their organelles[67]. The limitations of this emerging hallmark are as follows. Firstly, it has been shown that some tumours consist of two subpopulations, with different substrate requirements in respect to energy metabolism. One subpopulation requires glucose with lactate waste, with the other subpopulation requiring the same lactate waste for its metabolism, thus making them co-exist symbiotically[68]. Taken together therefore, it means this emerging hallmark may not exactly be applicable to all tumour cells and that the metabolic twist may simply be one of the routine adaptation features for cells in general, and maybe more with tumour cells.

1.2.8 Evading immune destruction

Protection offered by the immune network should also entail surveillance for tumours and thus preventing them from becoming established. For tumour cells to become established therefore, they will have to devise a means by which they are

able to evade this immune surveillance or destruction. The fact that the incidence of certain cancer types increases in immunocompromised states[69], may add credence to the above proposition. An experiment to further illustrate the importance of the immune system against tumour formation, using immunodeficient mice showed that a deficiency in either T cells or natural killer cells (NK) increased susceptibility to tumour formation[70]. In support of this, transplantation experiments showed that, weakly immunogenic cancer cells originating from immunocompromised primary hosts fail to thrive or seed when implanted unto immunocompetent secondary hosts, unlike when they are transplanted unto correspondingly weak secondary hosts[71]. From the clinical epidemiology point of view, colon and ovarian tumours are said to be less aggressive after massive infiltration with both cytotoxic T lymphocytes (CTLs) and NK cells, unlike those that lacked the immune cells[72]. Similarly, patients who receive organ transplants may develop donor-derived tumours due to their state of immune-suppression, whereas their donors have had the cancer cells dormant, possibly as a results of their enhanced immunity[73]. An obvious loophole in this emerging hallmark is the fact that there is currently no data suggesting that immunocompromised individuals are on an overwhelming majority in terms of cancer sufferers.

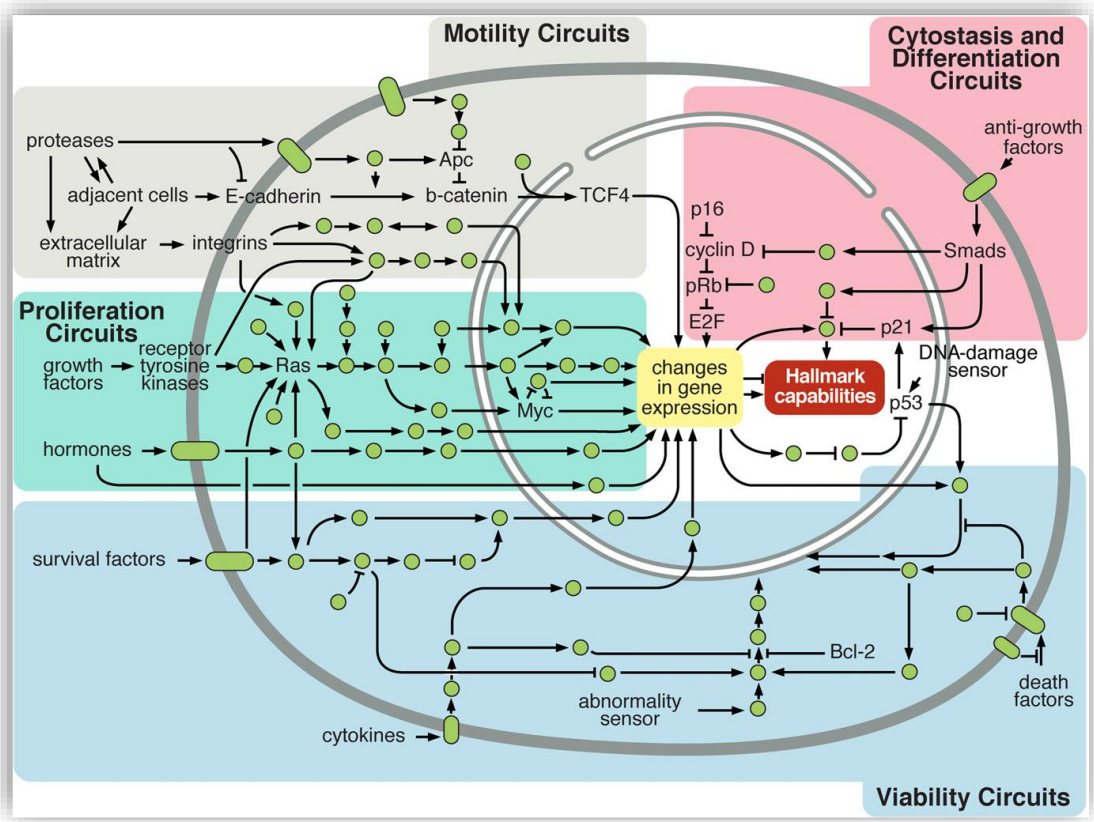

Figure 1.8 circuits and sub-circuits in cancer cells:

A simplified schematics of circuits and sub-circuits operating in cancer cells to regulate the hallmarks discussed[2].

1.3 Enabling characteristics of cancer

1.3.1 Genome instability.

It is generally accepted that for cells to become cancerous, on the basis of genetic changes, mutations accumulate to trigger or sustain carcinogenesis[74]. Healthy cells under normal physiological conditions are therefore unlikely to become cancerous, having inherent checks against cell cycle aberrations in addition to mechanisms in place for repair of damaged DNA[75]. The fact that cancer occurrence is generally more frequent than expected does suggest that cancer cells may be more susceptible to mutations, for them to be able to acquire a sufficient number of mutations put together to trigger carcinogenesis[76]. In colorectal cancer for instance, DNA repair is commonly aberrant, leading to an accumulation of muatations[77]. This susceptibility may be in the form of depreciation in the mechanisms acting as checks against cell cycle abnormalities, and those responsible for repair of damaged DNA. This is exemplified with loss in function of the p53 DNA damage repair pathway, noticed in several cancer types[78,79].

1.3.2 Tumour-promoting inflammation

Almost every tumour is infiltrated to some degree by immune / inflammatory cells[72]. It is thought that the infiltrating immune cells, particularly those of the innate immune system are helpers for tumour progression rather than the logical opposing role they are expected to play[80]. It is proposed that the mechanism by which they

achieve this has to do with the inflammatory cells enabling increased bioavailability of important molecules such as growth factors for increased proliferation, survival factors, proangiogenic factors and possibly ECM anchorage factors. All of these working together would enhance tumour invasion and metastasis[80,81]. In addition, the inflammatory cells are likely to enhance production of reactive oxygen species which enable neighbouring settling cancer cells acquire full status and thus promote malignancy[82].

1.4 The oral cavity:

The oral cavity is one of the major openings into the human body. It is important for digestion, speech, taste and respiration. Component parts are; the upper and lower lips with their labial mucosa and commissures, the upper and lower vestibules, the gingiva, the buccal mucosa, the mandible and maxilla including the dentition, the floor of the mouth, the anterior two-third of the tongue, also known as the oral tongue, the hard palate, and the retromolar region. The oral cavity opens posteriorly into the oropharynx which traditionally comprises the soft palate, tonsils and the posterior one-third of the tongue (**Figure. 1.9**). Some component parts are concealed to an extent, as a result, diseases or tumours may easily go unnoticed at their early stages. Patients with squamous cell carcinoma of the retromolar region for instance often present late[83], and nasopharyngeal cancers are not easily detected because of their anatomical location[84]. A good understanding of the gross anatomy of the region is therefore important.

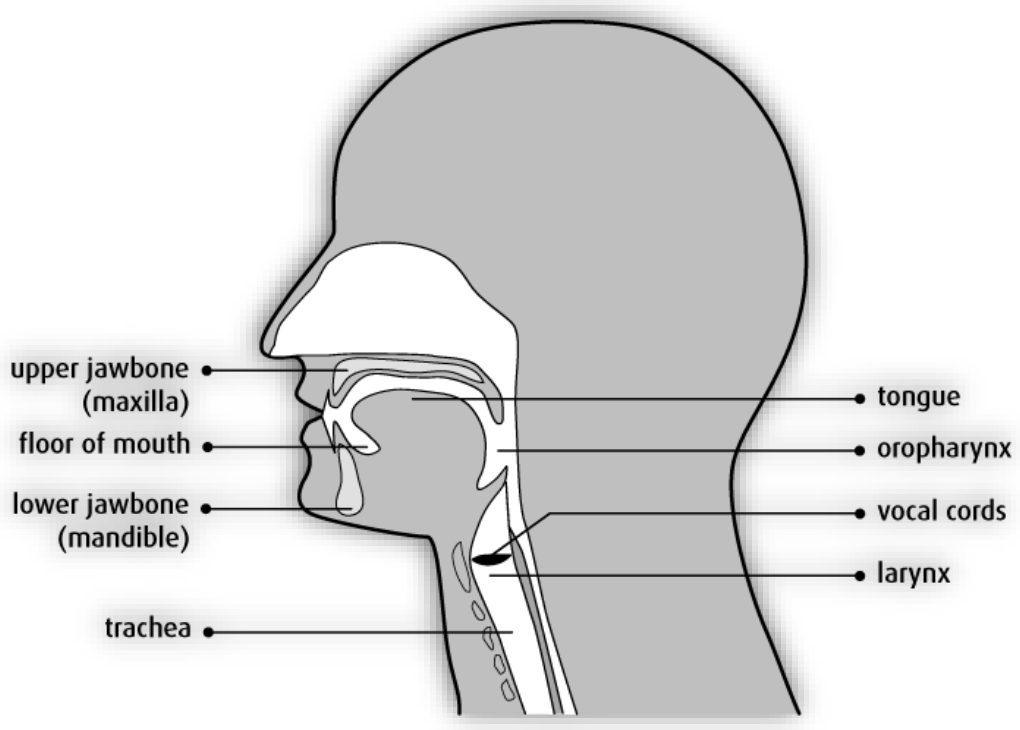

Figure 1.9 lateral cross section of the head and neck:

A lateral cross section of the head and neck region showing the position of the oral cavity in relation to other parts of the head and neck. The image is obtained from the Canadian cancer society

1.4.1 The lip

The oral cavity is bounded anteriorly by the lips, laterally by the cheeks, inferiorly by the floor of the mouth, superiorly by the hard palate and posteriorly continues into the oropharynx (**Figure 1.9 & 1.10**). The upper and lower lips form the surrounding to the opening of the oral cavity and play important roles in competence of the mouth and facial expression, while also aiding mastication and phonation. The upper lip

extends from the base of the nose superiorly and runs laterally towards the nasolabial folds, ending inferiorly at the vermilion border. The lower lip extends from the mandible inferiorly and runs laterally to meet the upper lip at the commissures. Histologically, from superficial to deep, the upper and lower lips comprise the epidermis, subcutaneous tissue, orbicularis oris, and the mucosa. The vermilion with its characteristic colour is composed of nonkeratinised squamous epithelium. Apart from the vermilion part of the lips, there are numerous minor salivary glands, sebaceous glands and hair follicles[85-87].

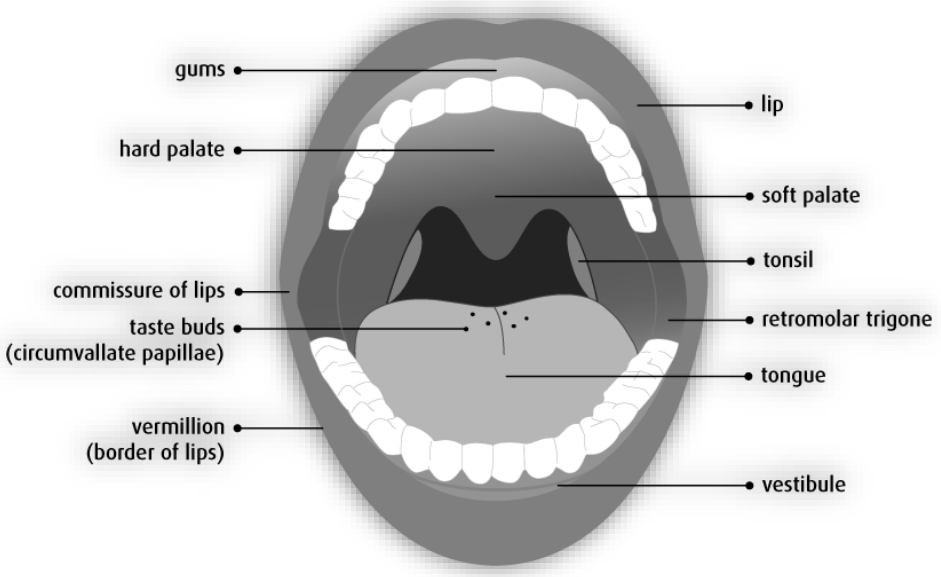

Figure 1.10 anterior view of the oral cavity:

An anterior view of the oral cavity showing its main component parts. Image obtained from the Canadian cancer society[87].

1.4.2 The tongue

The anterior two-thirds of the thick muscular tongue is part of the oral cavity and it is almost entirely covered by mucous membrane, with a characteristic appearance due to covering by lingual papillae[88].

1.4.3 The floor of the mouth

The main excretory duct of the submandibular gland, also known as Wharton`s duct, is found in the floor of the mouth with other smaller duct openings from the sublingual gland. The floor of the mouth is the inferior limit of the oral cavity.

1.4.4 The hard palate

This comprises of the anterior two-thirds of the palate, and it is much bonier compared to the soft posterior one-third of the palate. It basically separates the oral cavity from the nasal cavity[89]. It is bounded antero-laterally by the maxillary teeth, and superiorly by the respiratory epithelium of the nose. Its inferior border is the masticatory epithelium of the oral cavity, while continuing posteriorly with the soft palate. Feeding and phonation are the main functions of the hard palate, with both functions hampered in deformities such as cleft palates[89].

1.5 Oral cancer

Oral squamous cell carcinomas (OSCC) arise from stratified squamous epithelium of the oral mucosa[90]. OSCC incidence increases with age, common with people above the age of 40 years, with the most frequently affected sites being lateral tongue, lip and floor of the mouth [91-93]. Head and neck cancer was reported to be the eighth most common cancer type in the UK in 2014. Worldwide, it is the sixth leading cancer type by incidence with more than 550,000 cases and about 300,000 deaths in 2014[93]. Oral squamous cell carcinomas (OSCC) are the commonest forms of head and neck cancer[94]. Incidence of oral cancer varies from region to region due to marked differences in nutritional as well as socio-cultural habits[95]. Risk factors for all Head and neck cancer anatomical sites include; tobacco, alcohol, betel quid, family history, ionising radiation, and age. Other, more site-specific risk factors include infections such as human papillomavirus (HPV) in oropharyngeal cancer[96], Epstein-Barr virus (EBV) in nasopharyngeal cancer[97] and Burkitt`s lymphoma[98], as well as Human immunodeficiency virus (HIV) and Acquired immune deficiency syndrome (AIDS) in Kaposi`s sarcoma[99]. Immune system deficiencies resulting from conditions such as organ transplant and autoimmune conditions are also risk factors[100], as are occupational hazards such as exposure to acid mists, asbestos, formaldehyde, wood dust and rubber production[93]. Rare inherited disorders such as Fanconi anaemia[101], Li Fraumeni[102] and Tylosis[103] have also been implicated as risk factor for head and neck cancers. Oral cancers are often diagnosed rather late with two-third already significantly locally advanced before they are diagnosed[104]. Symptoms of oral cancer include: swelling or thickening of the affected part, non-healing ulcers, leukoplakia

(white patch), erythroplakia (red patch), pain on chewing, swallowing or speaking, bleeding, numbness, halitosis, mobile teeth, weight loss and neck lumps[105]. As a consequence of genetic and epigenetic alterations which form the basis for which carcinogenesis occurs, constituent cells for each cancer type do not only appear morphologically similar, but also tend to show upregulation/downregulation of specific proteins considered biomarkers. For OSCC, deregulation is commonly reported with genes such as p53, retinoblastoma gene, VEGFR, EGFR and recently notch[92,106]. Treatment modalities are by surgical excision, chemotherapy or radiotherapy, or a combination of any two or the three[107,108].

Classification or grading of oral cancer is important for the determination of prognosis and for effective treatment planning[109,110]. The TNM classification for instance, which is based primarily on anatomical location, is important for overall effective clinical care, also to aid in determining cases for clinical trials, for stratification, clinical and molecular research, as well as policy making[110]. Staging has been shown to be of importance, with cases treated differently according stage, with success[111]. Among other criteria, oral cancer may be classified according to primary site – cancer of the lip, tongue, floor of the mouth, palate, mandible, retromolar region, maxilla and vestibule. Also according to the pattern of the tumour invasion front or based on the level of differentiation of tumour cells[92,112]. Staging oral cancer puts clinical and pathological features into consideration and overall, the tumour stage gives an idea of extent of tumour and its prognosis[113]. The TNM form of staging considers tumour size (T), involvement of regional lymph nodes (N), and metastasis (M)[114]. **Table 1.2** shows details of the TNM staging system.

1.5.1 Genetic predisposition to head and neck squamous cell carcinomas.

It is already common knowledge that certain factors such as alcohol, tobacco and viral infections such as HPV are risk factors for the formation of head and neck cancers. In addition, individuals may be additionally predisposed or with an increased risk of developing HNSCC, genetically. Patients with the autosomal recessive Fanconi anaemia syndrome and families with mutations in CDKN2A and ATR genes have been shown to have an elevated tendency of developing head and neck cancer[115-118] . This is in addition to predictions that abnormalities in DNA damage repair pathway for instance may further add to susceptibility to risk factors such as alcohol and tobacco causing HNSCC[119].

1.6 Other forms of head and neck cancer

Apart from oral cancer, other common cancer sites in the head and neck region include: oropharyngeal cancer, nasopharyngeal cancer, laryngeal cancer and hypopharyngeal cancer.

1.6.1 Oropharyngeal cancers

Oropharyngeal cancers affect the oropharynx which is the part of the throat directly posterior to the mouth (**Figure 1.11**). Functional parts of the oropharynx include the

soft palate, base of the tongue, part of the throat occupied by the tonsils, and the posterior pharyngeal wall. The commonest histological form is oropharyngeal squamous cell carcinoma. Other forms include sarcomas, lymphomas, melanomas, and a few affecting regional salivary glands[120]. Common risk factor of oropharyngeal cancer include alcohol, smoking, chewing tobacco, HPV infection and poor diet. Symptoms include unexplained weight loss, appearance of a painless neck swelling, sore throat/tongue, ear pain, altered voice and halitosis. Treatment in the UK is through one or a combination of surgery, radiotherapy and chemotherapy[121,122].

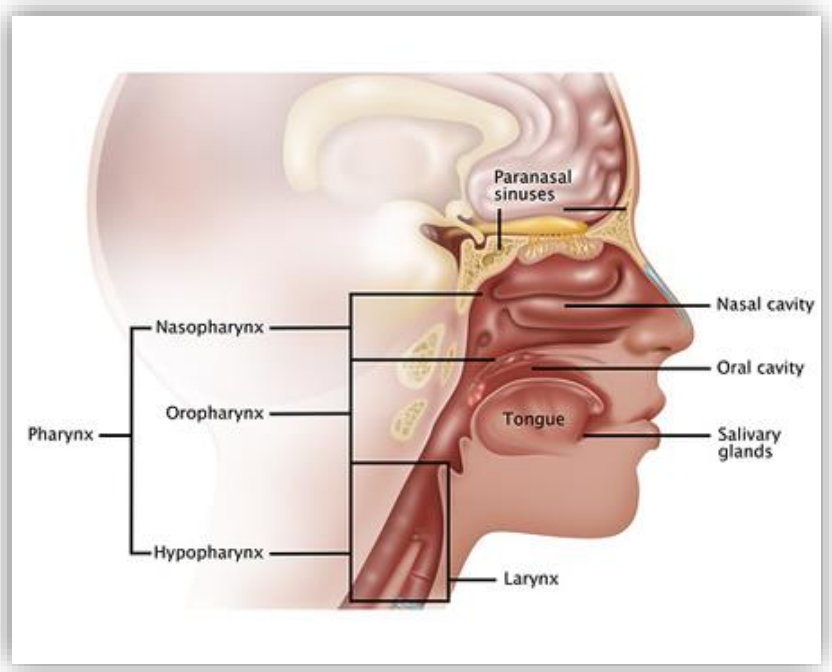

Figure 1.11 Lateral view of the head and neck:

Lateral view of the head and neck region highlighting the oropharyngeal space[123].

1.6.2 Nasopharyngeal cancers

Nasopharyngeal cancers affect the nasopharynx, which is part of the throat just posterior to the nasal region (**Figure 1.11**). The squamous cell carcinoma form is one of the histological variant, with others such as non-keratinising carcinomas and basaloid squamous cell carcinomas. In areas where nasopharyngeal cancers are prevalent, such as Southeast Asia and Southern China, the non-keratinising carcinoma variant is commonest with an incidence of as high as 90%[124]. Its main risk factor apart from the general risk factors for head and neck cancers is EBV (Epstein-Barr virus) infection[98], reported to be clonally present in almost a hundred percent of all undifferentiated nasopharyngeal cancer cases[125]. Notable symptoms include painless upper neck swelling, ear pain with possible leakage of fluid from the ear, blocked nose with bleeding, headache and hearing difficulties[126]. The main treatment modality is radiotherapy, but there may be a combination with chemotherapy[127].

1.6.3 Laryngeal cancers

Laryngeal cancers affect areas around the vocal cords (glottis). The larynx is essentially the voice box with the sub-regions, the superior supraglottis, the glottis, and the inferior subglottis (**Figure 1.12**). Cancer variants in this region include squamous cell carcinomas, sarcomas, lymphomas, adenocarcinomas and neuroendocrine carcinomas[128]. Symptoms of laryngeal cancer include classical hoarseness of the voice and neck swellings which may be painful[129,130]. Treatment

modalities include surgery, radiotherapy, chemotherapy and recently gene therapy[131,132].

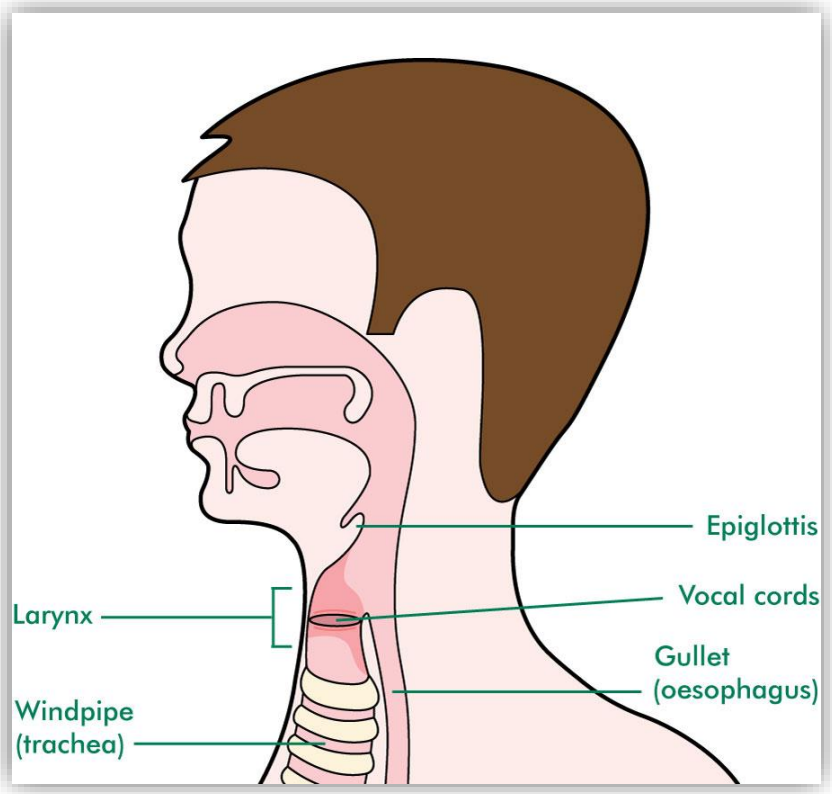

Figure 1.12 Lateral view of the head and neck:

Lateral view of the head and neck region showing the larynx[129]

1.7 Genetics of oral cancer.

Formation and progression of oral cancers, like other cancer types have been attributed to genetic alterations or abnormalities. Chromosomal instability resulting in altered number of chromosomes, often arising from defects in chromosome segregation is common with cancer cells[133]. Significant chromosomal instability is observed in 80% of HPV-negative HNSCC cases, and these include changes with the chromosomal arm-level as well as smaller focal alterations[134]. Using fluorescence in situ hybridisation (FISH) to analyse fine needle aspiration biopsy (FNAB) specimens, instability in chromosomes 7, 9 and 11 alone was demonstrated in 11.7% of OSCC patients[135]. Apart from aberrations in cell cycle, common in cancer, aneuploidy, which is the gain or loss of one or more chromosomes thereby altering the total number of DNA assembly of a cell, is also a commonly observed characteristic[136,137]. In a TMA study involving 47 non-metastasised and 39 metastasised primary OSCC cases, aneuploidy was demonstrated in all the cases as well as all affected lymph nodes[138]. Also, in a multi-centre analysis of tongue squamous cell carcinoma in 37 patients to determine correlation between DNA ploidy and clinicopathological characteristics, aneuploidy was detected in 86.5% of the cases[139].

Oncogenes and tumour suppressor genes are also affected by DNA copy number alterations, often due to deletions and duplications, with the tumour suppressor gene, CDKN2A/2B and the MTAP metabolic enzyme found to be co-deleted in 6/16 cancer cases in a study[140]. Primary OSCC cells were shown to have acquired a metastatic form by gaining metastasis- associated copy number alteration. In a study on copy number aberrations, using metastatic primary tumours and their paired

affected lymph nodes, gains and losses were most commonly observed in (3q, 9q, 11q13, 14q, 16p, 18p, and 20q) and (3p, 4q, 8p, 9p, 10p, 13q, 18q, and 21q) respectively in more than 50% of cases[141]. Loss of heterogeneity is another genetic occurrence that may lead to affected cells becoming cancerous[142,143], and this has been shown in oral cancer cases, with the loss of heterogeneity mostly affecting tumour suppressor genes and oncogenes. This was highlighted in a study demonstrating large-region-LOH in 3p, 17p and especially 9p chromosomes, with 9p housing genes such as KDM4C, CCDC171, IL33 and FREM1, all thought to be tumour suppressor genes for HNSCC[144]. Loss of heterogeneity in *p53* gene was notably demonstrated in oral cancer cases, and the *p53* gene is well established as a major tumour suppressor gene[145]. With the use of microarray technology and next generation sequencing, researchers have recently been able to carry out a comprehensive genomic profiling of head and neck cancers and their commonly mutated tumour suppressor and oncogenes (unravelling the molecular genetics of head and neck cancer through genome-wide approaches).

Table 1.2: TNM staging system for oral cancer (obtained from the International agency for research on cancer, IARC)[146]

T – Primary tumour size

TX	Primary tumour cannot be assessed
T0	No evidence of primary tumour
Tis	Carcinoma in situ
T1	Tumour 2 cm or less in greatest dimension
T2	Tumour more than 2 cm but not more than 4 cm in greatest dimension
T3	Tumour more than 4 cm in greatest dimension
T4a (lip)	Tumour invades through cortical bone, inferior alveolar nerve, floor of mouth, or skin (chin or nose)
T4a (oral cavity)	Tumour invades through cortical bone, into deep/extrinsic muscle of tongue (genioglossus, hyoglossus, palatoglossus, and styloglossus), maxillary sinus, or skin of face
T4b (lip and oral cavity)	Tumour invades masticator space, pterygoid plates, or skull base; or encases internal carotid artery

N – Involvement of regional (cervical lymph nodes)

NX	Regional lymph nodes cannot be assessed
N0	No regional lymph node metastasis
N1	Metastasis in a single ipsilateral lymph node, 3 cm or less in greatest dimension
N2	Metastasis as specified in N2a, 2b, 2c below
N2a	Metastasis in a single ipsilateral lymph node, more than 3 cm but not more than 6 cm in greatest dimension
N2b	Metastasis in multiple ipsilateral lymph nodes, none more than 6 cm in greatest dimension
N2c	Metastasis in bilateral or contralateral lymph nodes, none more than 6 cm in greatest dimension
N3	Metastasis in a lymph node more than 6 cm in greatest dimension

M - Distant metastasis

MX	Distant metastasis cannot be assessed
M0	No distant metastasis
M1	Distant metastasis

Overall stage grouping

Stage 0	Tis	N0	M0
Stage I	T1	N0	M0
Stage II	T2	N0	M0
Stage III	T1, T2	N1	M0
	T3	N0, N1	M0
Stage IVA	T1, T2, T3	N2	M0
	T4a	N0, N1, N2	M0
Stage IVB	Any T	N3	M0
	T4b	Any N	M0
Stage IVC	Any T	Any N	M1

1.8 Gene mutations and alterations in HNSCC.

It is a common trend for literature to site data from HNSCC as a whole, rather than specifically OSCC, and I will be following the trend. Gene mutations have been shown to be common in sporadically occurring (apart from the familial cases) cancers. A

study of 30 different tumour types ranked HNSCC as the 9th highest in terms of gene mutation load (ranging from 1-100 mutations per Mb)[147] . **Table 1.3** shows a summary of commonly mutated genes arising from three studies of head and neck cancer and the Indian LGC[134,148]. A cohort of the commonly mutated genes are hereby discussed.

Table 1.3 Tumour suppressor genes and oncogenes commonly associated with HNSCC[134].

Oncogenes

Location	Gene	Status
3q25	*CCNL1*	Candidate
3q25	*PARP1*	Candidate
3q26	*PIK3CA*	Established
3q26	*TP63*	Candidate
3q26	*DCUN1D1*	Candidate
7p11	*EGFR*	Established
7q31	*MET*	Established
8q24	*MYC*	Candidate
8q24	*PTK2*	Candidate
11q13	*CCND1*	Established
11q13	*CTTN*	Candidate
11q13	*FADD*	Candidate

Tumour suppressor genes

Location	Gene	Status
3p14	*FHIT*	Candidate
3p21	*RASF1A*	Candidate
8p23	*CSMD1*	Candidate
9p21	*CDKN2A*	Established
9p23	*PTPRD*	Candidate
10q23	*PTEN*	Established
17p13	*TP53*	Established
18q21	*SMAD4*	Established

1.8.1 p53

The transcription factor and tumour suppressor gene, *p53*, is known to be frequently mutated (46-73%) in HNSCC[148]. It contains the highly conserved DNA binding domain (DBD) and is activated in response to cellular abnormalities such as oxidative stress and DNA damage. This leads to cell cycle arrest to allow repair, failure of which leads to either apoptosis or senescence. Both missense and nonsense mutations are characteristics of the p53 mutational spectrums, with nonsense mutations being randomly distributed, but missense mutations directed at the DBD[149]. The fact that p53 mutations are also present in pre-malignant lesions strengthens the theory that p53 mutation is important in the early stages of cancer formation [106,150-152]. p53 may also be inactivated via upregulation of its negative regulator, MDM2[153,154]. In terms of significance of p53 mutation, a study using a cohort of about 420 HNSCC patients showed that mutations in p53 correlated with poor survival, and further worsened if mutations are in the DBD [155].

1.8.2 CDKN2A, CCND1 and RB1

The important cell cycle progression moderator, Retinoblastoma protein (RB1) is regulated by the upstream CDKN2A/CCND1 pathway[156]. For this reason therefore, the three proteins are mentioned together. In about 30% and 20% of HNSCC cases, CDKN2A gene is deleted and mutated respectively[134,157]. The cell cycle genes-CDKN2A, CCND1 and RB1 are frequently altered in HNSCC. Mutations in the CDKN2A gene, including splice site changes, nonsense mutations and frame shifts, generally

lead to inactivation of the gene, and this effect is increased where there are additional epigenetic alterations[158] . Cyclin D1 is a cofactor, together with CDK4 and CDK6 for the phosphorylation of Rb and its gene[159,160]. CCND1 is reported to be altered in form of amplification in over 20% of tumours, with low levels of mutations and epigenetic alterations also reported. In about 5% of patients, the retinoblastoma gene, Rb1 is shown to be either mutated or deleted [161]. Put together, it has been shown that differential deregulation of the genes of the CDKN2A/CCND1-CDK4-RB1 pathway is associated with the pathogenesis of HNSCC[162]. The biggest impact came from the deregulation of CDKN2A, especially in the early stages of disease, with deregulation of the other component genes thought to add to the effect and prominent at the later stages of disease[162].

1.8.3 PIK3CA and Epidermal growth factor receptor

PIK3CA is hereby discussed with Epidermal growth factor receptor (EGFR), having been shown that mutations in both genes frequently coexist[163]. PIK3CA is another commonly mutated gene in malignancies generally, including HNSCC, whose deregulation is thought to play significant roles in tumour growth and metabolism [164-166]. EGFR is able to indirectly activate PI3K after dimerization with members of the erbB family. This activation leads to further activation of AKT via phosphorylation of phosphatidylinositols. AKT either acts as a direct downstream effector of the PI3K pathway or indirectly by activating mTOR which is important for the regulation of cellular nutrient levels and energy stores[134] . Overall, PIK3CA mutation has been

reported in as many as 20% of HNSCC cases[167], particularly in HPV-positive tumours[168,169].

Activation of the epidermal growth factor receptor (EGFR) upon binding to its ligand leads to dimerization with other members of the tyrosine kinase erbB group of membrane receptors to which it belongs. This eventually leads to conformational changes and subsequent activation of downstream target genes/pathways such as RAS/RAF/MAPK which are important regulators of cellular features such as proliferation, metastasis, invasion and angiogenesis [170]. EGFR is expressed in majority of HNSCC tumours and a correlation has been shown between level of expression and prognosis[171]. Therapeutic interventions targeting EGFR have however not been as successful as expected. This may be due to a lack of understanding of the precise mechanisms by which EGFR plays its pathogenic role, or basically as a result of the presence and effect of some other non-EGFR alternative pathways[172-176].

1.9 Notch pathway

1.9.1 Overview of Notch signalling pathway

The notch pathway is one of the major pathways acting both individually and co-ordinately to interpret and transmit extrinsic signals, presenting such as distinct transcriptional responses[177]. The Notch signalling family consists of a group of transmembrane proteins coded for by the notch family of genes: Notch 1, 2, 3 and 4[178,179].

Discovered about a century ago in Drosophila through notches in their wing margins, these proteins are generally composed of a large extracellular and a smaller intracellular domain (**Figure 1.13**). Five notch ligands: delta-like1, delta-like3, delta-4, Jagged-1&2[180-182], have been identified in mammalian systems[183], and they are equally membrane bound like their receptors[184] (**Figure 1.14**). The activation of the Notch receptor is controlled by regulated intramembrane proteolysis (RIP) in which, the binding of a Notch ligand is believed to initiate a proteolytic cascade resulting in the release of the Notch intracellular domain (NICD) and subsequent activation of immediate downstream target genes such as *Hes-1*, *Hes-5*, *Mash-1* and *Neuro-D*[185,186] (**Figure 1.13 & 1.14**). Recent studies reveal that apart from the well-established fact that the Notch pathway takes part in differentiation of cells / tissues[184,187-190], it is now widely believed that both proliferation and apoptotic events can be modulated by Notch signalling[191].

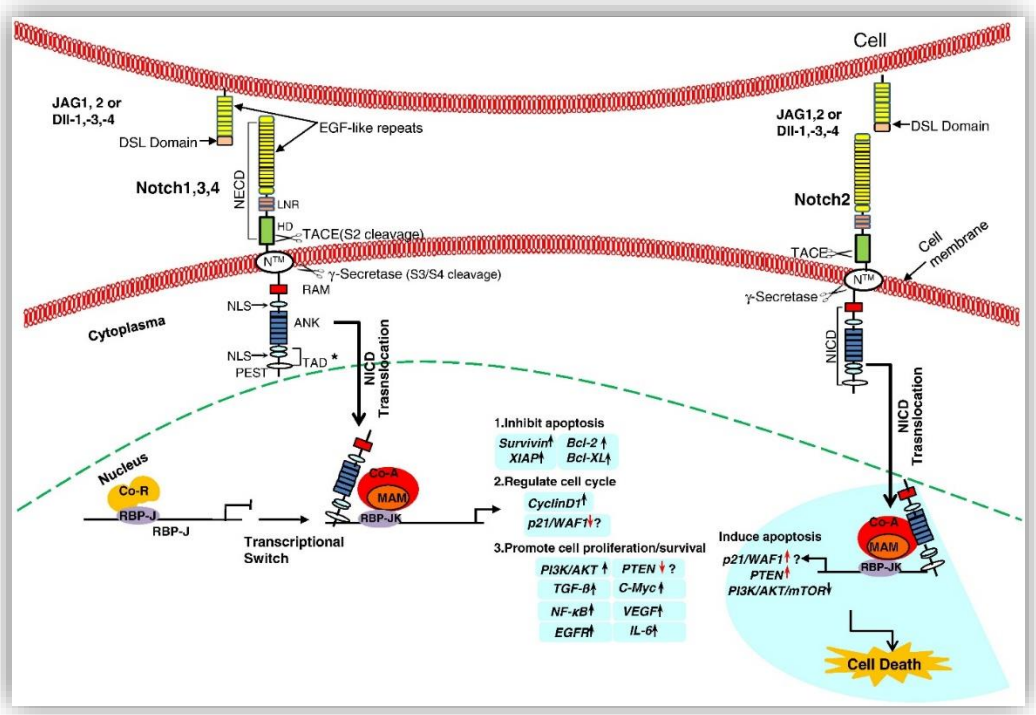

Figure 1.13 Notch signalling pathway illustrated[192].

1.9.2 Role of Notch signalling in HNSCC

The exact role of the Notch signalling pathway in the pathogenesis of head and neck cancers has been on the spotlight of recent investigations, with defects in this notch signalling pathway linked with the pathogenesis of HNSCC[193,194]. Mutations in Notch genes and receptors[195-197], altered RNA / protein expression[197-199], and constitutive activation of Notch without need for ligand binding, have all been reported in HNSCC[200]. With regards to Notch mutations, Notch1 mutation has been reported in as much as 10% to 15% of HNSCC cases, making it only the second most mutated

gene in HNSCC, with p53 the most commonly mutated[197]. In their comprehensive study which involved the use of a cohort of 44 HNSCC and 25 normal samples, a bimodal pattern of Notch pathway alteration was observed with a more obvious inclination towards activating mutations rather than inactivating mutations[197].

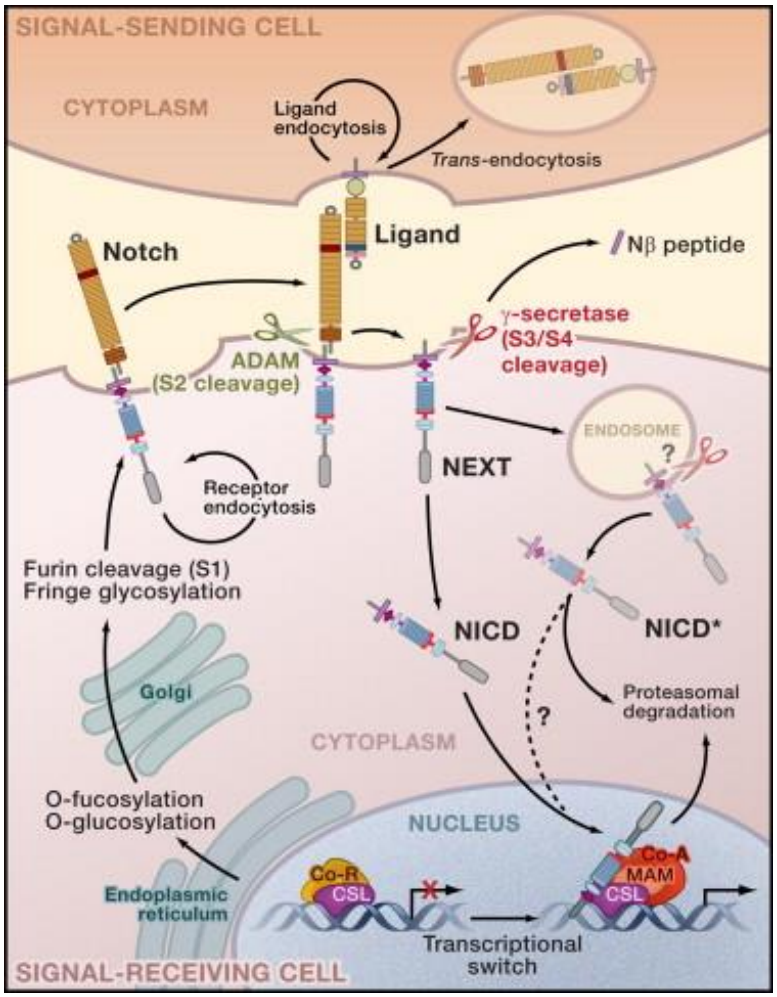

Figure 1.14 Notch signalling by RIP:

Schematic to illustrate notch signalling being mediated by regulated proteolysis. Image adopted from Raphael Kopan[201]

A smaller cohort of 11% of tumours analysed interestingly showed inactivating mutations in Notch1 receptor. Activating mutations were however demonstrated in the larger subset with increased expression or increase in gene copy number of receptors and ligands, and increased downstream pathway activation[197]. In a "whole exome" and transcriptome sequence experiment, to characterise alterations in Notch genes in early-stage (T1-T2) tongue squamous cell carcinomas (TSCC), in which 29 patient-derived tumour samples were used, Notch pathway was shown to be indeed activated in TSCC patients[202]. A bimodal mutation pattern was also observed, but unlike the study previously described, a lower inactivating Notch1 mutation of 4% was characteristic. A consistently higher frequency level of activating mutation was observed in 59% samples (17 of 29 patients). These activating mutations were observed in all the components of the Notch pathway including receptors, ligands and downstream target genes[202]. Importantly, in the same study, Notch1 was shown to be essential for survival, migration and stemness of TSCC tumour cells[202]. In another study to characterise the expression of transcriptionally active Notch1 intracellular domain (NICD1) in HNSCC, using immunohistochemical (IHC) approach, the cleaved Notch1 was shown to be associated with HNSCC high risk factors, in addition to its being highly expressed in HNSCC[199]. In the study, IHC was performed to analyse the distribution / expression of the cleaved Notch1 using 79 already sequenced HNSCCs whose mutation status were already determined. NICD1 was shown to be indeed associated with mutation status ($p<0.001$), and most interestingly, positive staining was observed in a combined 81% of the samples, with the remaining 19% recording negative stainings[199]. 58% of the positive stainings were characteristically peripheral, while the remaining 42% were non-peripheral. The high

level of NICD1 expression does signify increased Notch activation, and the fact that the general expression was in association with mutation status does indicate that the mutation was more of an activating, rather than inactivating type[199].

1.9.3 Correlation of increased Notch signalling with prognosis and tumour aggressiveness

High expression levels of Notch1 are thought to confer poor prognosis in HNSCC, with results obtained from correlation of Notch1 expression levels, with levels of resistance to Cisplatin, which is considered the main chemotherapeutic agent for the treatment of HNSCC[203] (p=0.000). Upregulation of Notch pathway was also shown to correlate with increased patient mortality[200]. It also correlated with increased expression of FGF1, which is a pro-invasive gene, with in vitro activation of Notch in HNSCC cells leading to increased transcription of FGF1[200]. This in turn was shown to induce an obvious increase in both cell migration and invasion, with subsequent FGF1 knock-down bringing about an abrogation of the increased migratory and invasive effects initially associated with over-expression[200].

1.9.4 The contradictory evidence for Notch as a tumour suppressor and / or oncogene

It is still debateable if its main role is oncogenic or as a tumour suppressor, or if down-regulation rather than its up-regulation is key for the formation of cancer. Its actual role has also been shown to depend on the cancer type or setting[204].

It is proposed that, while some members of the Notch family are considered more of tumour promoters, others may be classified as tumour inhibitors. Indeed, there have been cases where the same Notch subtype has been ascribed opposite roles by different researchers, as highlighted below. This is not coming as a surprise, considering the opposite roles Notch actually plays in developmental processes where it enhances stem cell potentials on one hand with a suppression of differentiation, while on the other hand it promotes differentiation and commitment to other cell/tissue lineages[205]. Overall, Notch has been repeatedly linked with the pathogenesis of head and neck cancers.

A recently published work has also suggested that down-regulation of the *Notch4* gene is associated with recurrence in cases of OSCC (oral squamous cell carcinomas), with a *p*-value of 0.001[193]. Priority is now placed on better understanding of the Notch signalling pathway which entails rather complex molecular alterations of the pathway. In the study by Wenyue et al. the possible activation of Notch signalling pathway in HNSCC (head and neck squamous cell carcinomas) was investigated[194]. In that study, the mRNA expression of *HES-1* and *HEY-1* was significantly higher in HNSCC tumours than in normal mucosa, having used a cohort of human tissue samples comprising of tumours (n=44) and paired normal (n=25). Using expression array analysis, they were able to demonstrate that JAG1, JAG2 and *NOTCH3* genes were overexpressed in tumour compared to normal tissues, therefore signifying possible up-regulation of notch in HNSCC. This is somewhat in contrast with an earlier report by the same investigators[198]. They also found out that a total of 31.8% of HNSCC tumour samples examined showed over-expression of *HES1* and/or *HEY1*

genes. Findings were further validated using an independent cohort of HNSCC samples along with a set of normal tissues, using quantitative RT-PCR. Significantly measured expressions of the two genes *HES-1* and *HEY-1* were found in HNSCC as against normal tissues[194]. In general, experimental reports in favour of an oncogenic role for Notch are more, however, reports are available as shown, where down-regulation of Notch has been attributed to tumorigenesis, thus ascribing to it a tumour suppressor role[206].

Notch 1 has been shown to play a tumour suppressor role in neuroendocrine tumours in a study where activation of the same notch subtypes did correlate with down regulation of tumour markers specific for the tumour type[207]. In another study using lung cancer cell lines and mouse models, investigators were able to demonstrate opposing roles for Notch1 and Notch2, with Notch2 deletion resulting in increased carcinogenesis, suggesting a tumour suppressor role[204]. Notch 1 was shown to play a tumour suppressor role in skin cancer by another group of investigators, with a knockdown of Notch 1 leading to the development of skin cancer following epidermal hyperplasia[208]. Notch signalling was shown to induce cell cycle arrest in small cell lung cancer cells[209]. These, and the previously well highlighted examples suggest indeed that Notch could act on both sides of the divide, as tumour suppressors or "promoters".

Two proteins, ADAM17, and iRhom2, are believed to be involved in the biochemistry of signal transduction by notch, with ADAM17 proposed to be responsible for the S2 cleavage in the Notch signalling system[210]. This S2 cleavage which occurs at an extracellular site and between Ala (position 1710) and Val (position 1711) residues results in the production of NEXT (Notch Extracellular Truncation)[211,212]. This is despite the fact that ADAM10 is commonly credited

with being the principal sheddase of Notch[213]. ADAM17 and iRhom2 are discussed shortly.

1.10 Consequence of the development of cancer

A notable consequence of the development of cancer is believed to be alterations or deregulation of growth signalling pathways in cancer cells[214], with cancer cells now known to adopt a means by which they are able to set up an autocrine production of essential growth factors, maintained by an organised positive feedback mechanism independent of their environment[215]. The rhomboid proteins (particularly iRhom2), are an emerging, newly identified class of proteins thought to be involved with trafficking and regulation of other proteins, and now implicated in the pathogenesis of a number of cancer types including; oesophageal cancer[216], head and neck cancer[217] and ovarian cancer[218]. The iRhoms, a subset of the rhomboid family have been evidently linked with trafficking/activation of very important growth and signalling factors such as TACE (tumour necrosis factor α convertase)[219], EGFR[216], and TGFα (transforming growth factor α)[220]. Of uppermost interest in this study is the link between the iRhom2 protein and the sheddase TACE/ADAM17, which is already known to be important in the shedding activities and subsequent activation of notch, thought to be an oncogene[194].

1.11 ADAM17:

The ADAM family of proteins has been widely studied and members are thought to be key players in the activation/deactivation of proteins by a process known as shedding, an important regulatory process which remains poorly understood despite its importance[221]. The process of shedding involves proteolytic cleavage of proteins and a subsequent release of their ectodomain[222]. This important molecular mechanism could also result in a change in the functional properties of the affected proteins[223], and other metalloproteases such as members of the matrix metalloproteases (MMP) family have also been implicated[224] in this role. Sheddases are therefore generally able to regulate cell activities by directly shedding membrane receptors or indirectly, through soluble mediators arising from the shedding of other membrane bound inactive precursors or ligands[225]. Most of this shedding process is reported to take place on the cell surface and the surface expression of the protein has been reported to be tightly regulated[226]. Most of the protein in its immature, and therefore inactive form is stored intracellularly, with only a fraction of the eventual mature / activated form demonstrated to be available on the cell surface[227-229].

Numbered according to order of discovery, 22 members of the ADAM family of proteins have been identified in the human genome, with a dozen encoding active enzymes[230]. Structurally, they are made up of an N-terminal, a pro-domain, a metalloprotease domain, a disintegrin domain, a cysteine-rich domain, an EGF-like domain, a transmembrane domain and a cytoplasmic domain[231] (**Figure 1.15**). The N-terminal consists of a signal sequence which directs the enzyme into the secretory pathway in the first instance[232,233]. The pro-domain serves as the inhibitor of the

enzyme, maintaining it in an inactive form. This is therefore cleaved off in the trans-Golgi apparatus to render the enzyme active[234-236]. The metalloprotease domain, which contains a zinc ion chelating sequence, is also known as the catalytic domain and is responsible for the actual shedding or proteolytic activity of the enzyme[237].

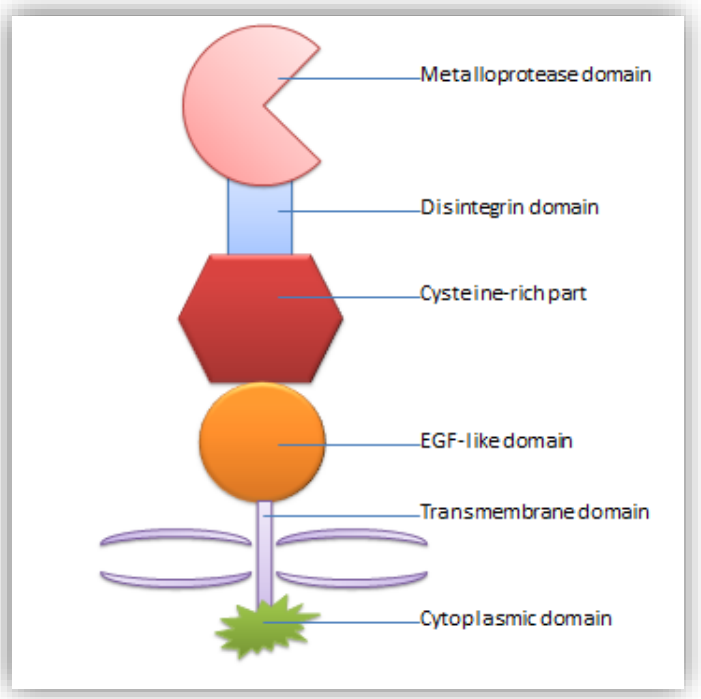

Figure 1.15 Structure of a typical ADAM protein showing its various components.

It comprises of a large extracellular part and a smaller intracellular part. The extracellular part comprises of the domains such as the Metalloprotease, Disintegrin and EGF-like domains, and the Cysteine-rich part. The intracellular part is made up of the Cytoplasmic domain.

The disintegrin domain contains a 14-amino acid sequence also referred to as the disintegrin loop, responsible for the interaction between the enzyme and integrins[236,238]. Example of such interactions is with $\alpha_5\beta_1$, with both molecules co-localising in HeLa cell membranes[239]. The cysteine-rich domain is associated with cell adhesion and fusion, and possibly interacting with ECM (extracellular matrix) and its vital constituent molecules, necessary for control of cellular activities, as well as cell to cell adhesion / interaction[230]. The cytoplasmic domain is shown to interact with proteins involved with intracellular activities such as trafficking, signalling and the maintenance of cell structure. Therefore, though primarily sheddases, the ADAMs also play other important cellular roles[236,240,241]. Functions of the EGF-like domain which is absent in ADAM17 and ADAM10 remain largely unknown[241].

Now thought to be expressed in a variety of cells/tissues and organs[242,243], their activities have also been shown to be quite diverse, ranging from sperm-interactions[244] to cell fate determination in nervous system[236]. Other functions include cell migration, muscle development and various aspects of immunity[236]. Here, focus will be on an important member of the family, ADAM17, also known as TACE (Tumour Necrosis Factor-α converting enzyme) whose activities are related to and somewhat similar to those of another member of the family, ADAM10.

1.11.1 Roles of ADAM17

Roles of ADAM17 have been investigated and documented to be indeed diverse. It is involved in the shedding of proteins, many of which are important signalling molecules such as TNFα, TGFα, EGF, HB-EGF, and VEGFR2, and adhesion molecules such as L-selectin, syndecans, CAMs (Cell Adhesion Molecules) and cadhesins[245-247]. Some of these molecules are largely involved in the regulation of cell proliferation, survival, migration and invasion, and thus may have implications in the development of cancer. These properties are often a result of the crosstalk between ADAM17 and epidermal growth factor receptor (EGFR)[231,248], and the Notch pathway[249], both of which have been linked with head and neck cancers. EGFR, a notable member of the ErbB family of receptors is widely known for its inherent ability to stimulate epithelial cells, causing them to proliferate[250], and is now thought to be an oncogene of head and neck cancers[251]. Using a 250k single nucleotide polymorphism array for analysis of subchromosomal alterations in OSCC, Jim Sheu et al were able to demonstrate the most frequent amplification in HNSCC to be that at 7p11.2 (in about a third of the cases), and this contains the EGFR. They also showed EGFR to be the most frequently amplified and highly expressed gene among the ErbB family, using both human and mouse oral cancers. The pattern of up-regulation of EGFR in oral cancer was further verified using immunofluorescence analysis and fluorescence in situ hybridization[251]. This data is in addition to data from several other studies which have implicated EGFR signalling in the pathogenesis of HNSCC[252-256], tagged it a possible prognostic / diagnostic / predictive biomarker[257-260], and shown the importance and effectiveness of targeting it (especially as a co-target) for therapy[261-264].

Several investigations have demonstrated up-regulation of ADAM17 in cancer, and the level of expression appears to correlate with tumour aggressiveness and rate of growth[246,265-270]. It is therefore gradually becoming a potential prognostic biomarker in a number of cancer types[271]. The exact role played by ADAM17 and its mechanism of operation has been shown to vary, functioning in both tumour formation and progression via proteolytic and / or adhesive properties[272]. Its metalloprotease and disintegrin domains are responsible for shedding and adhesion properties respectively[231].

In a study using OSCC (oral squamous cell carcinoma) cell lines and orthotopic murine tumour models, Simabuco et al were able to demonstrate that ADAM17 overexpression interferes in the biological processes associated with tumorigenesis of oral cancers[273]. In that study, ADAM17 overexpressing cells were subjected to in vitro functional studies, and injected into the immunodeficient mouse models with MS-based proteomics of resultant tumour tissues. Increases in tumour size, migration rate, invasion (measured via level of tissue collagenase activity), viability and adhesion were all demonstrated with increased expression of ADAM17[246]. Observations from mass spectrometry based proteomics in which several Erk regulatory proteins were found to be up-regulated in the tumour tissues from the mouse models give credence to suggestions ADAM17 also has a downstream molecular regulatory effect in addition to phenotypic role it plays. This will however require further research, considering the Erk pathway is downstream of EGFR as well, and thus may just be as a result of increased EGFR signalling via increased EGF or TGF release.

In another study on renal cancers by Franovic et al, ADAM17 was shown to be key in enabling tumour cells acquire survival capabilities such as migratory and invasive properties, as well as growth autonomy and tumour inflammation[274]. Using mouse models, In vivo formation of originally highly malignant renal carcinoma tumours was demonstrated to be sufficiently suppressed through silencing of ADAM17. Mechanism of operation of ADAM 17 was proposed to be via making available soluble TGF-α which in turn is an EGFR ligand[274].

In their study on breast cancer, using the breast cancer cell lines MCF-7 and MDA-MB-435, McGowan et al reported increased in vitro invasion and proliferation of cancer cells with overexpression of ADAM17, and a decrease in these processes with down regulation of ADAM17[275]. In this study, using ELISA and western blot techniques on a set of tumour samples, a relationship was shown to exist between ADAM17 levels and standard prognostic factors for breast cancer. High grade carcinomas had significantly higher concentrations of ADAM17 (p=0.017) compared to the lower concentrations in low grade carcinomas. Also, poor overall survival was associated with higher concentrations of the protein[275].

Suppression of ADAM17 function either through decreased expression of the protein or through inhibition of its protease activity, was shown to reverse the malignant phenotype using 3D culture models of human breast cancer cells by Kenny and Bissel. The inhibition resulted in reduced growth of the cell lines and reversal of their features similar to those of non-malignant cells. This reversal of morphological features was absent where there was overexpression of soluble pre-cleaved mutants

of AREG or TGF-a, but not the case with full length AREG or TGF-a. This thus suggests a role for ADAM17 in the early stages of malignant transformation[276].

Also, in a study by Zhang-Xuan et al to evaluate the clinical significance of ADAM17 in the progression and prognosis of gastric cancer, the protein was found to be up-regulated in tumour lesions compared to adjacent normal tissues[277], making it a potential biomarker.

The experiments and studies highlighted have overwhelmingly supported the proposition that ADAM17 plays an oncogenic role in the pathogenesis of a wide variety of cancer types. Highly likely to be involved in both formation and progress of tumours, primarily as a result of its key role in the proteolytic cleavage of an array of proteins.

As mentioned earlier, ADAM17 is also known as TACE (**T**NF-**α** **C**onverting **E**nzyme), due to its important role of releasing the active form of TNF-α from its precursor. The release of TNF-α, and the associated inflammation in turn has been directly implicated in liver, intestinal and ovarian cancer[278-282]. These studies as well as many more have been able to provide strong evidence that ADAM17 plays a role in the formation and progression of cancer.

1.12 ADAM17, iRhom2 and cancer

In an experiment by Colin Adrian et al, utilising in vitro differentiated macrophages from the bone marrow of mutant mice, loss of TNF shedding with the loss of iRhom2 was shown to be responsible for a complete abolition of activity of TACE[219]; the protein, iRhom2 already established to be predominantly expressed in macrophages. Inhibition of TACE in wild type cells (macrophages) by the matrix metalloproteinase inhibitor BB94 gave rise to a phenotype similar to iRhom2$^{-/-}$ macrophages, implying a shedding defect with the loss of iRhom2[219]. Overall, they investigated the regulation of ectodomain shedding by genetic and cellular approaches in both Drosophila and mammalian cells, generating null mutations in *RHBDF2* which encodes for the iRhom2 protein. Firstly, the resultant iRhom2$^{-/-}$ (Knock out) mice appeared normal. To mimic inflammation, where among other cytokines TNF was expected to be up-regulated, the iRhom2$^{-/-}$ mice were challenged with lipopolysaccharide (LPS) stimulation, but TNF induction was nevertheless observed to be almost completely abolished in the mutant mice. Equally, in vitro differentiated bone marrow derived macrophages (macrophages being the major sources of TNF) from iRhom2$^{-/-}$ mice failed to secrete TNF in response to LPS. With RNA levels of TNF unaffected, and protein levels actually elevated in iRhom2$^{-/-}$ mice, it was not a lack of expression, but rather a shedding defect.

These findings therefore implied that loss of iRhom2 as with the mutant mice does not interfere with the induction or with the intracellular trafficking of TNF, rather, it suggests a defect in the shedding process necessary for its eventual activation. Also, to show that the impact of iRhom2 on TACE has to do with trafficking to its site of

action, already established to be the membrane, TACE was found to be absent on the surface of iRhom2$^{-/-}$ macrophages in contrast to WT cells.

Equally, in the absence of iRhom2, TACE never became endo-H resistant, demonstrating the fact that it was never able to reach the Golgi, which further points at a defect in trafficking. They therefore concluded that, while trafficking from the ER is a limiting step for TACE maturation, iRhom2 is also an essential component of the biological mechanism that functions to release it to the Golgi apparatus. In the absence of iRhom2 therefore, TACE will not reach the Golgi apparatus to become activated. To examine these findings directly, mouse iRhom2 was expressed in human embryonic kidney (HEK) cells, with its effect on endogenous human TACE assayed. It was observed that overexpression of iRhom2 caused excess TACE to leave the ER which resulted in more furin-processed TACE, and thus an overall increase in TACE enzymatic activity[219]. The rhomboid-like proteins are hereby discussed, with emphasis on iRhom2.

1.13 The rhomboid-like proteins:

1.13.1 The rhomboid-like family of proteases.

It is the systematic exploration of Drosophila EGFR and the important roles it plays in a variety of intracellular events that led to the discovery of the rhomboid family of proteases[283], now known to be the main activators of the EGFR signalling pathway in this organism[284,285]. The activation process was initially thought to be only via direct

interaction with the main EGFR ligand, Spitz (a TGFα-like protein), but additional ligands and functions / mechanisms are now thought to be highly likely[286,287]. More recently, several studies have turned their focus on these other possible adjuvant roles for the rhomboid proteases apart from the traditional growth factor signalling role. Rhomboids are intramembrane serine proteases (IMP), with their active and catalytic residues buried in the lipid bilayer of the cell membrane (**Figure 1.16**). This localisation of their catalytic region enables them to easily cleave or activate / inactivate membrane proteins within their transmembrane helices (TMH)[288], 6 in prokaryotes and 7 in eukaryotes, in a two-step process, docking and scission. It is important to note however that, outside their catalytic/active site, other substrate-rhomboid interactive sites known as exocites have been described[289,290], and in substrate binding, the initial docking or interrogative step is shown to take place at the exocites.

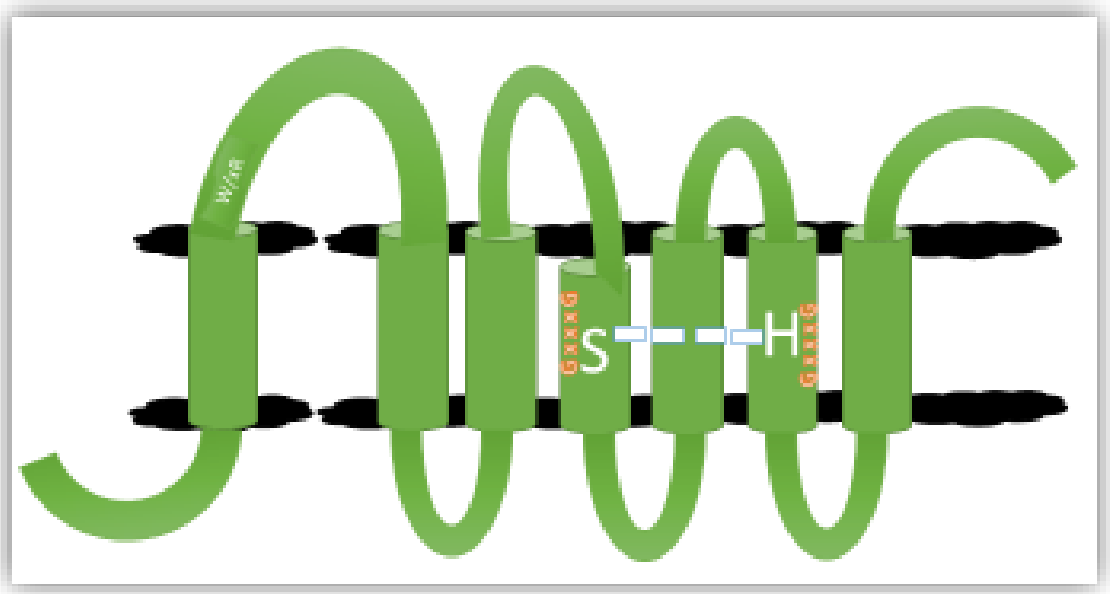

Figure 1.16 traditional rhomboid protein illustration:

Schematic illustration of a traditional rhomboid protein, showing the seven transmembrane helices (TMH) connected by loops. Both serine (S) and histidine (H) residues which make up the catalytic centres are shown on the fourth and sixth TMHs respectively, with their helix dimerization GxxxG sequences, important for structural stability. Between the first and second TMHs is the relatively long L1 loop which also houses the W/xR sequence.

Apart from the active core buried mostly in the membrane, most rhomboids in addition contain N- or C-terminal accessory regions outside the membranes. These accessory regions may function as extra exocites, an example is the extra ubiquitin

interacting motif (UIM) associated with RHBDL4 and found in its cytosolic region[291]. Peculiar with all rhomboid-like proteins is a rhomboid fold which consists of six or seven TMHs. In eukaryotes, a seventh TMH is added either at the C-terminal or the N-terminal, giving rise to a 1+6 TMH in the case of an addition to the N-terminal, or 6+1 TMH with the addition at the C-terminal[292]. These are referred to as the topology classes or topology classification. The active centres are the serine and histidine residues, located in the fourth and sixth TMH respectively (**Figure 1.16**), and this is known as the catalytic dyad, different from the classical catalytic triad of (D-S-H) common with other soluble serine proteases[292-294]. C-terminal addition is common with rhomboids in the secretory pathways, and N-terminal addition is localised to organelles such as mitochondria rhomboids. Five rhomboid-like proteases named RHBDL1-4 and PARL (Presenilins-associated-rhomboid-like), and a group of nine pseudoproteases make up the broad super family of rhomboid-like proteases.

The catalytic centres mentioned earlier are highly conserved in all rhomboids except the inactive pseudoproteases with the catalytic centres somewhat mutated[295-297]. Crucial for rhomboid structure stability is the helix dimerization GxxxG sequence. This is also highly conserved in rhomboids (active and inactive), possibly due to its importance in maintenance of rhomboid stability[292,298]. Another highly conserved motif in active rhomboids is the short W/xR sequence, situated in the rather long L1 loop between TMH1 and TMH2[288]. The long L1 loop is thought to be key in maintaining structural integrity in active rhomboids.

1.13.2 RHBDL1, 2, 3 & 4 and PARLs.

RHBDL1-4 are active in the secretory pathway, while PARLs, localised to the inner mitochondria membrane where they cleave mitochondria membrane bound proteins, and are thus involved with the overall homeostasis of the mitochondria[299]. A number of substrates/targets have been identified for PARL and RHBDL4, but not RHBDL1,2 & 3 which remain only poorly characterised[300,301]. RHBDL2 has been shown to effectively cleave proEGF for subsequent activation of EGFR signalling[302]. ADAM17 and ADAM10 are traditionally known for the above role[303], therefore, we hypothesise that the process by which RHBDL2 cleaves proEGFR might be an alternative pathway necessary in case of low supply of the primary sheddases. Increased activation of the EGFR pathway is known to be associated with cancer, thus implicating the rhomboid proteases in cancer formation or progression via the EGFR activation pathway. Indeed, overexpression of RHBDL2 has been shown to correlate with increased cell proliferation and resistance to anoikis in malignant epithelial cells[304]. Loss of cell proliferation in the form of reduced wound healing has also been demonstrated with loss of RHBDL2[305], and this may be due to a reduction in one of RHBDL2 substrates – soluble thrombomoduline[306]. Although the molecular mechanisms of carcinogenesis are under discussion and indeed remain unclear, RHBDL4 has been implicated in several cancer types, including colorectal cancer[307,308], liver cancer[309], and glioblastoma[310]. This Rhomboid protein is generally known to be localised to the ER[291] where it is primarily involved with ER-associated degradation (ERAD).

1.13.3 Rhomboid pseudoproteases.

These include iRhoms (iRhom1 and iRhom2) and Derlins, and have been shown to influence the fate of their targets by playing key roles in their intracellular trafficking or degradation[311]. It has been suggested that the inactive rhomboids have arisen from repeated duplications of the active rhomboids followed by diversification and loss of function[311,312]. iRhoms are the inactive homologues of rhomboids and are structurally different from their active counterparts in that they lack the traditional active residues, and contain both an extended cytoplasmic amino acid terminus as well as a Cys-rich luminal loop domain (iRhom homology domain) between TMH1 and TMH2[313] (**Figure. 1.17**). Two iRhoms, iRhom1 (RHBDF1) and iRhom2 (RHBDF2) have been identified in mammals.

1.13.4 iRhom2.

iRhom2 has been shown to be highly expressed in macrophages and involved with the intracellular trafficking of other proteins, ADAM17 a notable example[219]. iRhom2 has been directly linked with disease conditions such as tylosis and oesophageal cancer[216], and in epithelial ovarian cancers[218].

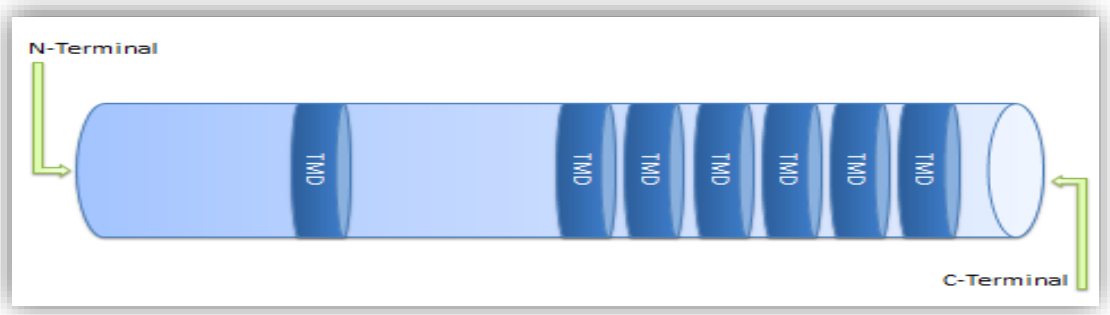

Figure 1.17 Structure of an iRhom showing its TMHs:

Structure of an iRhom showing its TMHs (TMD – Transmembrane domains) arranged between its two terminals, C and N.

Recently, experiments in mice have shown that iRhom2, a proteolytically inactive member of the rhomboid-like family of proteins, is required for the trafficking and maturation of TACE[219] (ADAM17). Produced in the Endoplasmic reticulum, TACE acquires its maturation in the Golgi apparatus where its pro-domain part is removed by a furin-type PRO-PROTEIN convertase or by autocatalytic removal, and iRhom2 is an important component of the mechanism responsible for its release into the Golgi apparatus[219,314,315].

Independent of the ADAM metalloproteinase pathway, EGF has also been shown to be directly regulated by iRhom1 and iRhom2 in COS-7 and HeLa cells, with both proteins being co-precipitated with FLAG-tagged EGF. This direct effect was shown to occur via ERAD (ER-associated degradation), with ADAM family proteins inhibited in

the experiment[316]. The cleavage of EGF (Myc-tagged) by iRhom2 with subsequent activation of the EGFR pathway has also been reported[317]. Taken together, this will suggest that, apart from EGFR activation via iRhom2 and ADAM17 partnership, the same activation of EGFR might occur with the aid of iRhom2, and in the absence of ADAM17, following a different pathway. ADAM17 therefore cannot be considered indispensable for EGFR signalling, considering the availability of an alternative pathway. EGFR signalling is known to be very vital in developmental processes, and has been repeatedly shown to be deregulated in several cancers including breast cancer[318], lung cancer[319], pancreatic cancer[320] and oral cancer[321]. Furthermore, Blaydon's report showed that keratinocytes, from individuals with a mutated form of iRhom2 were unaffected in terms of wound healing potential when starved of exogenous EGF[322]. This was proposed to be due to a sustained endogenous delivery of the growth factor in the presence of up-regulated iRhom2[216]. This missense mutation in the gene *RHBDF2,* which codes for iRhom2, is the underlying cause of tylosis, an autosomal dominant inherited condition which is associated with familial oesophageal cancer[216] and mutations in the same region of RHBDF2 has been reported in other familial oesophageal cancer[323].

1.14 Conclusion

Aside the original link with EGFR signalling which did herald its discovery (rhomboid-like family of proteases in general)[283], it is becoming quite evident that the rhomboid protein, iRhom2 is a major influence in the eventual shedding role of the very important sheddase, ADAM17[219]. Also, ADAM17 being an important sheddase in the

activation of the Notch signalling pathway[324] makes the cellular partnership between ADAM17 and iRhom2 entirely vital for signal transduction of Notch, and possibly a few others.

If up-regulation or indeed down-regulation of Notch is proven to be linked with carcinogenesis, there could be corresponding increase or decrease in expression levels or activities of ADAM17 and iRhom2 in such cancer cases.

Currently, there is sufficient data to suggest that ADAM17 is associated with HNSCC[273]. Data is equally gradually building up to indicate that iRhom2 is upregulated in HNSCC, and that iRhom2 is vital in the intracellular trafficking of ADAM17, while also favouring its activation / maturation[325]. However, little experimental work has been carried out in clinical tissues, nor has the expression of the protein been correlated with clinical outcome. ADAM17 and its close relative, ADAM10 have already been known to traditionally cleave Notch to enhance its activation[213]. There exist some controversy with regards to an entirely oncogenic role for Notch in HNSCC[197], but there is robust data in favour of an oncogenic role. Importantly, studies have shown reduced carcinogenesis with downregulation of ADAM17 and iRhom2, using mouse models[219]. Putting all of the available data together, it may be suggested that the oncogenic role of Notch is enabled by the shedding activity of ADAM17, which is further made possible by the intracellular trafficking afforded by the rhomboid protein, iRhom2 (**Figure 1.18**). This therefore leads to our working hypothesis that, **Increased expression of iRhom2 in oral cancer cells, through its interaction with ADAM17, contributes to tumorigenesis in this cancer type**.

Aim: To demonstrate that iRhom2 controls ADAM17 expression in HNSCC and that this contributes to tumour pathogenesis.

Objectives:

- To show that expression of iRhom2 and ADAM17 proteins is altered in HNSCC tissues and is associated with clinicopathological features suggestive of tumour aggression. Two cohorts of clinical tissues with clinical, pathological and outcome data will be assayed by western blot and immunohistochemistry.
- To demonstrate that iRhom2 controls the expression of the mature form of ADAM17 at the cell membrane in HNSCC. A series of in vitro experiments will investigate the consequence on ADAM17 expression, of up- and down-regulation of iRhom2.
- To investigate the effect of changes in iRhom2 and ADAM17 expression on HNSCC cell phenotype. Functional analysis of HNSCC cell lines will explore the effect of altered iRhom2 and ADAM17 expression on tumorigenic characteristics such as proliferation and migration.

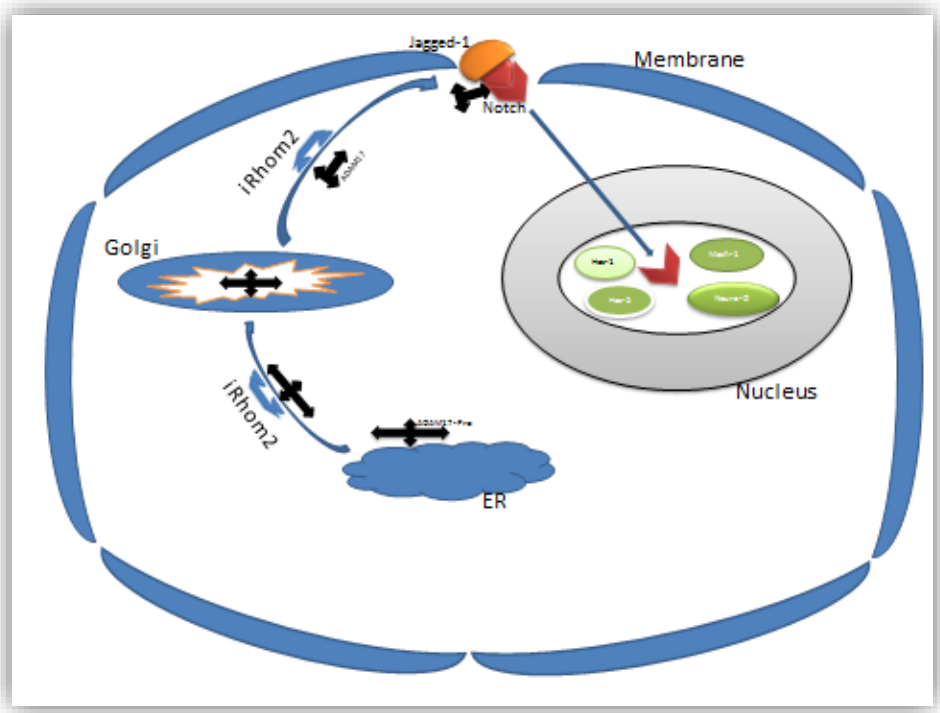

Figure 1.18 Diagram illustrating the binding of a notch ligand to initiate a proteolytic cascade. The signalling cascade is shown to involve iRhom2, ADAM17 (TACE) and Notch. Synthesised ADAM17 is trafficked by iRhom2 from point of synthesis, ER (Endoplasmic Reticulum), to the Golgi for maturation, and eventually to the cell membrane where it is involved with Notch activation. Notch activation is seen to lead to the release of an intracellular fragment – red arrowhead, NICD (Notch intracellular domain), which translocates into the nucleus for downstream target activities.

CHAPTER 2:

MATERIALS AND METHODS

2 Chapter 2: Materials and methods

2.1 Introduction

This study was split into two main parts. Investigations with the use of clinical specimens in form of tissue samples (tumour and paired normal), and scoring of TMAs (tissue microarray) was accommodated in the first part of the experiment, while the second involved the use of cell lines and determination of cellular functional changes following transfection.

2.2 TMA (tissue microarray) scoring and analysis.

A cohort of oral cancer and adjacent normal tissue from 122 patients had been used previously to construct two TMAs containing triplicate cores[326]. These TMAs were stained immunohistochemically using standard methods on a DAKO autostainer (Dako, Ely, UK), using its proprietary kit, the Dako EnvisionTM FLEX/HRP Detection system. In brief, a high temperature antigen retrieval method was employed using the DAKO PT-Link system (Dako, Ely, UK) on 4µm sections of the TMAs and final dilutions of 1:300 anti-iRhom2 antibody (Prestige HPA018080, Sigma-Aldrich, Poole)

and 1:150 anti-ADAM17 antibody (ab2051, Abcam, Cambridge). Primary antibody was omitted from negative controls. IHC stained TMA blocks were analysed (consensus reporting by two observers), using a semi-quantitative method for scoring intensity of immunoreactivity, and graded: + (weak staining), ++ (moderate staining) and +++ (strong staining). Tumour, CAFs (cancer associated fibroblasts) and inflammatory cells were all scored according to their levels of staining. For statistical analysis and correlation with available clinicopathological data, only oral cancer cases were included, with oropharyngeal cases excluded, giving a total of 100 oral cancers.

2.3 Tissue collection:

Fresh, frozen tumour specimens were obtained from a total of 99 HNSCC patients, whose primary treatment was surgery, together with paired normal tissue taken from the tumour margins of 38 patients. Written consent was obtained from all patients and in accordance with the laws governing tissue collection, storage and use in the UK (REC numbers: EC.47.01 & 10/H1002/53). Tissues were snap frozen in liquid nitrogen before being transferred to -80®C for longer storage.

2.3.1 Analysis of tissue composition:

Tissue from each frozen specimen was embedded in OCT (CellPath Limited). Two 5µm sections were taken for H & E staining and for subsequent histopathological assessment of degree of tumour content by a consultant oral pathologist. Staining was carried out at room temperature thus:

- Paraffin wax was removed by incubating in xylene for 5 minutes (step repeated with fresh xylene)
- Incubate in absolute alcohol for 5 minutes, followed by
- 70% alcohol for 5 minutes and
- 50% alcohol for 5 minutes
- Incubated in haematoxylin (Thermo Scientific) solution for 5 minutes
- Washed under tap water for 2 minutes
- Dipped in acid alcohol 3 times
- Rinsed under running water
- Incubated in eosin (Thermo Scientific) solution for 15 seconds
- Washed in tap water
- Dehydrated thus:
- Incubated in 70% ethanol for 5 minutes (repeated using fresh ethanol), followed by
- 90% alcohol twice and then absolute ethanol twice
- Incubated in xylene for 5 minutes and then
- Mounted in DPX (Fluka) solution and coverslipped.

Tumour samples with less than 50% tumour cells in either of the 5µm sections were excluded from the cohort. Normal samples with more than 5% tumour cell content on either of 5µm sections were also excluded from the study. Also excluded, tumour or normal tissues, were those predominantly fibrous, bony or fatty tissues (**Appendix 1**).

2.3.2 Protein extraction and quantification.

5mm³ pieces of tissues were excised from each sample, using disposable scalpels and targeting areas with an increased number of tumour cells or lack of tumour as appropriate. Harvested tissues were resuspended in 300µl of protein extraction buffer (50 mM Tris–HCl, pH 6.8, 1% SDS, 1% EDTA, 0.25% glycerol, 0.25% β-mercaptoethanol) with protease inhibitor (Roche Diagnostics), and total protein was extracted with the use of a sonicator (Sonics and materials INC, 40-50 amplitude for 30 seconds). Extracted protein was stored in aliquots at -80°C until use. Total protein was quantified using the Bradford assay.

2.4 Western blot analysis.

2.4.1 Electrophoresis and electroblotting:

40µl of protein preparation containing between 20µg and 50µg of total protein were mixed with a half volume of sample loading buffer and boiled for 5mins prior to being loaded unto 10% SDS/PAGE gels (**Appendix 2**). Electrophoresis was carried out at 60mV / 34mA for 16 hours. TE3-IR2+, an oesophageal cancer cell line constitutively expressing iRhom2, was used as a positive control.

Following electrophoresis, gels were transferred to 0.45µmm PVDF membranes (GE Healthcare Life Sciences) and electroblotting carried out for 4 hours at 80mV / 350mA.

2.4.2 Antigen detection:

Prior to probing with primary antibodies, blocking of membranes was carried out for one hour at room temperature using blocking solution (PBS + Licor Blocking Buffer, ratio 1:1), and the incubated membranes placed on a rocker.

The following primary antibodies were incubated at 4^{o}C overnight; rabbit-anti-RHBDF2 (1:500: Sigma Aldrich HPA018080-10CUL), goat-anti-ADAM17 (C-terminal, 1:350: Santa Cruz, sc-6416 and N-terminal, 1:350: Santa Cruz, sc-13973) and mouse-anti-β-Actin (1:1000: Santa Cruz, sc-47778). Membranes were washed in PBS (with 2% Tween20, Sigma Aldrich), for 5 minutes x 3 rounds, prior to incubation in secondary antibody. Fluorescent secondary antibodies; IRDye@800 (goat anti-mouse, 926-32210, and goat anti-rabbit, 926-32211, both Licor) and Alexa Flour@680 rabbit anti-goat, A21088, were used at a concentration of 1:10,000 for 2 hours incubation at room temperature. 2% Tween20 (Sigma Aldrich) was added to the blocking solution and used to dilute the primary and secondary antibodies. Components of running buffer and transfer buffer are shown in **Appendix 3**.

2.4.3 Analysis of results

At the end of both primary and secondary antibody incubation, membranes were rinsed in 1 x PBS solution, three times for 5 minutes in each case. The membranes were scanned and visualisation of fluorescent secondary antibody localisation was undertaken on a Licor Odyssey scanner (3.0 Model).

Densitometry was used to normalise and semi-quantitate the levels of protein expression in comparison with the actin control. Briefly, the intensity of the β-Actin band in each lane was measured and a ratio of control intensity divided by sample intensity was created. This ratio was used to normalise the iRhom2 and ADAM17 protein expression levels thus:

2.5 Normalisation

Densitometry was used to normalise and semi-quantitate the levels of protein expression in comparison with the actin control. Briefly, the intensity of the β-Actin band in each lane was measured and compared to that of the positive control, TE3. The ratio obtained was used to derive a correction factor (how many times more the B-Actin of the control band is) (**Figure 2.1**). Multiplying the correction factor by the densitometry of the target band gives a value that indicates the level of expression (status) (**Figure 2.1**). Status of High, Moderate and No expression were ascribed

based on the cut-off (a choice of 75th percentile / upper quartile – shown in section) from the cumulative frequency curve of the data (**Figure 2.1 & Figure 3.5**).

Sample	A	B	C	D	E	Positive Control
β-Actin Values	20	10	40	160	8	80
Correction Factor (a)	X 4	X 8	X 2	X 0.5	X 10	X 1
iRhom2 Value (b)	3.5	0.5	2.5	10	0	50
(a) X (b) (% in relatn to Control)	14 28	4 8	5 10	5 10	0 0	50 100
Status						

Figure 2.1 Western blot normalisation:

Illustration of how the β-Actin values of individual samples were used to obtain a correction factor, in reference to a standard, in this case the positive control (TE3-wild type, an oesophageal cancer cell line). Eventual densitometry score for each sample, a product of correction factor and iRhom2 value (a X b), and expressed in percentage with reference to the control value, was graded. Grading/Status expressed as colour codes to represent over-expression (dark orange), normal expression (light orange), and non-expressing (white), were based on cut-off values of 11 and 20.

2.6 Peptide blocking / competition studies

This was done to determine iRhom2 and ADAM17 (mature and immature) bands of interest and differentiate such from non-specific bands. The cancer cell line, PE/CA-PJ15 was used, due to its high level of baseline expressions of both iRhom2 and ADAM17 proteins. The western blot experiment described in section 2.4 was followed, with two identical gels, containing the same protein lane arrangement. For antigen detection described in section 2.4.2, incubation of one of the identical membranes followed the exact protocol, with the second membrane having its primary antibody incubated in its complementary blocking peptide for four hours at room temperature prior to membrane incubation. Anti-iRhom2 antibody (Abcam, ab116139) already constituted at 1:500 in its antibody solution, and its complementary blocking peptide (Abcam, 216174) were mixed at 50:1 ratio by volume. Anti-ADAM17 antibody (Santa Cruz, sc-6416) already constituted at 1:350 in its antibody solution, and its complementary blocking peptide (Santa Cruz, sc-6416P) were mixed at 50:1. Steps described in section 2.4.3 were thereafter followed.

2.7 Cell line analysis

2.7.1 Short Tandem Repeats (STR):

DNA extracted from NOK, Liv37K and PE/CA-PJ15 cell pellets and diluted to a concentrations of 5ng/µl. STR was undertaken using GenePrint10® (Promega), and analysed to confirm the identity of the cell lines.

2.7.2 Mycoplasma testing

A similar aliquot of DNA in section 2.7.1 was allocated for mycoplasma testing. Mycoplasma testing was carried out using E-Myco PCR detection kit (CHEMBIO Ltd – 25235).

2.7.3 Tissue Culture:

The cell lines, PE/CA-PJ15, Liv37K and NOK (normal oral keratinocyte), were resurrected from liquid nitrogen store and cultured. **Table 2.1** summarises origin of the cell lines and culture medium used. Incubation was at 37®C and 5.0% Carbon dioxide. Monolayer of cells at approximately 85% confluence were harvested by trypsinisation to recover cells and reseeded into new flasks according to desired confluence.

Table 2.1 Summary of established cell lines used for cell line analysis. Liv37K and PE/CA-PJ15 are oral cancer cell lines while NOK (normal oral keratinocyte is a non-cancer cell line used as a control cell line in this study. The Liv37k cell line has been tested at > 40 passages and shown to grow indefinitely. The table includes sources of the cell lines, culture medium and the starting passage numbers The cell line Liv37K has the capacity to grow ell line Liv37K has the capacity to grow indefinitely (tested at >40 passages

Cell Line	Origin	Culture Medium
LIV37K Passage 8	Floor of mouth tissue of a 57 year old male patient with OSSC	Keratinocyte serum free medium, supplemented with 1% L-Glutamine and 10% foetal bovine serum (FBS)
NOK Passage 6	Human oral epithelium and immortalised	Keratinocyte serum free medium, supplemented with 1% L-Glutamine and 10% foetal bovine serum (FBS)
PE/CA-P515 Passage 5	Tongue tissue of a 45 year old male patient with OSSC	Dulbecco Modified Eagles Medium (DMEM)

2.7.4 Harvest of cell pellets:

Cell pellets for onward protein extraction and western blot analysis were prepared by scraping cell monolayers into 10ml PBS, followed by centrifugation at 1330g for 5 minutes to recover cell pellets. These were stored at -80®C prior to protein

extraction. Protein extraction, quantification and western blotting were carried out using the same protocol as for tissue.

2.8 Proliferation assays:

Crystal violet assay and MTT (**M**ethyl**T**hiazol**T**etrazolin) assay were used to estimate cell proliferation and to establish a G418 kill / survival curve for the various cell lines prior to transfection for over-expression experiments.

2.8.1 Seeding of cells and G418 selection:

Cells were seeded in a 12 well plate to achieve approximately 50% confluence after 24 hours (5K for PE/CA-PJ15, 10K per well for NOK and Liv37K). After 24 hours, G418 solution (Calbiochem, Cat: 345810-1GM) was added to give serial concentrations of 0, 200, 400, 800 and 1000µg/ml in culture medium for NOK and Liv37K, and, 0, 500, 1000, 1500 and 2000µg/ml for PE/CA-PJ15. All assays were undertaken in triplicate. G418 solution was renewed 24 hourly, and cell survival was estimated every 24 hours for 5 days as follows:

2.8.2 Staining with crystal violet solution:

Cells were washed briefly with PBS and air-dried for 5 minutes. Then stained with crystal violet (Sigma) solution (0.05% in PBS), incubating at room temperature for 30 minutes. Crystal violet solution was withdrawn and cells washed under running tap water a few minutes, and left to air-dry overnight at room temperature. The following day, 200µl of 10% acetic acid was added to solubilise the crystal violet and 100µl transferred into 96 well plates. Absorbance was read at 570nm using a Spectramax-Plus284 absorbance microplate reader (Molecular Devices), against a 10% acetic acid blank.

2.8.3 Staining with MTT solution

Cells were washed briefly with PBS. Then incubated in fresh culture medium containing 0.5mg/ml MTT solution at 37°C for 2 hours. MTT solution was withdrawn and the cells fixed with 500µl of chilled 3.7% formalin (pH 7.4) for exactly 12 minutes at room temperature. Formalin was withdrawn, and MTT solubilised with 400µl of DMSO. 100µl of the resultant solution was transferred to fresh plates (96 well) and absorbance read at 570nm using a microplate reader against a DMSO blank.

2.8.4 Survival / Kill curve:

Absorbance values were plotted against time (in days), and the minimum concentration of G418 sufficient to complete cell death (shown graphically by a decline in surviving cell population) was identified for each cell line.

2.9 Over-expression of iRhom2:

2.9.1 Plasmid:

Isoform 2 of the RHBDF2 gene was previously synthesised and cloned (Epoch Life Sciences Inc., Fort Bend County, Texas) into the multiple cloning site of-5.3kb pIRESneo vector (Cat No. 6060-1), (**Figure 2.2**). It contains a P (CMVIE) promoter region to allow expression in mammalian cells at 232-820, with its multiple cloning site occupying 909-974. Its synthetic intron (IVS) which helps with stability of mRNA is at 974-1269, while the internal ribosomal entry site (IRES) of the encephalomyocarditis virus (ECMV) occupies 1295-1880 to permit translation of two open reading frames from one mRNA. Next is the neomycin phosphotransferase gene (NPT II) at 1906-2709 to aid in the selection of transfected cells, a fragment containing the bovine growth hormone poly A signal at 2710-2998, and the ampicillin resistance gene at 5117-4257[327].

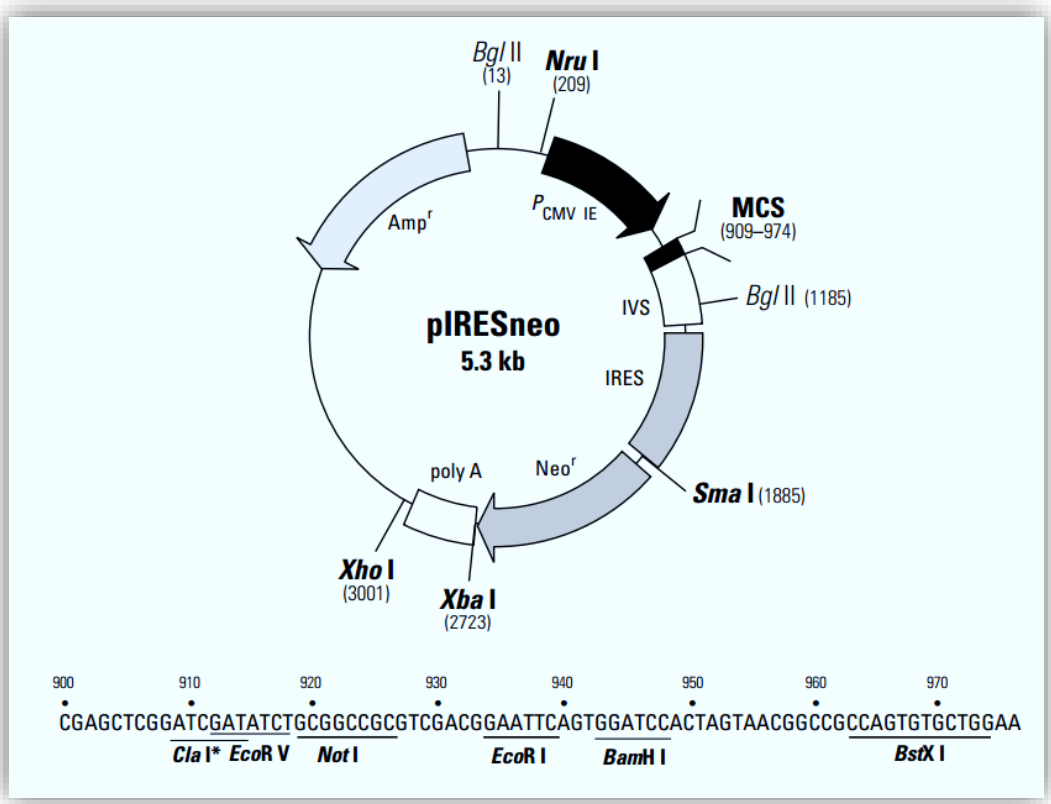

Figure 2.2 Restriction map of the pIRESneo vector:

Restriction map of the pIRESneo vector. Isoform 2 of RHBDF2 was cloned into the EcoR1 site of the multiple cloning site[327].

2.9.2 DNA extraction:

Bacterial stocks were streaked onto selective media (50mg/ml Ampicillin) and individual colonies used to inoculate 5ml LB broth which were cultured for 7 hours at 37^{o}C with shaking.

200µl of the resultant bacteria culture was further incubated overnight in 200ml of LB broth with same ampicillin concentration. Both rounds of incubation were undertaken at 225rpm / 37^{O}C.

Plasmid DNA was extracted using a QIAGEN plasmid midi kit, following the manufacturer`s protocol. Extracted DNA was quantified using a Nanodrop100 machine (Thermo Scientific) and stored at -20®C prior to use.

Gel electrophoresis was carried out on 1% agarose gels with 10µl of Cyto 60 added to the gels for direct visualisation using a Licor Odyssey scanner. A restriction digest was previously carried out to confirm DNA was as expected.

2.9.3 Production of over-expressing clones

Cells were trypsinised, centrifuged at 1330g speed to completely eliminate trypsin, reconstituted in culture medium and seeded into T25 flasks thus:

- NOK-50K cells per flask
- Liv37K-50K cells per flask
- PE/CA-P515-30K cells per flask

In order to achieve approximately 80% confluence after 24 hours. For each flask, a DNA solution was prepared containing:

- 340µl of OptiMem (Gibco)
- 30µl of plasmid DNA (at 200mg/ml)

- 6µl of Lipofectamin Plus (Invitrogen)

and a Lipofectamin LX solution containing

- 300µl of OptiMem (Gibco)
- 24µl of Lipofectamin LX (Invitrogen)

These solutions were mixed and allowed to incubate for 5 minutes at room temperature before adding 600ml of the combined solution to the culture medium in each T25 flask

The cells were incubated and the medium was left unchanged for:

- 72 hours in NOK flasks
- 72 hours in Liv37K-flasks
- 48 hours in PE/CA-PJ15 flasks

The incubation time for PE/CA/PJ15 was less as they were less tolerant to the transfection reagent. Thereafter, transfection medium was withdrawn, and replaced with fresh culture medium that was changed daily to allow surviving cells to recover from the trauma of transfection

After 48 hours, surviving cells were trypsinised to separate them from dead cells and reseeded unto new T75 flasks with 10ml of fresh culture medium introduced.

The cells were allowed to grow to about 60% confluence and then G418 added for clone selection thus:

- NOK-100mg/ml of G418
- Liv37K-100mg/ml of G418

- PE/CA-PJ15-1200mg/ml of G418

G418 solution was renewed every 48 hours for 10 days and then selection stopped to allow surviving cells recover. Cells were passaged after a further 2 days into 3 new T75 flasks, to create cells from which pellets would be derived for expression analysis by qPCR and western blotting.

2.9.4 Selection of single colonies:

Transfected cells were seeded at low density in 24 well plates with the aim of achieving small singular discrete colonies in some of the wells. Culture medium was renewed after 24 hours and wells checked for those with single colonies. Such wells were marked, G418 selection carried out and cells were allowed to grow to about 80% confluence before trypsinisation and seeding into T25 flasks to grow on. Resultant clones were checked for iRhom2 overexpression through western blotting and one clone selected for proliferation / migration assays.

2.10 shRNA knock-down:

Mission®shRNA plasmid bacterial glycerol stock (SIGMA – 09051604MN) and Mission®pLKO.1-puro BZM shRNA control plasmid DNA (SIGMA-SHC008-04021321MN), plus Mission®pLKO.1-puro Empty Vector Control Plasmid DNA (SIGMA-SHC001-04101509MN) were used. Bacteria culture, plasmid DNA extraction,

transfection of cell lines and culture followed the same protocol as for production of over-expression clones described in section **2.6**

In lieu of G418, 2µl of puromycin (5mg/ml) in 10ml of culture medium was used. Treatment was for 48 hours, after which it was withdrawn and replaced with fresh culture medium. Medium change was carried out every 24 hours for 3 days, and the level of knockdown was evaluated using western blotting. Individual clones were isolated following the same protocol outlined in section **2.8**, with the use of puromycin in place of G418. Western blotting was used to evaluate the resultant clones and one was picked for proliferation and migration studies. For the control knockdowns using control plasmid DNA, individual clones were not selected, rather, the resultant population was utilised for western blot verification

2.10.1 RNA expression analysis:

RNA was extracted from NOK, LIV37K and PE/CA-PJ15 cell pellets using QIAGEN RNeasy purification mini kit (Cat No. 74104), following the manufacturer`s protocol. RNA concentration was determined using the nanodrop machine (model and manufacturer).

500ng of total RNA was reverse transcribed in a volume of 20µl using High capacity cDNA reverse transcription kit (Applied Biosystems – 4368814) to obtain cDNA.

8µl of cDNA was amplified using FAM labelled RHBDF2 Taqman primer/probe set (Assay ID - Hs 01079432 – Applied Biosystems), assayed on an Applied Biosystems 7500 Fast Real- time PCR system. Data was subsequently analysed on the 7500

Software v2.3 (Applied Biosystems). Final values for RNA expression were in relative quantification values (RQ), calculated thus: $R=2^{(-(\Delta Ct_{sample}-\Delta Ct_{cal}))}$, with the mRNA expression of the wild type of each cell line used as a calibrator for each set. Assays were in duplicates, with the mean value used for analysis. B-Actin was used as the endogenous control.

2.11 Proliferation assay:

Wild-type, shRNA knock-down and overexpressing variants of NOK, Liv37K and PE/CA-PJ15 cell lines were all trypsinised and seeded in individual 6 well plates and in triplicates. 10k per well for NOK and Liv37K, while PE/CA-PJ15 were seeded at 5k cells per well. Culture medium was changed every 24 hours for 5 days and cells were harvested daily for crystal violet analysis as described in section **2.4**.

2.12 Scratch assay:

Cells were trypsinised and seeded into removable chambers (Ibidi). Experiments were done in triplicates with the removable chambers placed at the centre of wells of 6 well plates. All the NOK and Liv37K cell line variants were seeded at 25k cells per chamber, with PE/CA-PJ15 cells seeded at 10k cells per chamber. Medium was augmented after 24 hours and cells allowed to replicate a further 24 hours to

confluence of about 85%. The culture medium was withdrawn, followed by three rounds of washes with PBS, and the removable inserts were gently withdrawn before introduction of fresh culture medium. The plates were transferred to a 5% Carbon dioxide / 37^{o}C chamber attached to a microscope (Micro-manager 4 – Nitcon Eclipse TE300) for image capture at ten minutes intervals for 30 hours. Gap closure images were analysed on Image J and T-Scratch.

2.13 Statistical analysis:

Protein expression data from tumour and normal tissue was analysed using box plot analysis and paired sample T test (SPSS statistics, version 24). An Ogive (Cumulative frequency curve) was used to establish categorical groupings. Chi square and the Kaplan Meier survival test were used to analyse associations between tissue expression and clinicopathological features including, survival, recurrence, tumour stage, extracapsular spread, and tumour differentiation.

CHAPTER 3:

BASELINE EXPRESSION OF iRhom2 AND ADAM17 IN ORAL CANCER AND ORAL NON-CANCEROUS TISSUE

3 Baseline expression of iRhom2 and ADAM17 in oral cancer and oral non-cancerous tissues

3.1 Introduction and aims

It is being proposed that the rhomboid protein, iRhom2 may be implicated in a number of cancer types, including head and neck cancer. Its discovery was in connection with its role in EGFR activation and signalling[283], with EGFR signalling already widely implicated in cancer pathogenesis[171]. More recently, newer roles such as the trafficking and shedding of the metalloprotease, ADAM17 have been identified. Experiments have implicated deregulation of both proteins, iRhom2 and ADAM17 in carcinogenesis[219,325]. There is the current hypothesis that, increased expression of iRhom2 in cancer cells may be involved in the pathogenesis of cancer, and possibly promoting metastasis. The aim of this chapter is to estimate and compare the levels of expression of the two proteins, iRhom2 and ADAM17; in head and neck cancer tissues and adjacent normal or non-cancerous tissues, using western blotting and immunohistochemical of previously assembled TMAs containing archival tissue from 112 HNSCC patients[326]. Expression of these proteins in tumour and normal tissues was also correlated with a number of clinicopathological features that reflect tumour stage and aggression.

3.2 Results

3.2.1 Assessment of tumour content in tissues:

The cohort of 137 tissue samples (99 tumour and 38 paired normal tissues) selected for this experiment, were independently validated (by a pathologist) for tumour and normal tissue content by H & E staining of two 5µm sections from each sample to verify the tumour load of each sample (**Figure 3.1**). A cut-off of 60% tumour load was used for tumour samples to be included in this study, while > 5% of tumour cell population was unacceptable for normal samples. Using this criteria, a total of 68 tumours and 27 normal tissue specimens were used in this study (**Appendix 3**).

3.2.2 Blocking peptide / Competition studies

Initial western blot analysis probing for both iRhom2 and ADAM17 displayed multiple bands at the proposed molecular weights suggested by suppliers of the primary antibodies used, suspecting a lack of specificity. It was therefore necessary to identify bands that represented the iRhom2 and ADAM17 proteins.

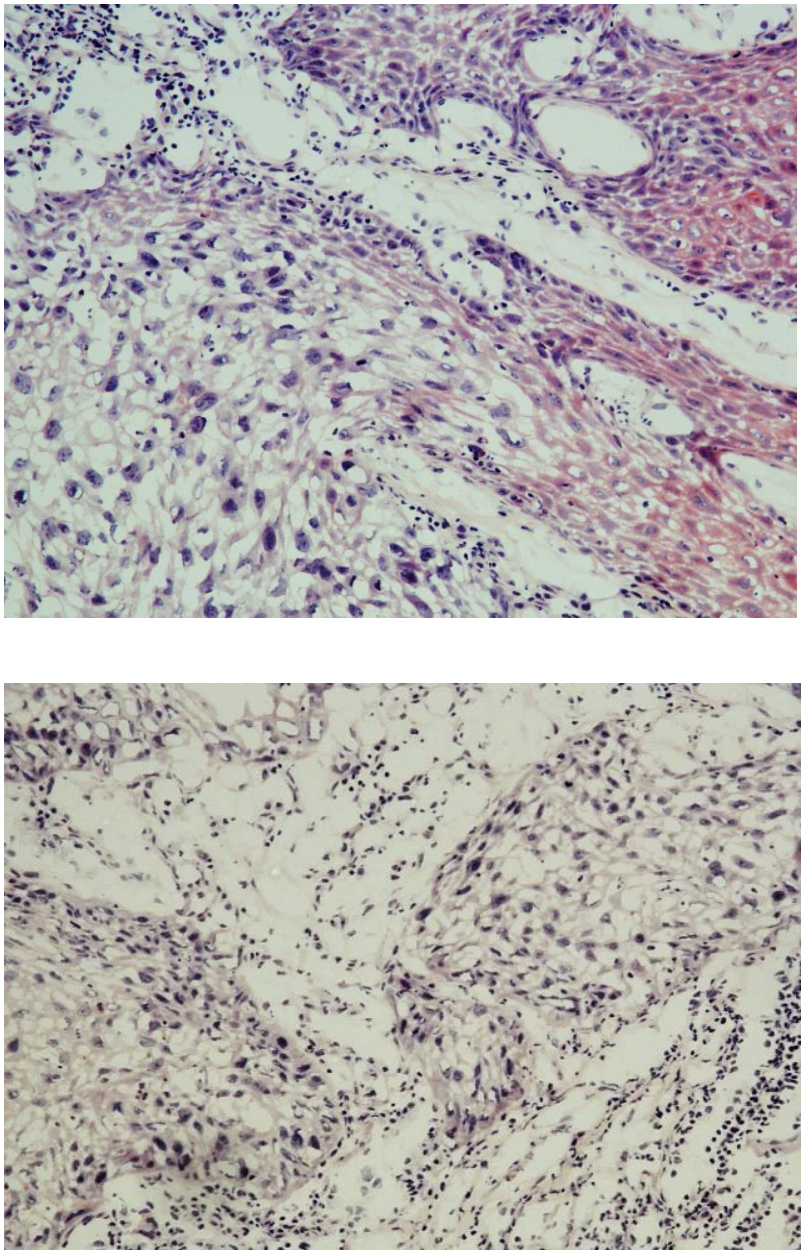

Figure 3.1 : H & E (Haematoxylin and Eosin) staining of tissue samples:

Two examples of H & E stained slides at X 4 magnification, to determine approximate amount of tumour cell content. Top panel shows sample with approximately 75% tumour content. There is also the presence of inflammatory cells. Bottom panel shows a slide with about 50% tumour cell content, with the other portion taken over by inflammatory cells and cancer associated fibroblasts.

Blocking peptide/competition studies were employed for this identification / confirmation step. iRhom2 blocking peptide experiments removed 2 proteins of molecular weights between 76KDa and 102KDa, and reduced the intensity of a smaller protein band between 32KDa and 46KDa (**Figure 3.2**). The two uppermost bands (close to 100KDa), are the isoforms of iRhom2, and the third band of interest about midway between 32KDa and 46KDa might be a cleaved product. Additional bands between 46KDa and 58KDa become more prominent on blocking iRhom2 antibody (**Figure 3.2**), indicating the presence of non-specific bands. In ADAM17 peptide blocking, three protein bands between 95KDa and 130KDa were removed when the C-terminal ADAM17 antibody was blocked (**Figure 3.3**), and prominent bands at approximately 70KDa disappearing significantly. Therefore, bands at approximately 100KDa were taken as indicative of iRhom2, those between 95KDa and 130KDa for the immature form of ADAM17, and at about 70KDa for the mature form of ADAM17.

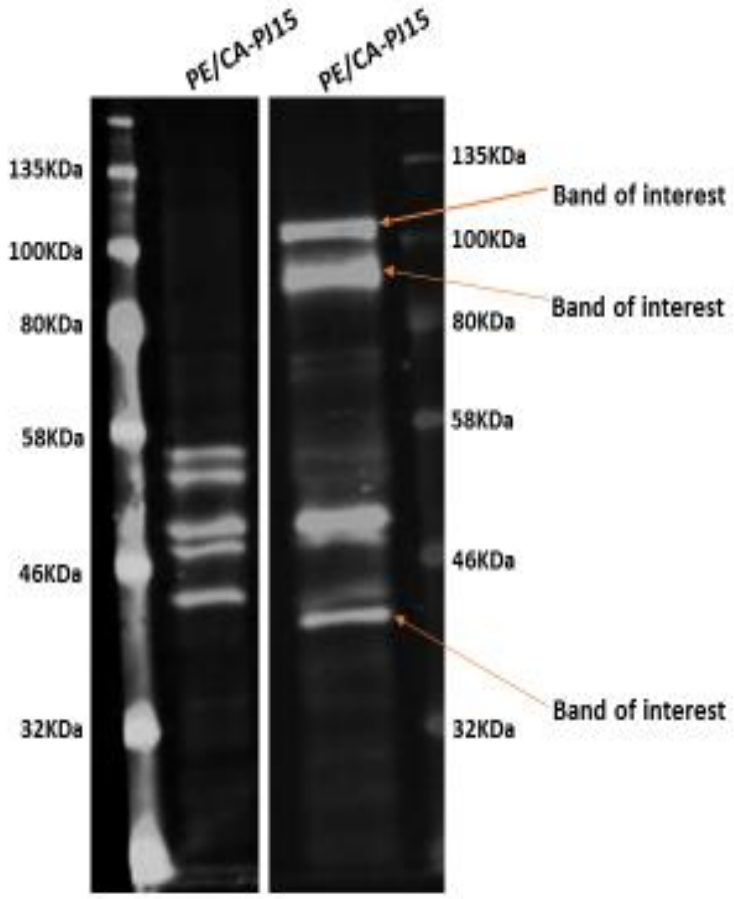

Figure 3.2 Blocking peptide / competition studies for iRhom2

Blocking peptide / Competition studies for iRhom2 using the cell line PE/CA-PJ15. Left panel**: -** iRhom2 expression in the presence of iRhom2 blocking peptide. Right panel: - iRhom2 expression pattern in the absence of iRhom2 blocking peptide. Three bands of interest are removed by the blocking peptide. The three bands are visible on the right, but not the left membrane (panel). The three bands include two, just above and just below the 100 KDa mark, and a prominent band between the 46KDa and 32KDa marks. The top two are two isoforms (1 and 2) of iRhom2 protein, while the lightest is thought to be an important degradation product of iRhom2.

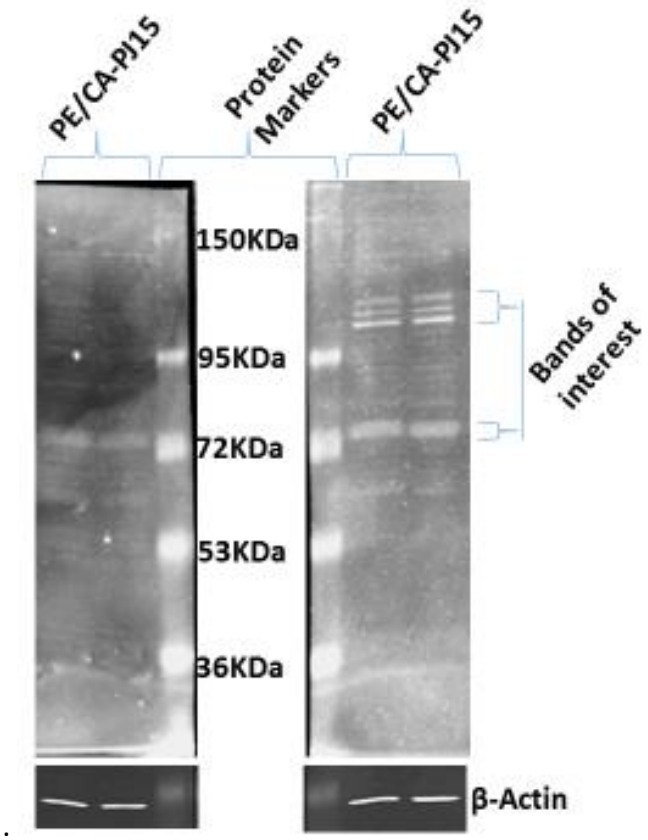

Figure 3.3 Blocking peptide / competition studies for ADAM17

Blocking peptide / Competition studies for ADAM17 using the cell line PE/CA-PJ15. Left panel**: -** ADAM17 expression in the presence of ADAM17 blocking peptide. Right panel: - ADAM17 expression pattern in the absence of ADAM17 blocking peptide. Four bands of interest have their intensities considerably reduced following the addition of the ADAM17 blocking peptide. Three of these bands are visible between the 150KDa and 95KDa marks, with the fourth just above the 72KDa mark. The three higher bands represent the immature forms of ADAM17, while the lowest, just above the 72KDa mark represents the mature form of the protein The C-terminal ADAM17 antibody (Santa Cruz, sc-6416) was utilised here to target both the immature and mature forms of the protein.

3.2.3 iRhom2 expression in tumour and adjacent normal tissues:

Variable levels of iRhom2 expression were demonstrated in the tissue samples (**Figure 3.4**). Densitometry was used for quantitative assessment of the levels of expression and the data correlated for loading, then normalised against the over-expressing TE3 positive control that was run on every gel (see **section 2.5** of materials and methods, and **Figure 2.1**). A status of High, Moderate and "no expression" were ascribed based on a cut-off of 20 arbitrary units determined from the 75th percentile / upper quartile of the cumulative frequency curve of the data (**Figure 3.5** and **Figure 3.6**).

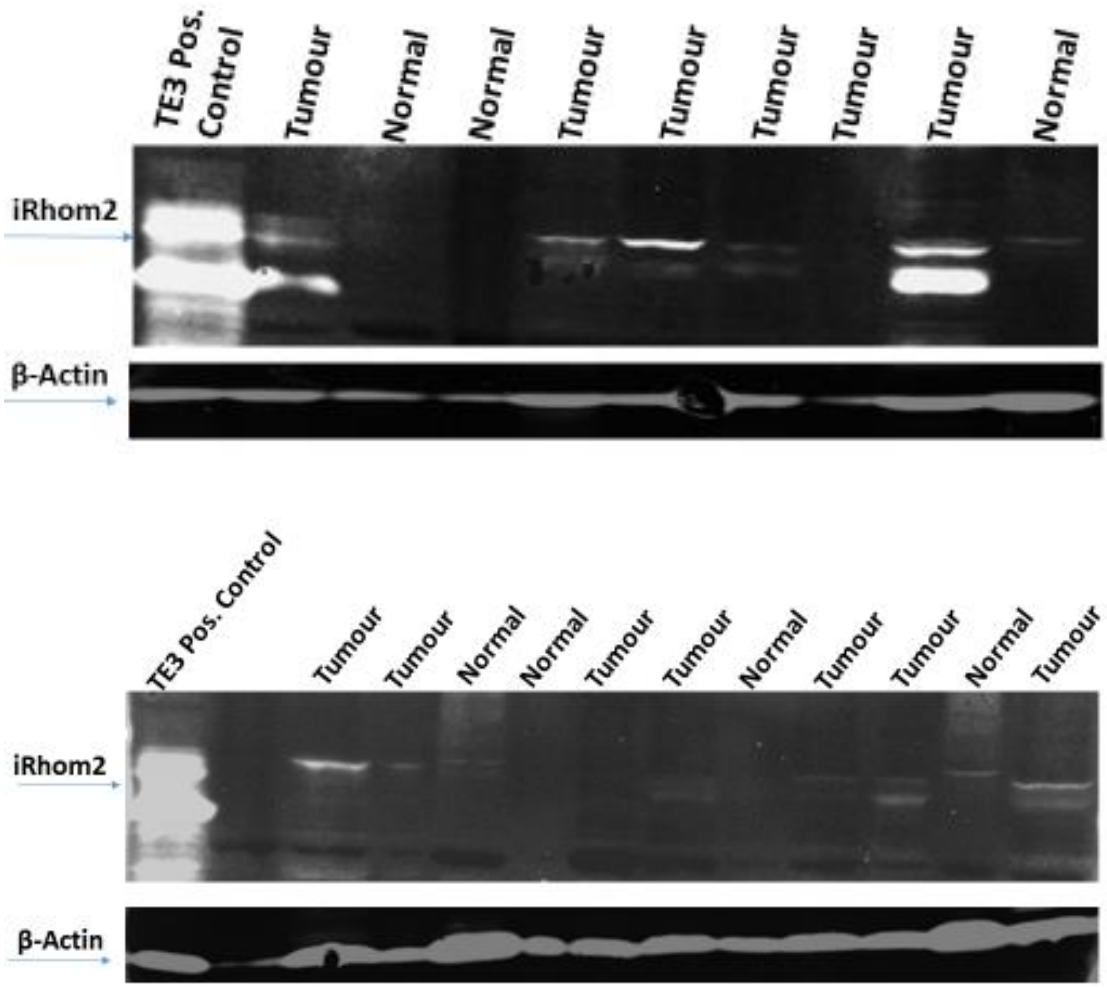

Figure 3.4 Examples of western blot for iRhom2 expression in tissues:

Upper and lower panels (membranes) show varying levels of iRhom2 expression in tumour and normal tissues. TE3 cells over-expressing iRhom2 were used as positive control in the first lanes (from left) on both panels. The position of iRhom2 isoforms is indicated, with β-Actin loading controls shown below the iRhom2 gels. Lane 2 from right, on the Top panel is a tumour sample, a good representation of iRhom2 over-expression. Lane 1 from right on the same membrane is a normal sample with no detectable iRhom2 expression, while lane 4 from right shows moderate expression.

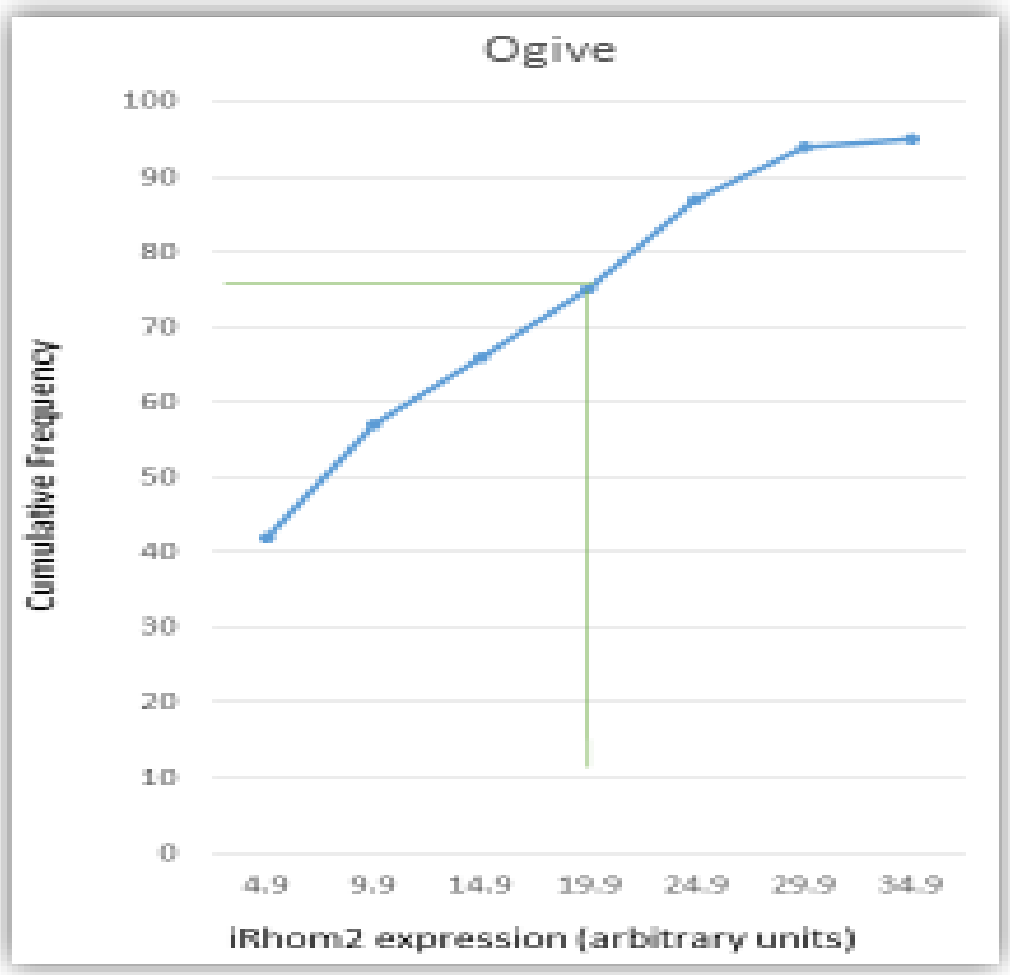

Figure 3.5 Determination of cut-off from Ogive.

Cumulative frequency curve generated using iRhom2 densitometry values for tumour and paired normal samples. A cut-off point of 20 arbitrary units was derived from the Ogive to correspond with expression at the upper quartile (75th percentile). Densitometry values above this cut off were taken to represent over-expression while those below it will represent moderate or no expression.

	Levels of iRhom2 expression	TUMOUR TISSUES			PAIRED NORMAL TISSUES		
CUT OFF: 11	FREQUENCY	27	18	23	2	4	21
	PERCENTAGE	40%	26%	34%	7%	15%	78%
CUT OFF: 20	FREQUENCY	19	26	23	1	5	21
	PERCENTAGE	28%	38%	34%	4%	19%	77%

Figure 3.6 Distribution of levels of iRhom2 expression:

Based on the cut-off point of 20 arbitrary units derived from the Ogive, and a second cut-off of 11 arbitrary units, obtained from the formula, **mean + 2 S.D** (representing densitometry values >95% average value for normal tissues), expression levels were graded. Dark orange - > cut off, Light orange - ≤ cut off, and White = zero arbitrary unit, and the table shows a summary of the distribution of levels of iRhom2 expression based on both cut-off points. Irrespective of the cut-off used, more tumour tissues over-express iRhom2; than normal samples. With a cut-off of 11 for instance, 40% of tumour samples were shown to over-express iRhom2, compared to 7% for normal samples.

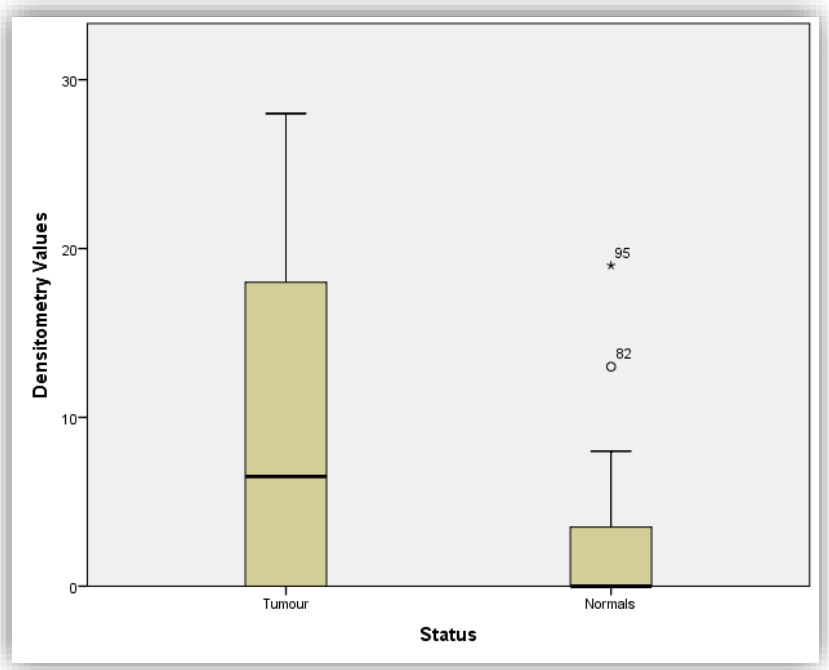

Figure 3.7 Summary of the levels of iRhom2 expression:

A boxplot showing a summary of the levels of iRhom2 expression in tumour and normal samples. Two outliers are conspicuous within the cohort of normal tissues, and these are thought to be normal tissues that might either have significant but yet undetected tumour cell infiltration, or those originating from skin or tissues rich in myeloid cells, which are known to be strongly positive for iRhom2[328].

A second approach to establish a cut-off was also used, in which overexpression in tumour tissues was ascribed to densitometry values >95% average value for normal tissues (**mean + 2 S.D).** Using this method, the cut off was set at a densitometry value of 11 [2.26 + 2(9.176)], giving the number of tumour samples with the "highly

expressing" of 27/68 (40%), compared with 19/68 (28%), when using the upper quartile method (**Figure 3.6**).

3.2.4 ADAM17 expression in tumour and adjacent normal tissues:

Probing for both the mature and immature forms of ADAM17 in the cohort of tumour and normal samples (using the C-terminal ADAM17 antibody) also produced evidence of variable levels of expression (**Figure 3.8**). The immature form of ADAM17, with an expected band about 110KDa, was observed in 63/68 (93%) of the tumour samples; and 14/27 (52%) of the normal samples. However, probing for the mature form of the protein, expected to be around 75KDa, demonstrated expression in 38/68 (56%) of tumour samples and 7/27 (26%) of normal samples. The activated (mature) form is expected to be concentrated at the cell membrane but likely in relative minute amount compared to the intracellular pool of immature ADAM17. Though yet unverified, we suspect that the concentration of mature ADAM17 at the membrane (where shedding activities are meant to be concentrated) may be a direct reflection of a number of factors including the level of abundance of its immature cytoplasmic pool.

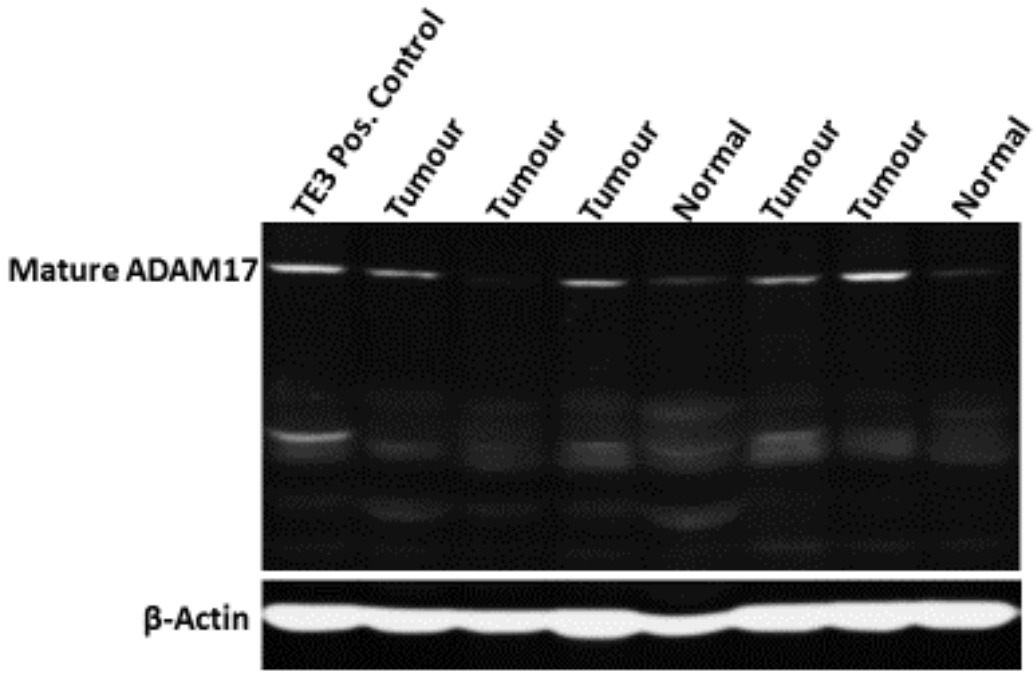

Figure 3.8 Expression of ADAM17 in tissues:

Mature ADAM17 of about 75KDa is shown to be expressed in varying levels by tumour and normal tissue samples. The same TE3 cell line used for iRhom2 expression is maintained as positive control. From left, lanes 2, 4, 6 and 7 are examples of ADAM17 over-expression, with lanes 3, 5 and 8 showing normal ADAM17 expression. β-Actin loading controls have been shown below the ADAM17 gel.

3.2.5 Correlation of iRhom2 and ADAM17 expression with clinicopathological data.

Having established an increased iRhom2 expression pattern in tumour samples compared to paired normals, an attempt was made to establish possible correlations between levels of protein expression and clinicopathological features that may directly or indirectly serve as indices for malignancy. iRhom2 and ADAM17 expression in tumour samples was compared with the following features: tumour site, size, extra-capsular spread, histological differentiation and survival. Only oral cancer cases were included in these analyses. Oropharyngeal cases which had been included in the western blot experiments were excluded. There was no significant correlation between iRhom2 expression and any of the clinicopathological features except for survival. ADAM17 expression did not correlate with any clinicopathological features.

3.2.5.1 iRhom2 expression and survival.

For this analysis, survival was taken as the time from the date of surgery to death (or date last seen, for patients who are still alive) in months. iRhom2 expression was categorised as over-expressed as defined by the two densitometry cut-off values derived earlier, 19.9 and 11, and Kaplan Meier curves were constructed. With a densitometry cut-off of 11, iRhom2 expression was shown to correlate negatively with survival (p=0.000 for the higher cut-off of 19 and p=0.007 for 11 cut-off) (**Figure 3.9**).

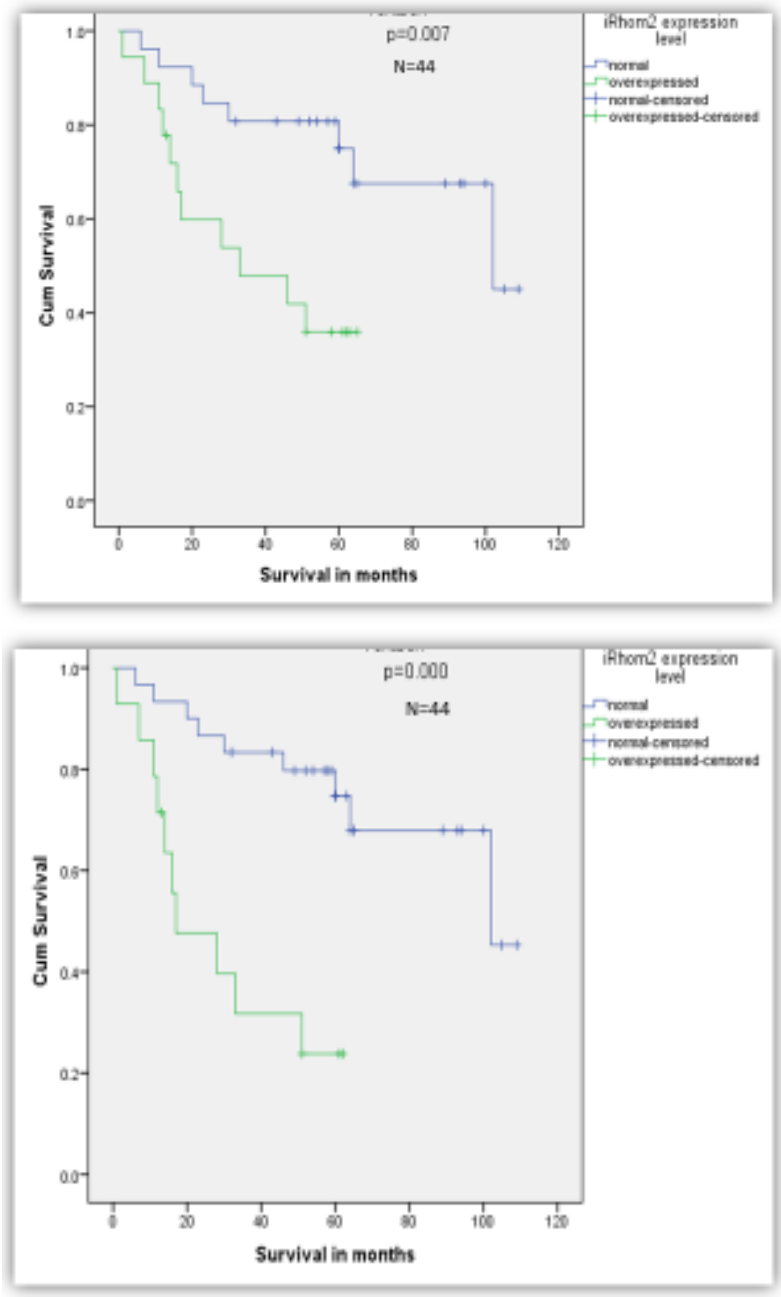

Figure 3.9 Kaplan Meier survival analysis:

Kaplan Meier survival analysis of 44 clinical samples in relation to levels of iRhom2 expression. Top panel: cumulative survival with cut-off set at 11 arbitrary densitometric units. Bottom panel: cumulative survival with cut-off set at 19.9 arbitrary densitometric units.

3.2.6 Intracellular localisation of iRhom2 and ADAM17 by IHC of TMAs

A set of TMA cores previously assembled were scored in an attempt to determine the location and degree of expression among different cell types in intact oral cancer tumour tissues. Unexpectedly, all of the iRhom2 stained cores were either negative or weak. This may be due to relatively small amounts of the protein iRhom2 or the need for improved optimisation of the protocol. For instance, it is a possibility the antibody used is not suitable for IHC on FFPE (formalin fixed paraffin embedded) sections, considering some antigens are not detectable after FFPE treatment. This is while assuming the control sections may not have been stained adequately.

ADAM17 expression was evaluated on the TMAs. The staining was however observed to be likely non-specific with regards to discriminating between the mature and immature forms of ADAM17. ADAM17 is thought to be relatively abundant in its pro-form in the cytoplasm and in relatively smaller amounts as active or matured ADAM17 at the cell membrane[234]. It is this active form at the cell membrane that is thought to carry out shedding activities on other proteins towards their subsequent activation[219]. It is therefore important to be able to differentiate between the two forms as the former is likely to only be a store and is non-functional. The antibody used was intended to primarily target the active form of the protein at the cell membrane, but TMA cores showed mainly abundant cytoplasmic staining and only a handful of weak membranous staining. This shows that expression of functional ADAM17 protein was infrequent. It was also noted in some of the cores that the strength of staining varied from one part of the cytoplasm to the other. One

explanation could be that, since activation or maturation of ADAM17 takes place in the Golgi apparatus, and the mature molecule is then transported to the cell membrane, some of this active or mature form of the protein can be observed in the cytoplasm enroute to the cell membrane. Despite these reservations, it has been demonstrated for other cancer associated proteins E.g. FANCD2, that altered cellular localisation of proteins may be associated with clinical parameters[329]. However, no correlations between ADAM17 staining and clinicopathological features were observed in this cohort. The bioavailability of the protein may be reduced at the cell, such that detecting it via routine protocols becomes a challenge.

3.2.7 TMA (tissue microarray) scores and analysis.

In order to determine the location of increased iRhom2 and ADAM17 expression in intact tumour tissue, TMAs containing triplicate cores from tumour and normal adjacent tissue from 112 patients[326] were probed for iRhom2 and ADAM17. ADAM17 expression ranged from “no staining” to “strong staining” (**Figure 3.10**).

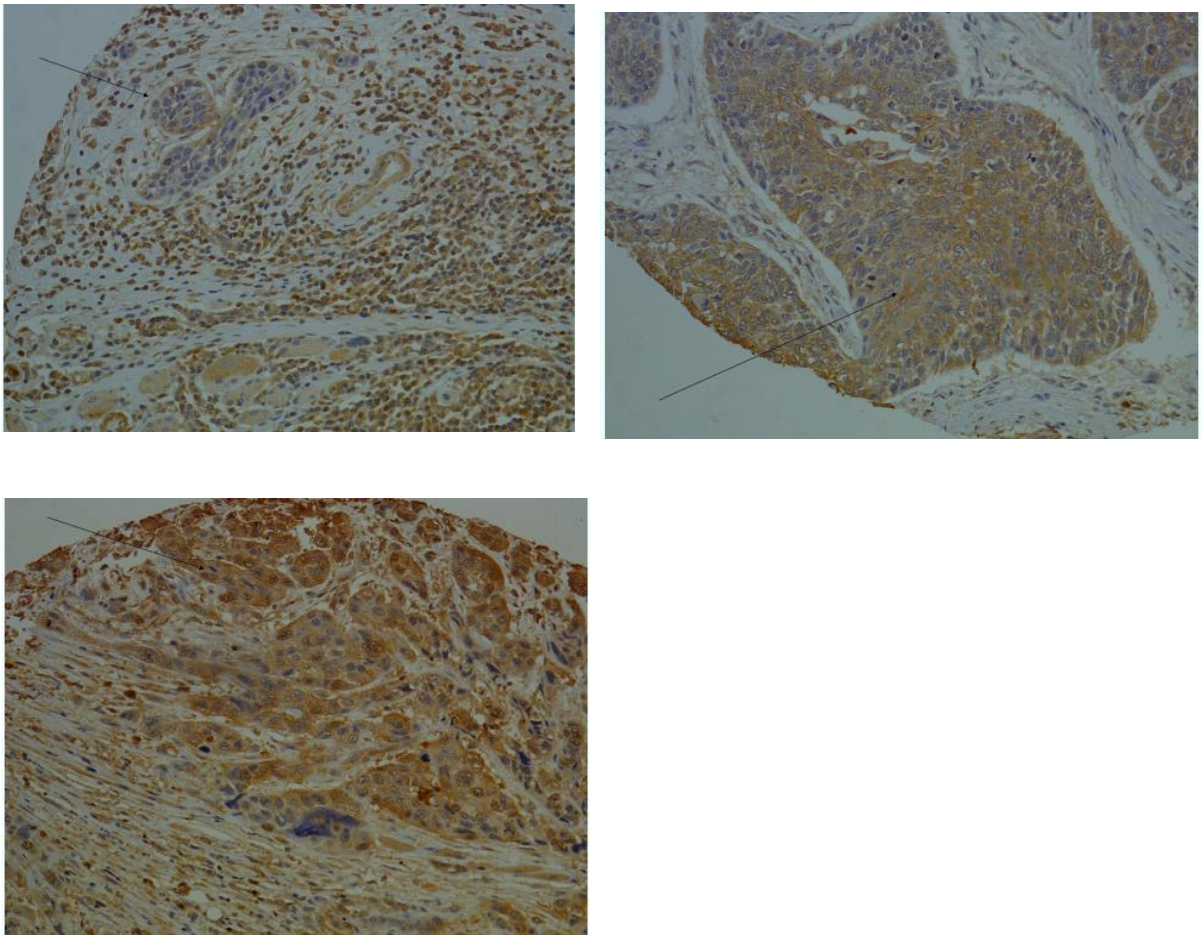

Figure 3.10 ADAM17 staining on tumour cores:

Figures showing different levels of ADAM17 staining on tumour cores. **Top-left** panel shows a core with weak (+), **Top-right** panel demonstrates moderately staining tumour and the **Bottom** panel illustrates strongly stained tumour. Tumour areas are illustrated by arrow heads.

A number of the cores demonstrated more than one level of intensity across the tissue, in which case the most prevalent staining pattern was taken as representative degree of staining. Apart from a few cases, most of the triplicates were not far from each other in terms of staining intensities. For each triplicate set, the most

representative score (i.e. present in 2 or more cores) was adopted as a consensus score (**Table 3.1**). Following the removal of data from non-oral cancer cases, a smaller cohort of 88 patient samples was analysed.

Table 3.1 Examples of TMA triplicate scores and the consensus scores arrived at.

Core Score	Core Score	Core Score	Consensus
Negative	Negative	+	+
Negative	+	+	+
+	++	++	++
+	+	++	+
++	+++	+++	+++

Very few wholly negative or weakly staining cores were observed for ADAM17 (**Table 3.2**), so data from “negative” and “weak” were consolidated into a single category.

Unexpectedly, the staining for iRhom2 was almost exclusively negative and were not analysed further.

Table 3.2 The distribution of ADAM17 consensus staining in TMAs

Consensus Score	Negative	+	++	+++
Frequency	3	9	58	18

3.2.7.1 ADAM17 TMA expression and clinicopathological features.

Some of the less common sites of oral cancer were represented rarely in this sample set, so the primary oral tumour sites were regrouped into 3 categories, tongue, floor-of-mouth (FOM) and others. The "Others" category included those in the retromolar, lower and upper alveolus, lower alveolar ridge, and hard palate region. There was no significant correlation between ADAM17 expression and primary tumour site.

ADAM17 expression was also compared with other clinicopathological features, but did not show any significant correlation between levels of expression and survival, ECS (extracapsular spread), tumour size, nodal involvement, and recurrence.

3.3 Summary and discussion of findings

3.3.1 Assessment of tumour content of frozen specimens

A total of 137 clinical samples in form of tissues obtained from surgery and snap frozen were screened for inclusion in this study. Analysis of H & E stained sections was performed and results showed 28/137 were not suitable for inclusion in the final cohort. Apart from few which were too small in size for these experiments (particularly normal tissues, n=11), most of those excluded was on the basis of containing too little cancer cells to be confident that the data obtained was from tumour cells. Adopting 28/137 as a working ratio would mean that, if any new study is intended to analyse a particular sample size, then this ratio may be applied to increase overall number of tissues recruited in order to allow for tissues that may be discarded as inadequate.

ADAM17 expression was evaluated on the TMAs. The staining was however observed to be likely non-specific with regards to discriminating between the mature and immature forms of ADAM17. ADAM17 is thought to be relatively abundant in its pro-form in the cytoplasm and in relatively smaller amounts as active or matured ADAM17 at the cell membrane[234]. It is this active form at the cell membrane that is thought to carry out shedding activities on other proteins towards their subsequent activation[219]. It is therefore important to be able to differentiate between the two forms as the former is likely to only be a store and is non-functional. The antibody used was intended to primarily target the active form of the protein at the cell membrane, but TMA cores showed mainly abundant cytoplasmic staining and only a handful of weak membranous staining. This shows that expression of functional

ADAM17 protein was infrequent. It was also noted in some of the cores that the strength of staining varied from one part of the cytoplasm to the other. One explanation could be that, since activation or maturation of ADAM17 takes place in the Golgi apparatus, and the mature molecule is then transported to the cell membrane, some of this active or mature form of the protein can be observed in the cytoplasm enroute to the cell membrane. Despite these reservations, it has been demonstrated for other cancer associated proteins E.g. FANCD2, that altered cellular localisation of proteins may be associated with clinical parameters[329]. However, no correlations between ADAM17 staining and clinicopathological features were observed in this cohort. The bioavailability of the protein may be reduced at the cell, such that detecting it via routine protocols becomes a challenge.

3.3.2 Total protein expression of iRhom2 in oral cancer.

On western blot, variable expression of the iRhom2 protein was observed. This was expected, having been shown previously that some tissues probably did not express the protein. In my experiments, the frequency of any iRhom2 expression was higher in tumour samples with 45/68 (66%), than in normal sample 6/27 (22%) ($p<0.05$). Furthermore, the level of expression was generally greater in tumour tissues when either a stringent cut-off of 19.9 arbitrary densitometry units (top quartile of expression), or a “normal” cut-off of 11 units (mean of normal tissues + 2 SD) was set as the limit for overexpression. Analysis was based on expression of isoforms 2. The increased expression of iRhom2 in tumour tissues may be in direct response to an

increased demand for availability of mature ADAM17 at the cell membrane. This could be the case, with a number of studies already implicating ADAM17 in tumorigenesis[246,279]. It may also be that the effect is in iRhom2 expression (either upregulation or increased stability due to activating mutations)[330], resulting in increased availability of ADAM17 on the cell surface. This in turn activates, for example, the EGF or notch pathways. Tumour samples in which iRhom2 expression could not be demonstrated may therefore be those without inherent ability to express the protein, or where a different pathway is available to sustain tumour growth.

3.3.3 Total protein expression of ADAM17 in oral cancer

ADAM17 expression levels were variable in the tissues analysed. Generally, tumour tissues were found to have a higher level of ADAM17 expression, considering either expression of the immature form or the mature form. This is in keeping with available data suggestive of an oncogenic role for ADAM17, including oral cancer cases, where increased expression has been implicated in tumorigenesis[246]. We hypothesised that expression of the mature form might be in direct response to signals for increased shedding activities, therefore our correlation with clinicopathological features was based on the mature form. Also, iRhom2 protein expression correlated with both mature and immature ADAM17 expression ($p<0.001$).

3.3.4 iRhom2 expression correlates with patient survival

iRhom2 expression levels in tumour samples correlated with survival, but not with other clinicopathological features examined. However, ADAM17 expression did not correlate with survival.

CHAPTER 4:

FUNCTIONAL CHANGES IN HEAD AND NECK CELL LINES FOLLOWING UP/DOWN-REGULATION OF iRhom2

4 CHAPTER 4: Functional changes in head & neck cell lines following up/down-regulation of iRhom2

4.1 Introduction and aims:

The deregulation of iRhom2 and ADAM17 have been implicated in the development of a number of cancers[331-333], with my data now eliciting the inclusion of oral carcinomas to the list. There is the hypothesis that, increased expression of iRhom2 in cancer cells may be involved in the pathogenesis of cancer, and possibly supporting increased metastasis. Data from the previous chapter on tissue analysis shows that increased iRhom2 in oral cancer tumour tissues is associated with poor prognosis and may thus be a marker of "aggression". There was however no observable correlation between the levels of iRhom2 expression and other markers of aggression such as extra-capsular spread (ECS). The aim of this section is to investigate a possible role for iRhom2 in tumour aggression in head and neck cancer cell lines in which iRhom2 has been up/down-regulated.

4.2 Results:

4.2.1 Profiling of cell lines:

Baseline expression of iRhom2 and ADAM17 by a cohort of head and neck cell lines was determined by western blot (**Figure 4.1** and **Figure 4.2**). The cell lines; PE/CA-PJ15 and PE/CA-PJ14 showed relatively high levels of iRhom2 expression, while low expression was observed in NOK, Liv7, Liv72 and Liv22K, with a rather intermediate level of expression in Liv37K (**Figure 4.1**). All the cell lines analysed expressed high levels of the immature form of ADAM17 (**Figure 4.2**), with observed differences in the banding patterns, likely reflecting different post-translational modifications in different cell lines. For instance, the two PE/CA cell lines (and to some degree Liv37K) have an additional, strong band at approximately 100KDa. PE/CA-PJ15 and PE/CA-PJ41 also showed a prominent band representing the mature form of ADAM17 at approximately 76KDa, while a small fragment, likely the cleaved N-terminal region (not confirmed) was only detected in PE/CA-PJ15 (**Appendix 3**). The mature form of the protein was present at low levels in Liv37K, Liv22K, Liv72K, Liv7K and NOK. Two head and neck cancer cell lines, PE/CA-PJ15 and Liv37k, and the normal oral keratinocyte cell line, NOK, were selected for functional studies based on their expression pattern (**Figure 4.3**)

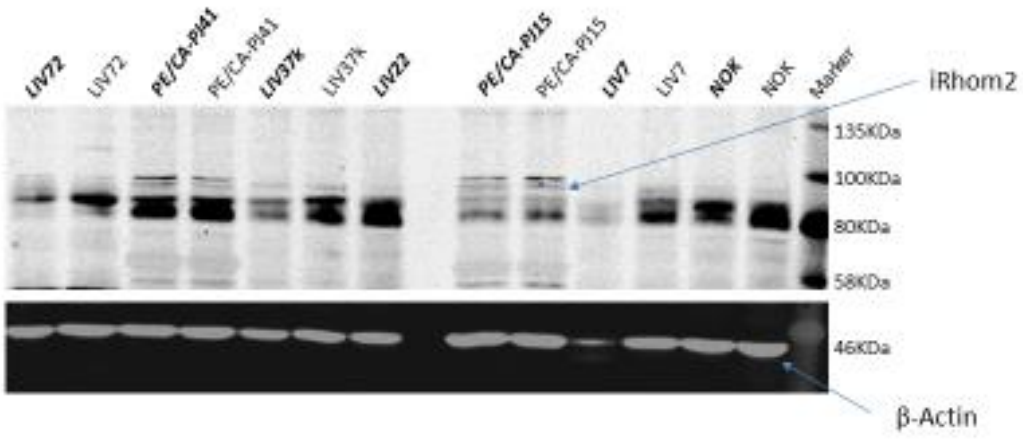

Figure 4.1 **Profiling of iRhom2 expression:**

Profiling of iRhom2 baseline expression in six oral cancer cell lines and normal oral keratinocytes (NOK) to determine suitable options for cell line analysis– "iRhom2 arrow" points at the target band (iRhom2 Isoform 2). The prominent band just above it is the iRhom2 Isoform 1, which is not the target band in this experiment. Cell lines were probed in duplicates with bold letterings representing proteins from a separate flask. The PE/CA-PJ cell lines (PJ15 and PJ41) are shown to have significant baseline levels of iRhom2, unlike the other cell lines.

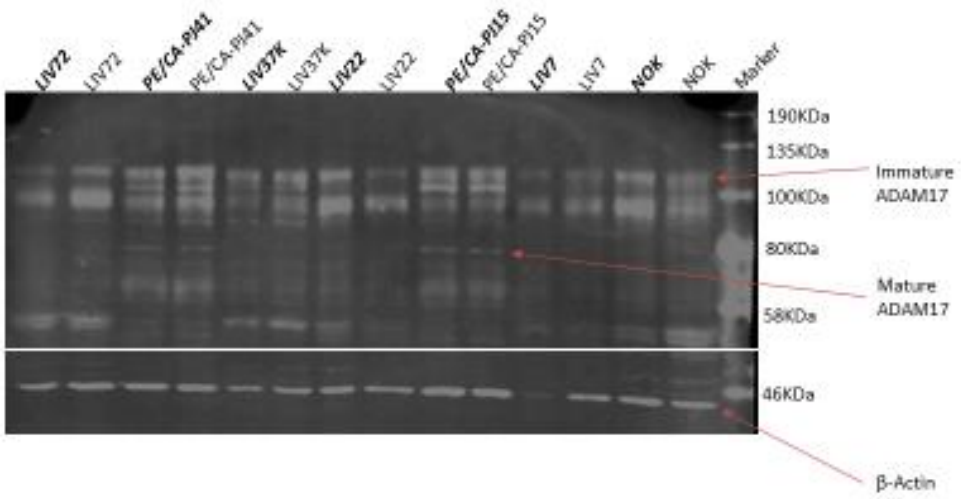

Figure 4.2 **Profiling of ADAM17 expression:**

Profiling of ADAM17 expression in six oral cancer cell lines and normal oral keratinocytes (NOK). Arrow heads point at bands representing the mature and immature forms of the protein. Apart from the Liv22 and Liv7 cells with moderate levels of immature ADAM17, all the other cell lines appear to have a high level of immature ADAM17 (seen between the 100KDa and 135KDa marks). The mature form of the protein (at about the 75KDa point) could only be demonstrated in the PE/CA-PJ cell lines (PJ15 and PJ41).

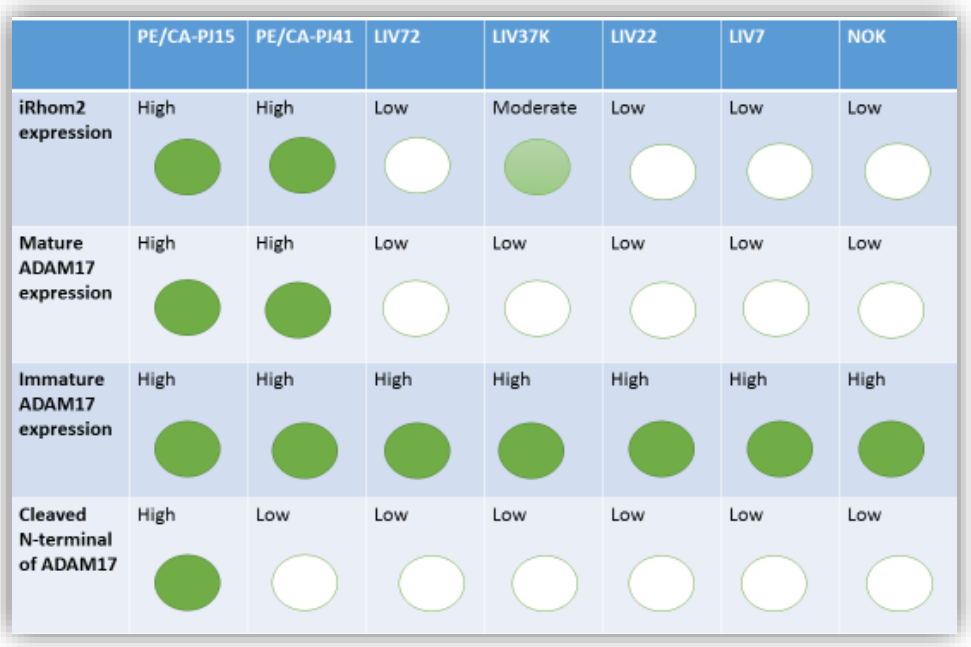

	PE/CA-PJ15	PE/CA-PJ41	LIV72	LIV37K	LIV22	LIV7	NOK
iRhom2 expression	High	High	Low	Moderate	Low	Low	Low
Mature ADAM17 expression	High	High	Low	Low	Low	Low	Low
Immature ADAM17 expression	High	High	High	High	High	High	High
Cleaved N-terminal of ADAM17	High	Low	Low	Low	Low	Low	Low

Figure 4.3 **iRhom2 and ADAM17 expression pattern:**

ADAM17 and iRhom2 expression patterns are represented as colour codes where, the darker the colour shade, the higher the relative level of expression of the protein (based on cut-offs from the constructed ogive). The mature form of ADAM17 protein is demonstrated in the PE/CA cell lines (PJ15 and PJ41), with all the cell lines shown to express its immature form. iRhom2 is shown to be highly expressed in the PE/CA cell lines, compared to moderate expression levels in the Liv37k cells.

4.2.2 Generation of G418 kill / survival curves:

Kill / survival curves were generated for PE/CA-PJ15, Liv37K and NOK in the presence of G418. Both Crystal violet and MTT assays were utilised to quantify total DNA and mitochondria activity respectively, with the assay continuing for up to 5 days. It was important to use both assays because this will not only produce a cell count, but those of viable cells. For NOK and Liv37K, a concentration of 200µg/µl of G418 was observed to be sufficient to kill cells within 5 days, while a concentration of 2000µg/µl was necessary for PE/CA-PJ15. For the eventual killing of untransfected cells, kill doses of 100µg/µl and 1500µg/µl were used respectively.

4.2.3 iRhom2 over-expression in NOK, Liv37K and PE/CA-PJ15 cells.

Transfection of PE/CA-PJ15, Liv37k and NOK cell lines with the iRhom2 overexpressing plasmid, pIRESneo, produced protein overexpression in all three cell lines. Single colonies were cultured for each cell line and three to four different colonies were analysed for the most efficient transfection in terms of level of iRhom2 over-expression (**Figure 4.6, 4.7 and 4.8**). The highest level of overexpression was demonstrated by PE/CA-PJ15 cells (**Figure 4.5**). An additional prominent band (50KDa) was consistently observed in all of the overexpressing variants, and may represent a degradation product. RNA over-expression was also observed (**Figure 4.4**).

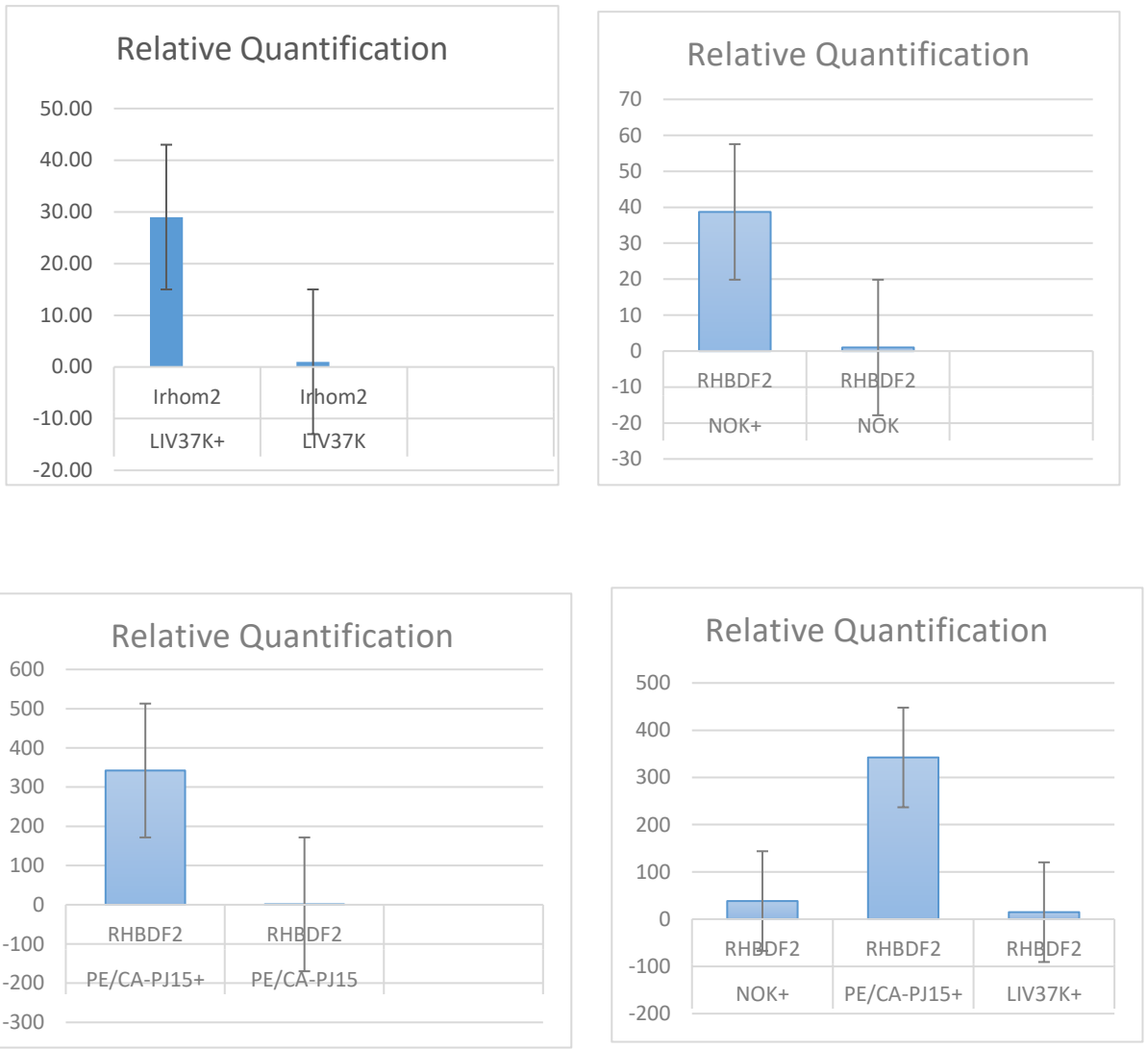

Figure 4.4 Relative quantification of *RHBDF2* overexpression:

Relative quantification (RQ) of levels of *RHBDF2* overexpression in the over-expressing variants of NOK, Liv37K and PE/CA-PJ15 cell lines, compared with the parental cell lines. The last image compares the relative level of overexpression among the three cell lines. Values represent those obtained from qPCR analysis, carried out in duplicates.

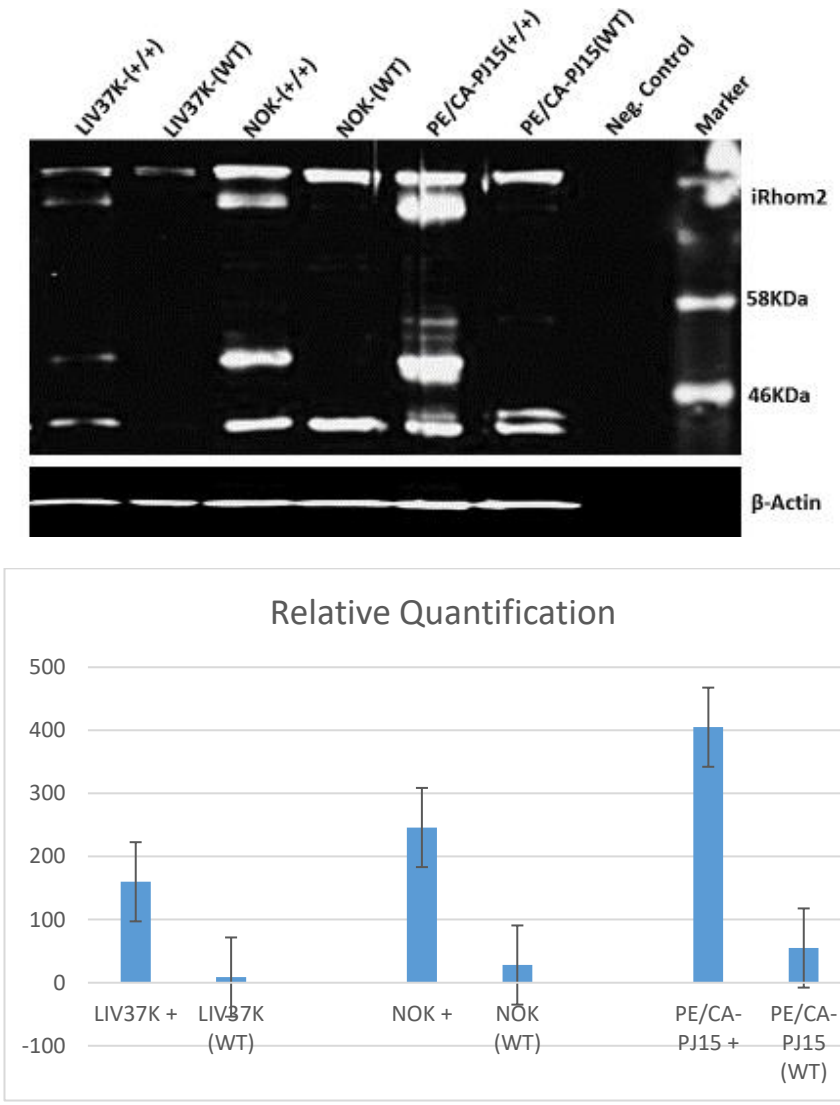

Figure 4.5 **iRhom2 protein over-expression:**

iRhom2 protein over-expression in NOK, Liv37K and PE/CA-PJ15 cell lines**:** Top-western blot following stable transfection with the iRhom2 isoform 2 overexpressing plasmid (pIRESneo). Transfected cells (+/+) are shown to have a higher level of expression of the iRhom2 protein compared to their corresponding wild types (WT). Bottom- relative quantification of iRhom2 isoform2 protein expression, using arbitrary densitometry units. The highest level of iRhom2 expression is shown to occur in PE/CA-PJ15, however, the biggest impact of over-expression is demonstrated with the Liv37k cells.

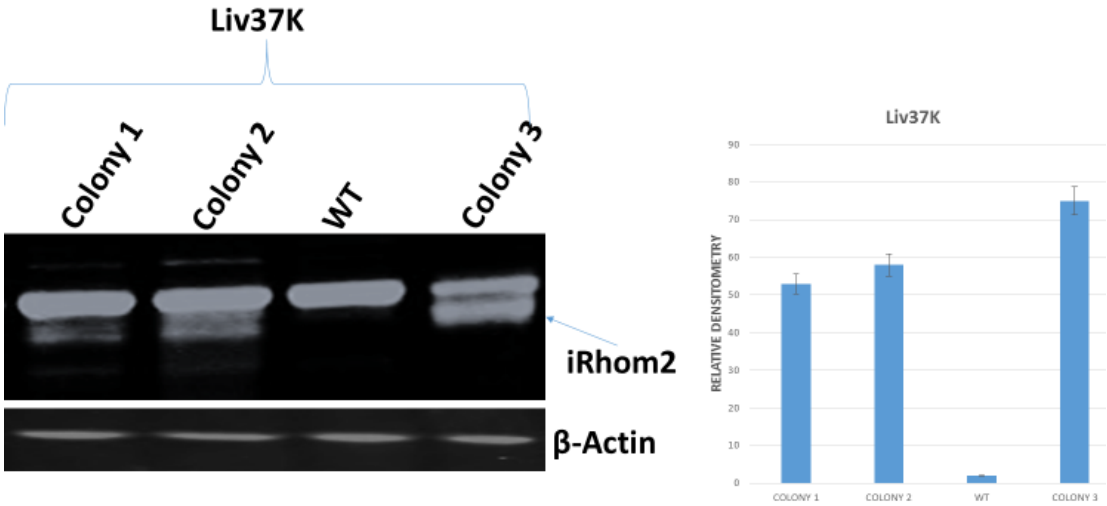

Figure 4.6 **Colony selection for Liv37K:**

iRhom2 protein over-expression in 3 different colonies of Liv37K cells, in comparison with the wild-type (WT). Left panel shows the western blot result, while the right panel is a bar chart to illustrate the degree of iRhom2 over-expression, using relative densitometry values. The bar chart includes percentage error bars. The greatest transfection efficiency was demonstrated in Colony 3 and these cells were used onward for Liv37K (+/+) variants.

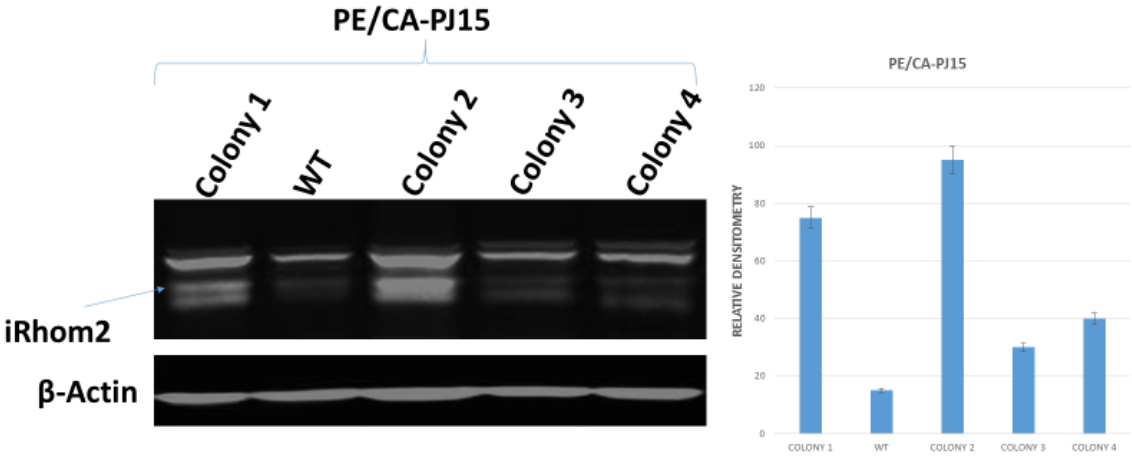

Figure 4.7 **Colony selection for PE/CA-PJ15 cells:**

iRhom2 protein over-expression in 4 different colonies of PE/CA-PJ15 cells, in comparison with the wild-type (WT). Left panel shows the western blot result, while the right panel is a bar chart to illustrate the degree of iRhom2 over-expression, using relative densitometry values. The bar chart includes percentage error bars. The greatest transfection efficiency was demonstrated in Colony 2 and these cells were used onward for PE/CA-PJ15 (+/+) variants.

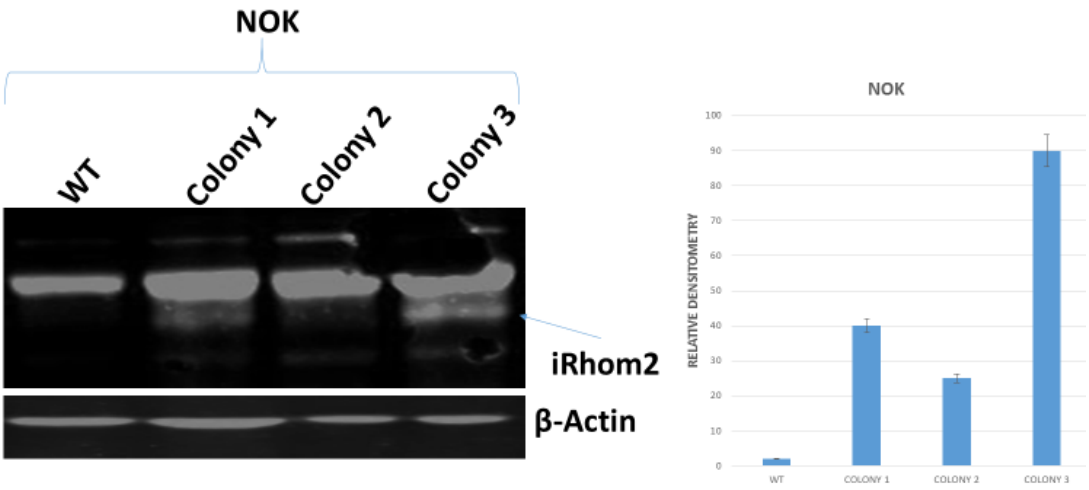

Figure 4.8 **Colony selection for NOK cells:**

iRhom2 protein over-expression in 3 different colonies of NOK cells, in comparison with the wild-type (WT). Left panel shows the western blot result, while the right panel is a bar chart to illustrate the degree of iRhom2 over-expression, using relative densitometry values. The bar chart includes percentage error bars. The greatest transfection efficiency was demonstrated in Colony 3 and these cells were used onward for NOK (+/+) variants.

4.2.4 shRNA knock-down of *RHBDF2*.

The previously transfected, over-expressing cell lines, were subsequently subjected to shRNA knock-down of the *RHBDF2* gene, targeting Isoform 2. Scrambled shRNA together with an empty vector were used as controls. Interestingly, iRhom2 expression was reduced below the levels observed in parental cell lines for both PE/CA-PJ15 **(Figure 4.9)** and NOK **(Figure 4.10),** using clone A (TRCN0000048685), 25

times less in PE/CA-PJ15 and 18 times less in NOK. Knock-down experiments using Liv37k cell lines did not yield appreciable knock-down (**Figure 4.11**). The two shRNA clones, A (TRCN0000048685) and B (TRCN0000048687) were utilised, separately and in combination, for possible *RHBDF2* knock-down in Liv37K, without appreciable knock-down effect (**Figure 4.12**). .

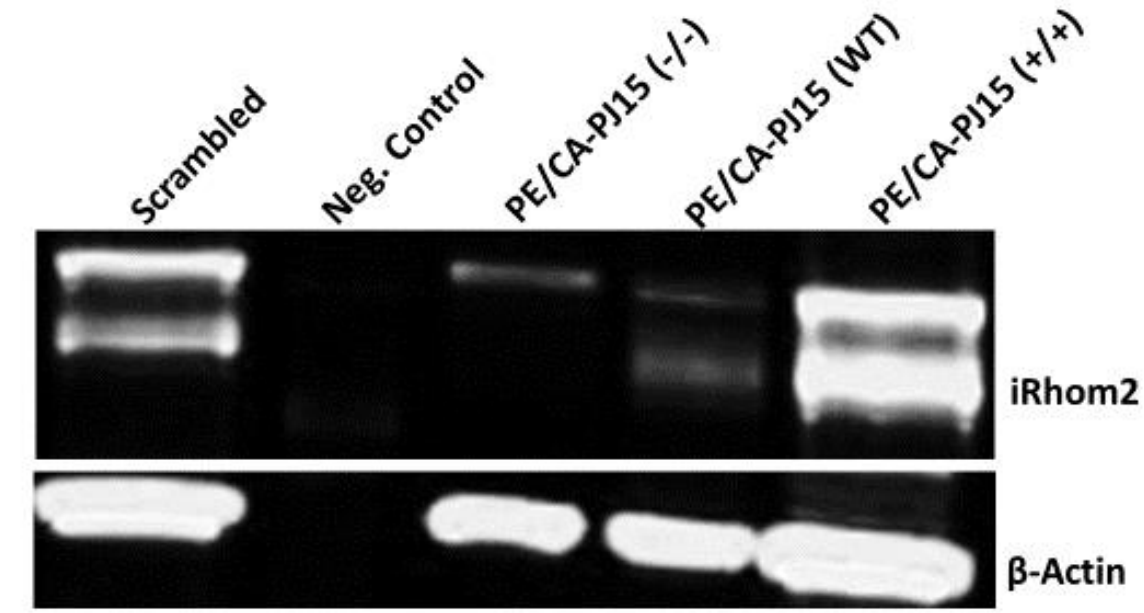

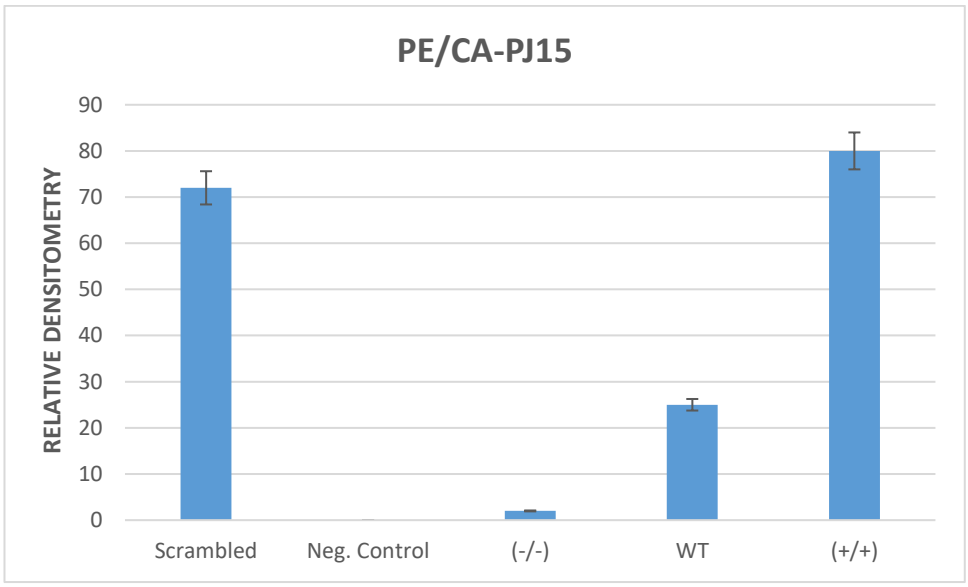

Figure 4.9 **shRNA knock-down of *RHBDF2* in PE/CA-PJ15 cells:**

Western blot (Top panel) and relative quantitation (Bottom panel) following shRNA knock-down of *RHBDF2* gene in over-expressing PE/CA-PJ15 clones. There is a significant knock-down effect following shRNA treatment, with iRhom2 expression level falling from around 70 relative densitometry units (over-expressing +/+ clones) to below 5 (knock-down -/- clones).

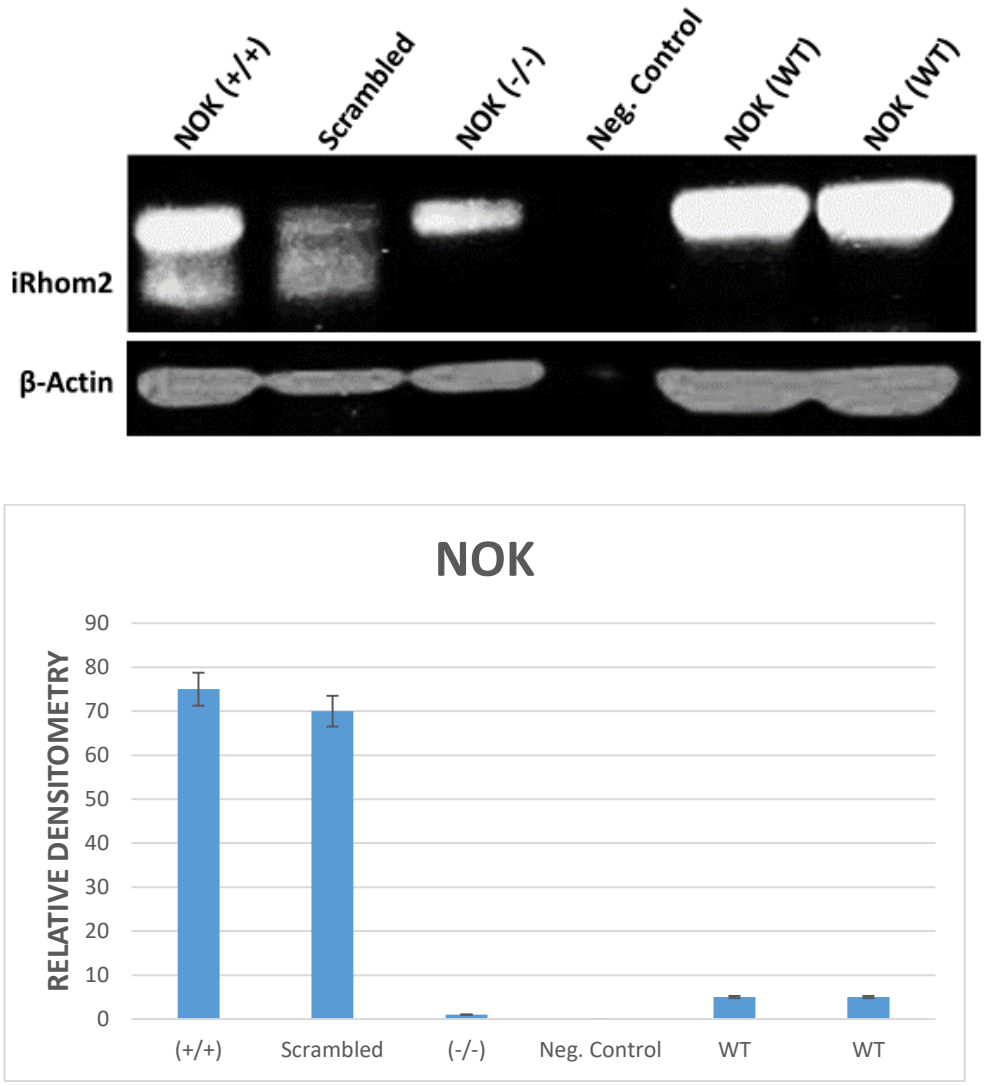

Figure 4.10 **shRNA knock-down of *RHBDF2* in NOK cells:**

Western blot (Top panel) and relative quantitation (Bottom panel) following shRNA knock-down of *RHBDF2* gene in over-expressing NOK clones. There is a significant knock-down effect following shRNA treatment, with iRhom2 expression level reducing from around 75 relative densitometry units (over-expressing +/+ clones) to below 5 (knock-down -/- clones).

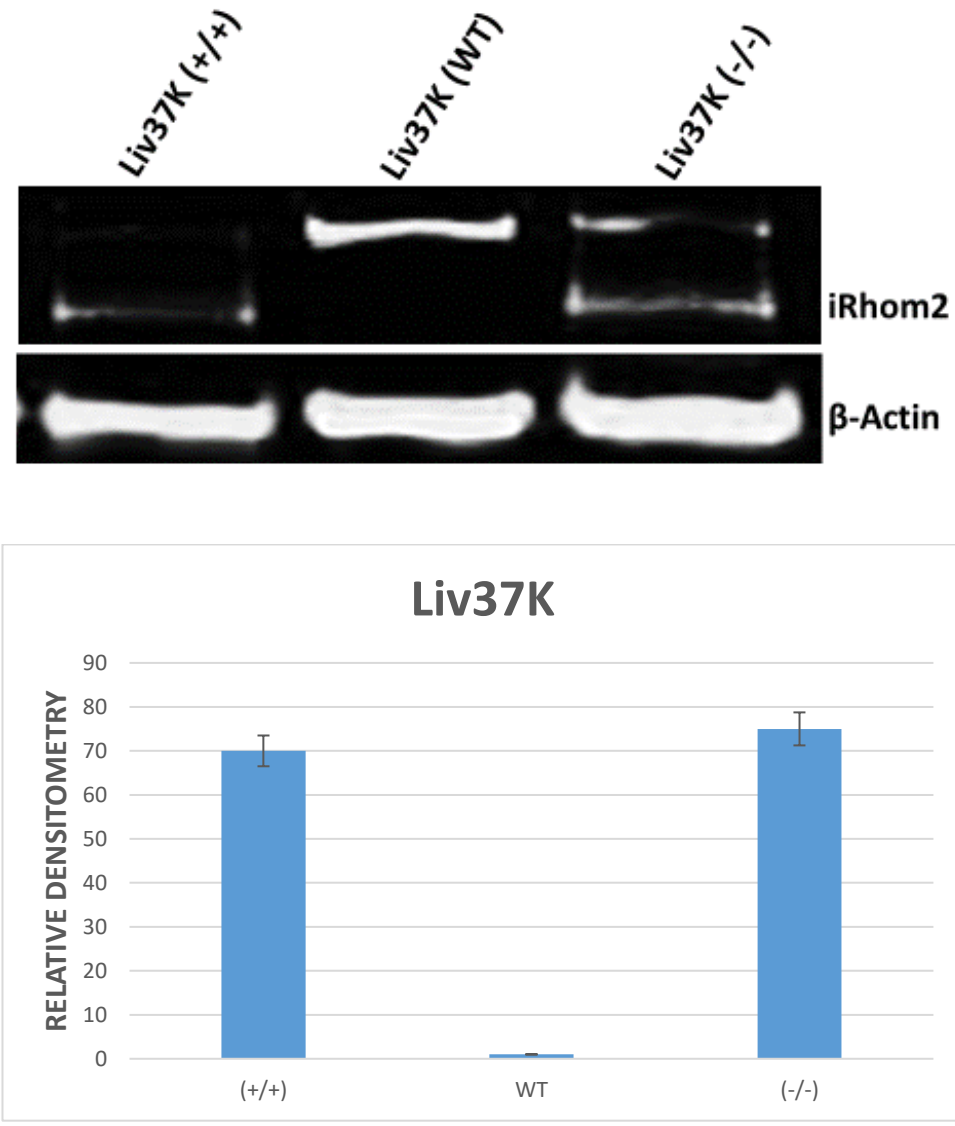

Figure 4.11 **shRNA knock-down of *RHBDF2* in Liv37k:**

Western blot (Top panel) and relative quantitation (Bottom panel) following shRNA knock-down of *RHBDF2* gene in over-expressing Liv37k clones. The knock-down effect is not significant, with the (-/-) cells appearing to have similar levels of iRhom2 expression to the over-expressing clones (+/+).

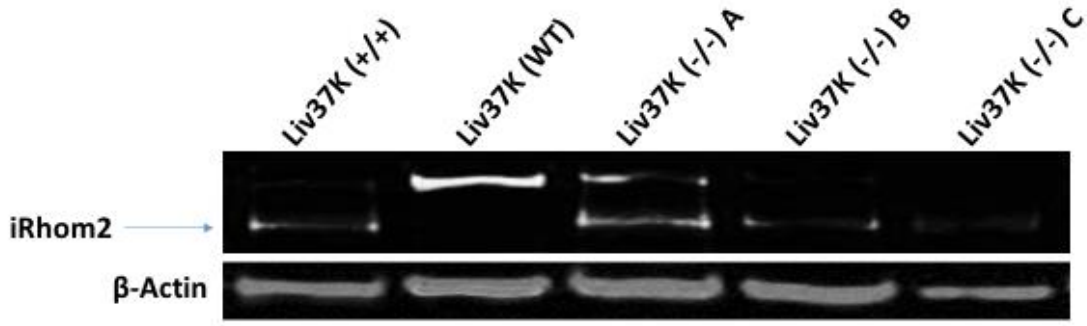

Figure 4.12 **RHBDF2 knock-down using multiple shRNA:**

Western blot following attempted shRNA knock-down of *RHBDF2* gene in over-expressing clones of Liv37K cells. The two shRNA clones, A and B, were used separately, and in combination as C to attempt knock-down effect, without success. All the knock-down clones (-/-), A, B and C appear to have similar levels of iRhom2 expression compared to the over-expressing clones (+/+).

4.2.5 ADAM17 expression following overexpression and shRNA knock-down of *RHBDF2*

The effect of up/down-regulation of iRhom2 on the expression of ADAM17 was investigated with immunoblotting, probing for both forms of ADAM17 (mature and immature). Increased expression of the mature form of the protein was clearly demonstrated in the over-expressing PE/CA-PJ15 cell lines, with a reduction of expression in the shRNA knock-down (**Figure 4.13 Top and Bottom panels**). However, mature ADAM17 expression could not be detected in any clones produced from the other two cell lines, NOK and Liv37k (**Figure 4.13**). Expression of the immature form

of ADAM17 was increased in iRhom2 over-expressing cell variants of all three cell lines, and reduced in 2/3 of the shRNA knock-down cell lines (**Figure 4.13**, **Top and Middle panels**). There was increased levels of expression of the immature ADAM17 with increased iRhom2 expression in both NOK and Liv37K cells, but not in PE/CA-PJ15 cells, where both overexpressing and knock-down cells expressed the immature form at relatively equal / elevated levels.

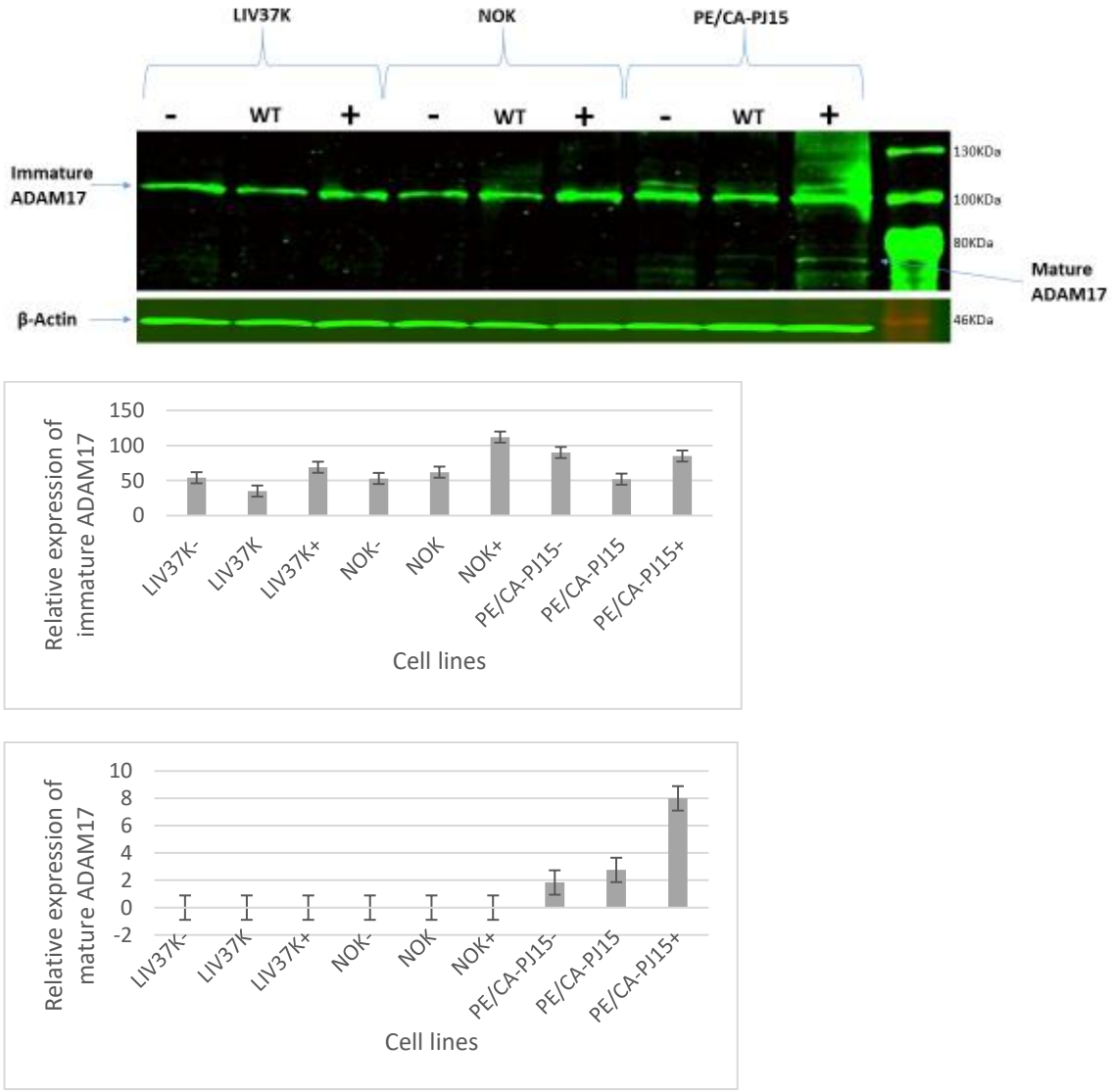

Figure 4.13 ADAM17 expression following upregulation of iRhom2:

Top panel – Western blot analysis of expression of mature and immature forms of ADAM17 following overexpression and shRNA knock-down of RHBDF2 in Liv37K, NOK and PE/CA-PJ15 cell lines. Levels of the immature form of the protein appear unaltered across the variants of all three cell lines. The mature form of the protein is however shown to be markedly increased in the PE/CA-PJ15 (+/+) cells. **Middle and bottom panels** – bar charts to illustrate relative quantification of levels of expression of the immature and mature forms of ADAM17 respectively. Error bars demonstrate mean plus 2 S.D for 2 replicates.

4.2.6 Functional analysis

4.2.6.1 Proliferation

The crystal violet assay was used to assay the rate of proliferation of PE/CA-PJ15, Liv37K and NOK cell lines and their overexpressing and shRNA knock-down derivatives. This assay suggested that overall growth / proliferation was unaffected by the changes in iRhom2 expression (**Figure 4.14**), except for Liv37k where over-expression of iRhom2 appeared to slow the proliferation rate.

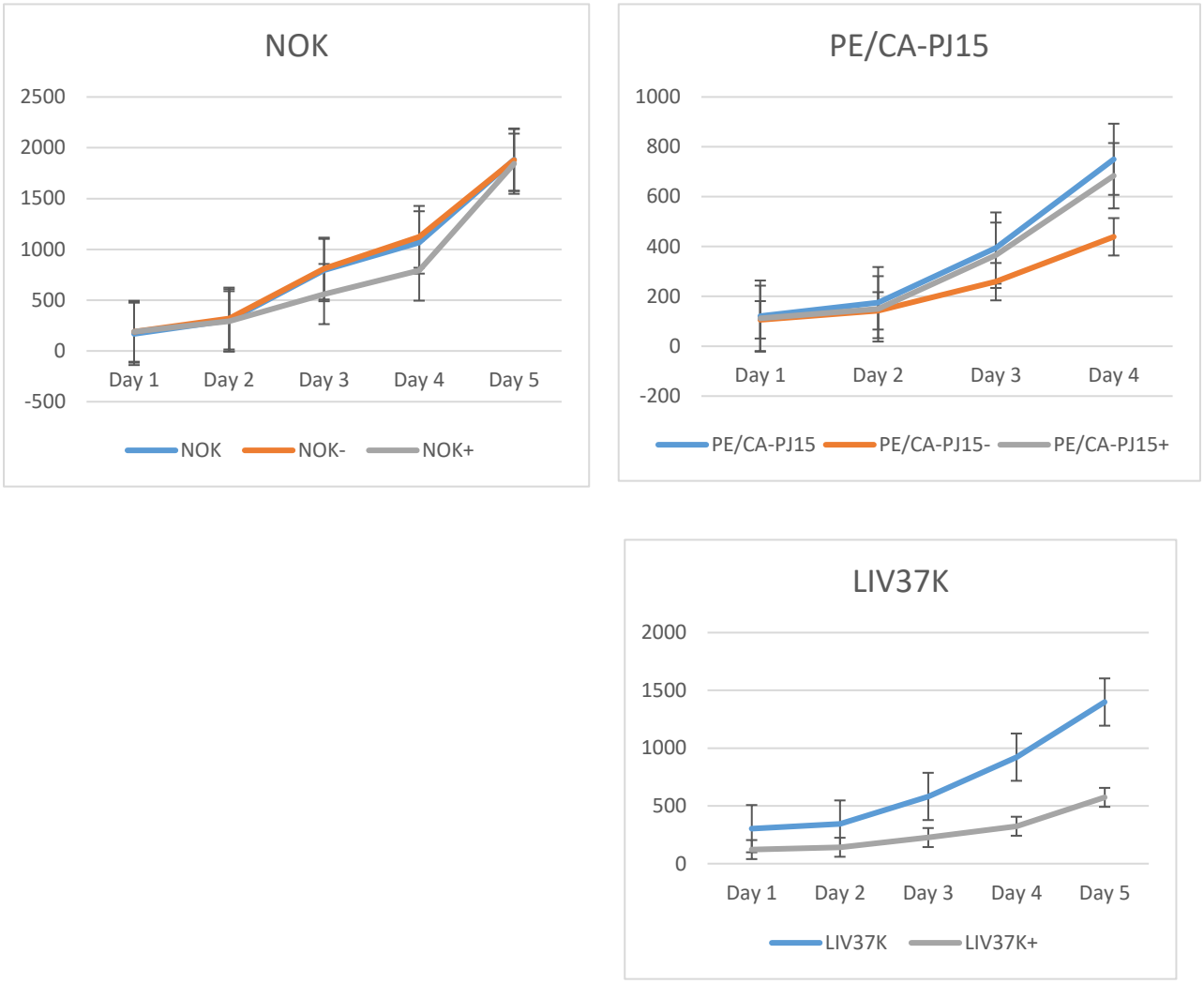

Figure 4.14 **proliferation assay:**

Crystal violet proliferation assay on NOK, Liv37K and PE/CA-PJ15 cells and their derivatives**:** Viable cell population, represented by the absorbance, is plotted against time in days. Blue line: parental cell line; orange line: shRNA knock-down of over-expressing clone; grey line: over-expressing clone. With all three cell lines, there seem to be no obvious added proliferative advantage following iRhom2 over-expression. Equally, there seem to be no proliferative setback following iRhom2 knock-down, with the slopes similar to each other.

4.2.6.2 Migration:

The wound healing assay (scratch assay) was used to assess changes in rate of migration between the wild type NOK, Liv37K and PE/CA-PJ15 cells and their derivatives. PJ15 (+/+) cells with up-regulated iRhom2 migrated faster than their wild-type and knock-down variants with the knock-down clone showing the slowest rate of migration (**Figure 4.15**). Complete wound closure by PJ15 (+/+) occurred after 18 hours but was not achieved by the wild type or knock-down variants until 32 hours. iRhom2 over-expression did not appear to alter the rate of migration of NOK cells (**Figure 4.16**). An increased rate of wound closure was observed for Liv37k upregulated cells compared with the parental cell line and the same increased rate of wound closure was observed in Liv37K cells which unsuccessfully went through the knock-down process (**Figure 4.17**). Considering the rate of migration (in terms of wound closure) between the wild type variants of the two cancer cell lines used, PE/CA-PJ15 and LIV37K, the PE/CA-PJ15 cells migrated slower than the LIV37k cells, in indirect proportion to their baseline iRhom2 expression. Wild type PE/CA-PJ15 cells closed the wound after 32 hours (**Figure 4.15**), unlike wild type LIV37K cells for which the same closure took an average of 17 hours (twice faster), (**Figure 4.17**). Baseline iRhom2 expression levels may therefore not be a direct measure for rate of migration. NOK cells migrated fastest. Again, the above observation has its limitations, considering the fact that the various cell lines were seeded at different confluence. It was not possible to seed cells at the same confluence for the three cell lines, considering they have different growth rates. Seeding at the same confluence therefore would have resulted to overcrowding for PE/CA-PJ15 where LIV37K and

NOK are considered adequate. If the rate of migration is directly and considerably influenced by the seeding densities, this will therefore explain the reason for the rather overall slower closure rate observed with PE/CA-PJ15, considering they were seeded least dense. Consistent with the two cancer cell lines, PE/CA-PJ15 and LIV37K, their upregulated variants migrated at approximately twice the rate compared to their wild type. This remarkable increase in rate of migration with increased iRhom2 expression in cancer cells, is an indication that iRhom2 is involved with cell mobility in cancer, but at different rates across cells.

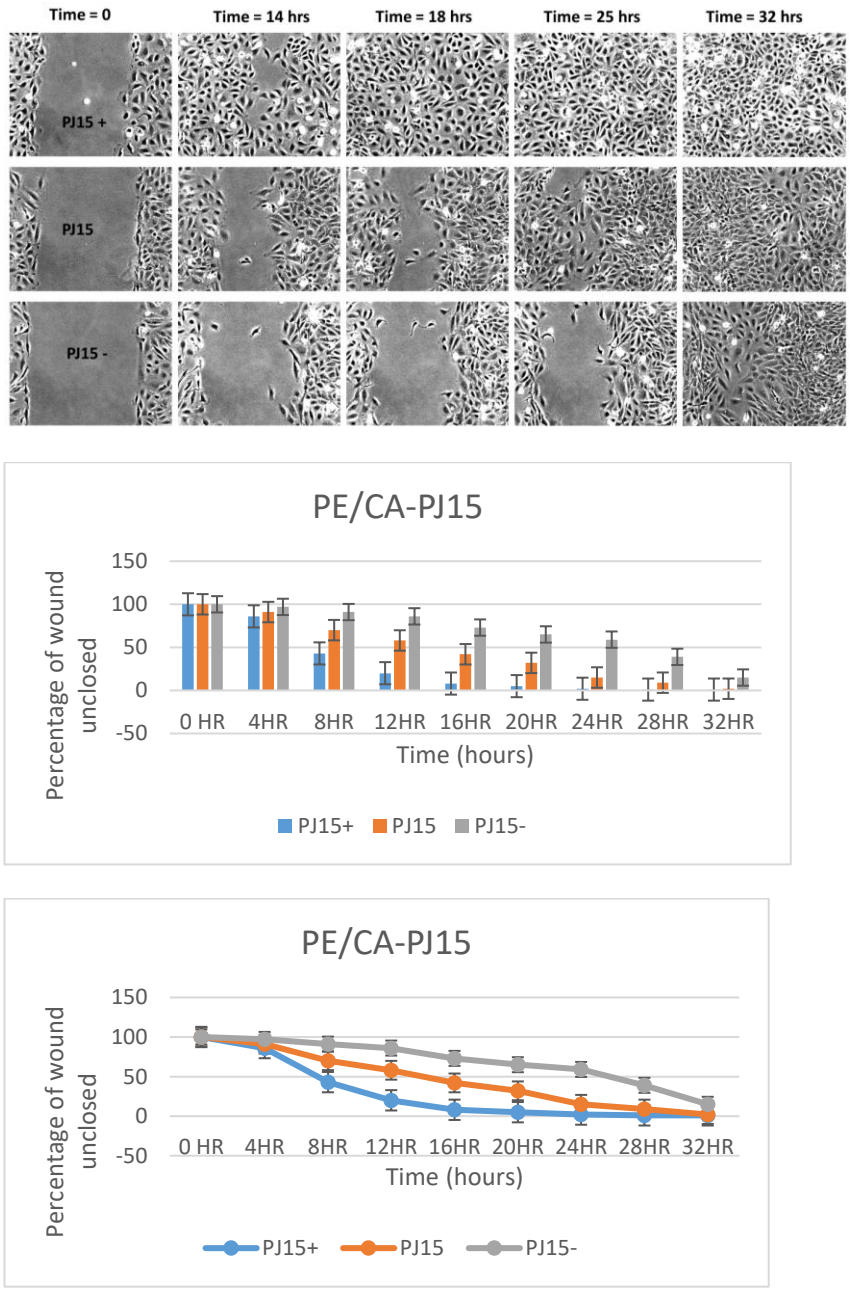

Figure 4.15 **Migration of PE/CA-PJ15 cell lines:**

Migration of PE/CA-PJ15 cell lines using the scratch assay. Top panel - Freeze photography taken at the time points indicated to reflect extent of open wound/closed area. Middle & Bottom panels – graphical representations of the relative rates of wound closure. Orange line/bar: parental cell line; grey line/bar: shRNA knock-down of over-expressing clone; blue line/bar: over-expressing clone. Experiments were performed in duplicates, with standard error bars shown.

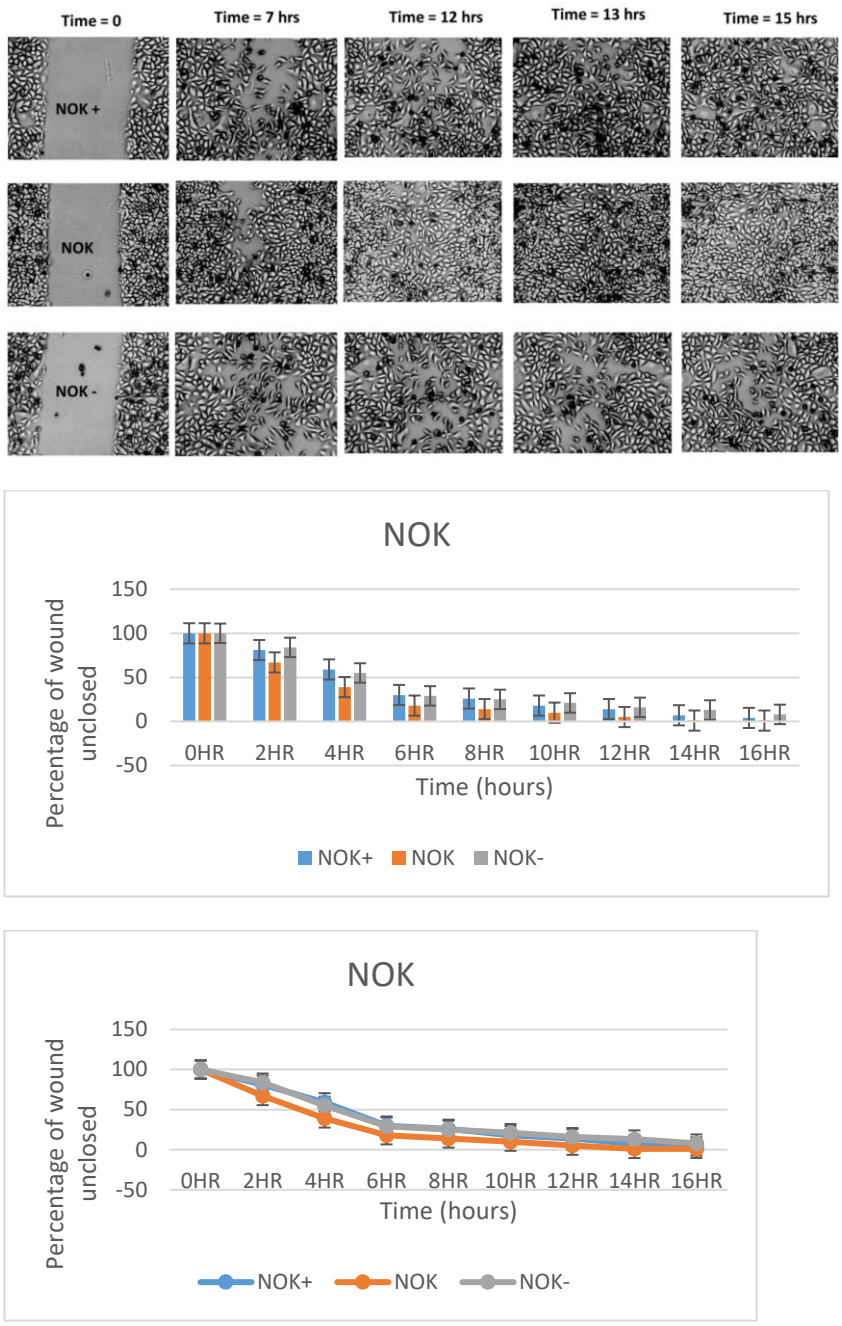

Figure 4.16 **Migration of NOK cell lines:** Migration of NOK cell lines using the scratch assay Top panel - Freeze photography taken at the time points indicated to reflect extent of open wound/closed area in NOK cell series. Middle & Bottom panels – graphical representations of the relative rates of wound closure among the variants. Orange line/bar: parental cell line; grey line/bar: shRNA knock-down of over-expressing clone; blue line/bar: over-expressing clone. Experiments were performed in duplicates, with standard error bars shown.

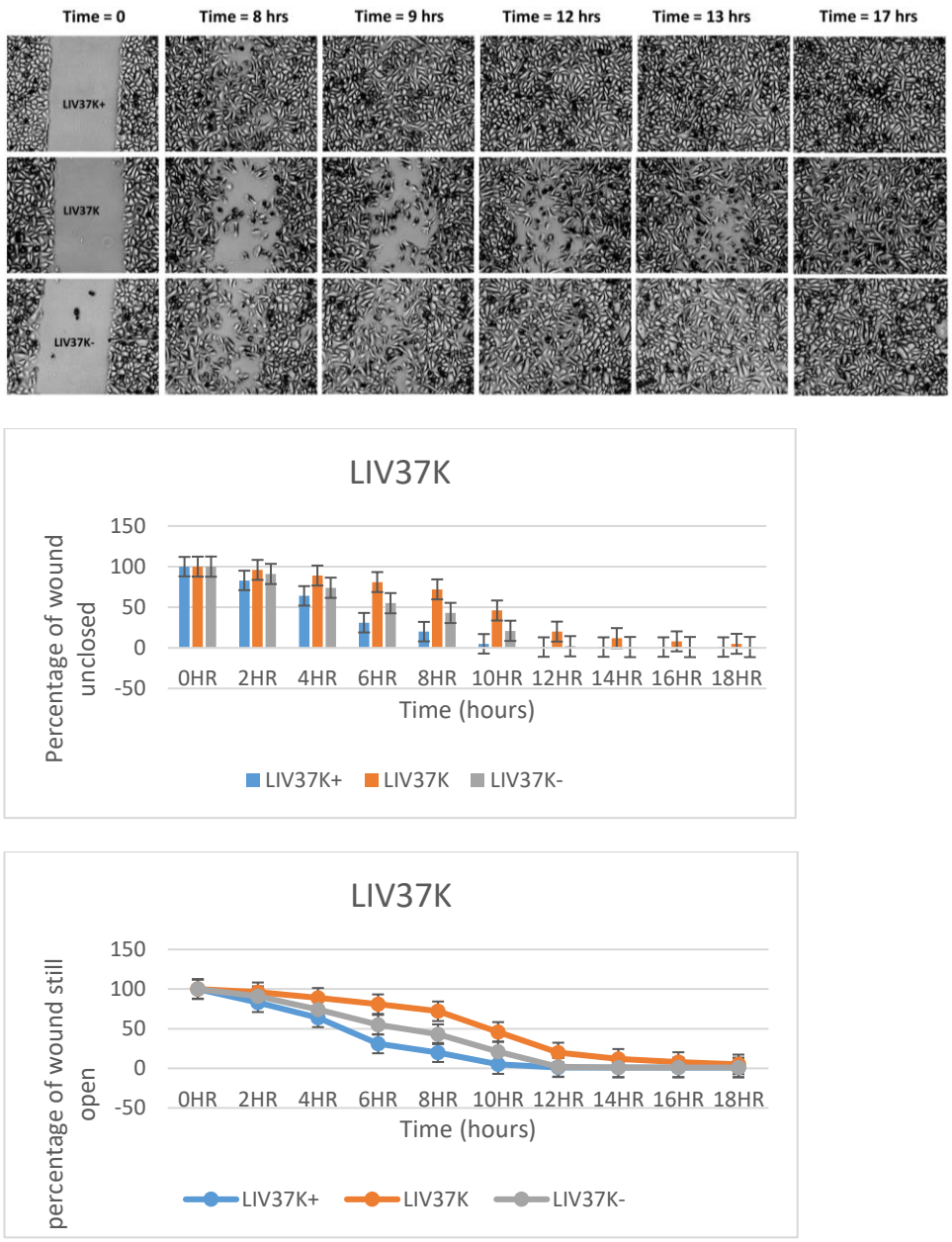

Figure 4.17 **Migration of Liv37k cell lines:** Migration of Liv37k cell lines using the scratch assay Top panel - Freeze photography taken at the time points indicated to reflect extent of open wound/closed area in Liv37K cell series. Middle & Bottom panels – graphical representations of the relative rates of wound closure among the variants. Orange line/bar: parental cell line; grey line/bar: shRNA knock-down of over-expressing clone; blue line/bar: over-expressing clone. Experiments were performed in duplicates, with standard error bars shown.

4.2.6.3 Morphological observations:

Morphological changes were observed between the various strains of PE/CA-PJ15 cells, with the up-regulated clones, PJ15 (+/+) appearing more spindle shaped compared to the WT and KD cells (**Figure 4.18**). There were no obvious morphological differences among the variants of NOK and Liv37k cells.

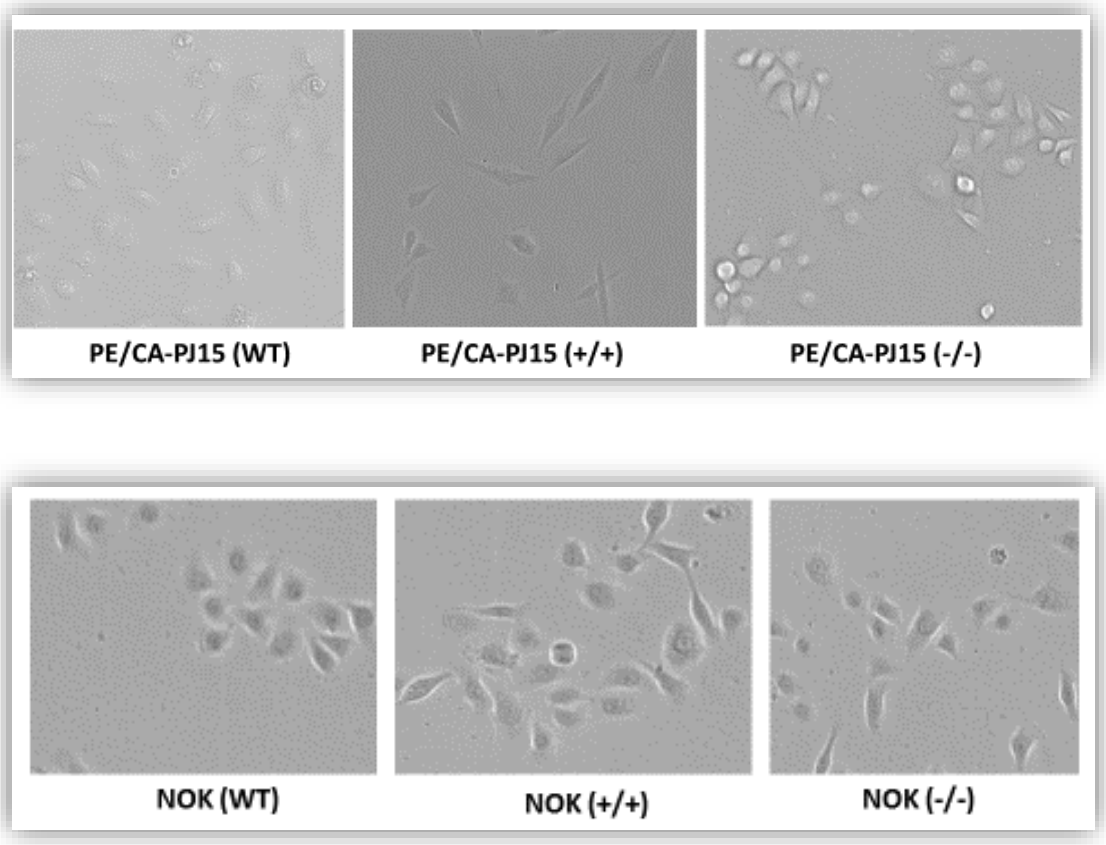

Figure 4.18 **Morphological changes:** Phase contrast images of PE/CA-PJ15 and NOK derivatives in culture. The PE/CA-PJ15 (+/+) over-expressing clones appear to be more elongated with what appears to be somewhat prominent spindles. A similar finding is observed with the NOK (+/+) clones, though their knock-down variants, NOK (-/-) also appeared similar to the over-expressing clones.

4.3 Summary and discussion of findings

4.3.1 Expression of iRhom2 and ADAM17 in cell lines

The parent cell lines profiled expressed iRhom2 and ADAM17 in varying levels. The marked variation in iRhom2 expression was expected, considering the variation in its expression by the cohort of clinical tissues used earlier, in addition to suggestions that certain cells / tissues may not express the protein[334]. For ADAM17 expression, all the cell lines seem to strongly express the immature form but not the mature form. Again, this comes as no surprise, considering the protein has been shown to be pooled largely in its immature form, with only a relative mature / active fraction at the cell membrane[227,228].

4.3.2 The effect of iRhom2 upregulation on ADAM17 expression.

Upregulation of iRhom2 was achieved in all three cell lines used, but to varying levels, as demonstrated on both western blot and by RT-PCR. The highest level of upregulation at the RNA level was observed in the PE/CA-PJ15 cell line (approximately 350 fold compared with 30-40 fold for Liv37k and NOK, respectively). However, relative over-expression at the protein level was greatest in Liv37k (approximately 150 fold compared with 8-12 fold for PE/CA-PJ15 and NOK, respectively), probably due to the fact that they demonstrated the highest baseline expression from the profiling carried out initially. Equally, there is the possibility that cells have a

maximum level of iRhom2 they may accommodate, in which case the increased level of RNA may not result in a corresponding protein level for PE/CA-PJ15. There is however no evidence to this in the literature. The expression of the immature inactive form of ADAM17 was observed to approximately double, compared to the parental cell line when iRhom2 protein was upregulated in all cell lines tested. However, increased expression of the active form was only demonstrated at significant levels in one of the cell lines, PE/CA-PJ15, following upregulation of the iRhom2 protein. The increased expression of mature (active) ADAM17 may be due to the increased bioavailability of iRhom2 (following its upregulation), proposed to be responsible for its intracellular trafficking and subsequent activation. The fact that this has not been reflected in the other two cell lines may be because, though likely increased, the levels might still be sub-optimal for detection by western blot. The increased expression of the immature / inactive form of ADAM17 on the other hand may be in response to feedback arising from rapid deployment of ADAM17 for trafficking by iRhom2. The difference is however less felt considering the fact that the immature store is already considered relatively abundant in the cytoplasm. Importantly, using **Table 4.2** as a guide, it could be argued that, X 350 upregulation of iRhom2 at the RNA level for PE/CA-PJ15 has not produced as much effect as X 40 for Liv37k, suggestive of the fact that there might be a stronger forward gradient in Liv37k due to lower baseline levels of iRhom2 in the parental cells. This means the iRhom2 levels even in the over-expressing variants may be nowhere near the optimal concentrations, and thus, a higher level of over-expression at both RNA and protein levels for Liv37k may eventually lead to a detectable amount of mature ADAM17 resulting from increased bioavailability of the carrier iRhom2.

Table 4.2 Relative upregulation of iRhom2 at both RNA and protein levels in PE/CA-PJ15 and Liv37k

	PE/CA-PJ15	Liv37K
Upregulation of iRhom2 at RNA level	X 350	X 40
Upregulation of iRhom2 at protein level	X 12	X 150

4.3.3 shRNA knock-down of RHBDF2 reduces iRhom2 and ADAM17 protein expression

The most pronounced level of knock-down was demonstrated in the PE/CA-PJ15 cell lines (to approximately 0.05 X the level in the parental cell line; 0.01 X the over-expressing clone), with NOK cells also being successfully knocked down (0.2 X parental and 0.01 X over-expressing clone). However, although clones were antibiotic resistant, the Liv37k knock-down did not reduce iRhom2 protein levels. This finding, followed the same trend with overexpression, and may therefore be due to general ease at transfecting the PE/CA-PJ cell line. In PE/CE-PJ15 cells, following shRNA knock-down of RHBDF2, the levels of immature ADAM17 protein are not affected, but the mature protein levels fall to 0.25 X overexpressing clone; in NOK cells there is a 2 x reduction of immature protein levels compared with the overexpressing clone but

this is approximately equivalent to the parental levels; As expected, no apparent change in Liv37K

A possible explanation would be that, since the knock-down cells are those which were previously overexpressing iRhom2, there is the possibility that an increased store of immature ADAM17 already available intracellularly will as a matter of fact take a longer time to become depleted, considering the fact that there is now less iRhom2 available following the shRNA knock-down to ensure trafficking away to the cell membrane. Indeed, (**Figure 4.13-Middle panel**) does show slightly more immature ADAM17 in the knock-down cells compared to their overexpressing variants.

4.3.4 Phenotypic effects of increased iRhom2

Over- or under-expression of iRhom2 did not appear to affect cellular proliferation. However, increased iRhom2 expression caused PE/CA-PJ15 cell lines to become slightly more spindle shaped when at low density. This phenotype may be associated with increased motility and was tested in scratch assays. No changes in morphology were observed in NOK and Liv37k cells following changes in iRhom2 expression. Increased rate of cell migration following upregulation of iRhom2 was observed with the PE/CA-PJ15 and LIV37K cell lines, but not the NOK cell lines which are also non-cancerous. The rate of migration equally reduced with reduced iRhom2 expression following subsequent shRNA knock-down of RHBDF2. The fact that earlier experiments on rate

of proliferation showed proliferation rates remained largely unchanged following upregulation or indeed down-regulation of iRhom2, indicates data on migration are likely not influenced by changes in cell proliferation. Considering the two cancer cell lines, recall that the real impact of upregulation of RHBDF2 on iRhom2 protein expression has been earlier shown to be more marked with Liv37k cells compared to PE/CA-PJ15 cells. Here, comparing rates of migration between parental cells and over-expressing variants, there is equally a slightly more pronounced change in rate of migration with Liv37k cells compared to PE/CA-PJ15. Liv37k over-expressing cells closed completely at 0.529 X the time taken for their parental cell to close up, while over-expressing PE/CA-PJ15 cells took a slightly higher 0.563 X the time for their parental cells to close the void. This may therefore imply that iRhom2 will likely play a key role in tumour cell (considering there was upregulation of iRhom2 had no noticeable influence on rate of migration in NOK cells) migration. Whether or not the mature form of ADAM17 plays a role in migration as does iRhom2, at this point can only be speculative, considering we were unable to measure changes in mature ADAM17 in Liv37k cell. It does appear mature ADAM17 plays a role in migration with PE/CA-PJ15, but this will require confirmation with Liv37k or any other HNSCC cancer cell line. Of the two cancer cell lines analysed, PE/CA-PJ15 showed some measure of increased proliferation with upregulation of iRhom2, but this was not the case with LIV37K in which the trend seemed to be slightly reversed. For the non-cancer NOK cell lines, various strains grew in similar fashion.

CHAPTER 5:

DISCUSSION

5 DISCUSSION

5.1 Introduction

The experiments described in this thesis were designed primarily to investigate the possible roles of iRhom2 in the pathogenesis of head and neck cancers. Particular interest has been channelled at the sheddase, ADAM17. We have used the squamous cell carcinoma variants of head and neck cancers, which are known to form the vast majority (over 90%) of head and neck cancers in terms of histologic classifications[335]. Expression of iRhom2 and ADAM17 proteins was investigated in two cohorts of HNSCC tissues using Western blotting and IHC (on a previously constructed TMA)[326], followed by correlation with clinicopathological features including recurrence and survival. The results obtained led to in vitro cell line work in which RHBDF2, which codes for iRhom2, was upregulated, and then down-regulated with shRNA knock-down, to determine possible changes in functional characteristics such as growth and migration as a result of deregulation of iRhom2.

This chapter will summarise the observations made, and discuss, limitations, challenges and future experiments aimed at better understanding of the role of iRhom2 in head and neck cancer.

5.2 Summary of findings

I have shown, by Western blot, that iRhom2 is often upregulated in head and neck squamous cell carcinomas, in comparison to adjacent normal tissues ($p<0.05$) and

that ADAM17 is also upregulated in these tissues. In particular, it should be noted that the levels of the immature, inactive form of ADAM17, in which the protein is stored in the cytoplasm are not significantly different between tumour and non-tumour cells, but the mature form is upregulated in tumour cases.

iRhom2 expression in oral squamous cell carcinoma correlated with survival ($p<0.05$), but not with any other clinicopathological features such as extracapsular spread, tumour size and recurrence.

In in vitro studies, cancer cell proliferation was not shown to be directly influenced by deregulation of iRhom2, with similar growth rates being observed in wild type cells and their variants, over- or under-expressing iRhom2.

However, upregulation of iRhom2 in established cancer cells increased their rate of 2D migration in a wound healing assay, but did not confer a similar advantage to a non-cancerous oral epithelial cell line.

An important finding was the observation of an increase in the level of expression of the mature (active) form of ADAM17, following upregulation of iRhom2 in the PE/CA-PJ15 cells. The immature pool of the protein was also shown to be increased following upregulation of iRhom2.

5.3 iRhom2 expression in head and neck squamous cell carcinoma

It has been demonstrated previously that iRhom2, while being highly expressed by some tissue types such as macrophages and those involved with secretory

functions[336], is expressed at very low levels or not at all in other tissues. It is a possibility that some others may either express it in very low amounts or not at all[337]. My western blot data using proteins extracted from tumour and normal tissues demonstrates variation in levels of expression across the two tissue types, with some specimens not expressing iRhom2 and others showing strong protein expression. In general, I noted increased expression of iRhom2 in tumour, compared with adjacent normal tissues. It is possible that it is not the epithelial-derived carcinoma cells that are expressing iRhom2 in these tissues, but that our data is due to infiltrating tumour associated macrophages in the cancer tissues. Data on iRhom2 expression is still relatively scarce, and not much has been published on iRhom2 localisation in cells. Zettl et al demonstrated over-expressed iRhom2 to be predominantly localised to the ER[316], and a large pool also shown to be cell membrane localised according to Maney et al[338]**.** The suggestion that increased iRhom2 might originate from surrounding immune cells remains to be substantiated. Previous data has however shown increased expression of iRhom2 in macrophages[328], suggesting cancer cells alone may not be the source of the increased measurements. To investigate this possibility, I undertook IHC staining of a TMA containing cores for 107 HNSCC tumours. However, majority of the cores stained negative for iRhom2, possibly due to the relative small amount of the protein in the cells. The few positive staining cores were those derived mainly from salivary and secretary tissues as suggested by the protein data base[339]. The lack of IHC data therefore makes it speculative to affirm that the cancer-derived epithelial cells are the origin of the iRhom2 expression in my western blot data. All of these claims will require further investigations discussed later.

5.4 Increased expression of iRhom2 and its effect

The rhomboid protein, iRhom2 has been implicated in carcinogenesis previously[325,340]. Ongoing research keeps shedding light on the exact mechanisms by which this happens. Like many other signalling proteins, mechanisms of action may not be exactly stereotyped, but varying from cell to cell or influenced by a combination of other factors / associated signalling molecules. Distinct mechanisms / pathways have been put forward to explain the role of iRhom2 in cancer. One has to do with mutation of *RHBDF2*, the gene which codes for iRhom2. In one study, and typically, it was shown that missense mutation of the *RHBDF2* gene was the main underlying cause of Tylosis with oesophageal cancer[322]. Gain-of-function mutations in the N-terminal domains of iRhom2 have been shown to enhance the stability of the short-lived protein[330]. This increased stability may augment its function E.g. in EGFR signalling and maybe ADAM17 trafficking and activation, leading to cancer formation or progression[341-343], with EGFR signalling and ADAM17 signalling already implicated in carcinogenesis[344,345346347].

I was able to demonstrate increased iRhom2 and ADAM17 expressions in cancer, using clinical tissues, though the increased expression of IRhom2 did not necessarily correspond with that of ADAM17. That is, some samples with increased iRhom2 expression did not necessarily show increased ADAM17 expression. This observation may be due to a number of reasons. It is a possibility that the upregulated iRhom2 in HNSCC is channelled into other signalling pathways other than via ADAM17[306,330], with EGF[330] and Thrombomodulin[306] and EphrinB3[348] (both with EGF-like domain), already known to be substrates for iRhom2.

5.4.1 Upregulation of iRhom2 leads to increased expression of ADAM17

Increased expression of both mature and to a lesser extent, the immature form of ADAM17 was observed in cell lines following upregulation of iRhom2. This is in keeping with published work which implicates iRhom2 in the intracellular trafficking of ADAM17 and therefore its activation and bioavailability for action at the cell membrane[219,349,350]. Thus, the increased expression of the mature ADAM17 in cell lines over-expressing *RHBDF2* is likely due to increased availability of iRhom2. This is corroborated by the observation that shRNA knock-down of *RHBDF2* in the overexpressing variants also produced reduced expression of mature ADAM17. Increased expression of the immature form was also demonstrated but was less marked compared to that with the mature form, raising questions as to whether the control of expression is both transcriptional as well as post-translational. Upregulation of iRhom2 caused about three-fold increment in expression of mature ADAM17, compared to about 60% increment for the inactive form. A lesser impact on the immature form is likely due to the fact that, there is already a highly detectable amount of the immature form (densitometry value of 52 for the immature compared to a value of 3 for the mature, following western blot on PE/CA-PJ15), such that increased availability of the trafficking protein, iRhom2, may not generate an overwhelming need for more immature ADAM17. The need will only probably arise when the immature pool is further depleted and approaches a certain baseline level to generate feedback. This is still speculative as there are currently no published work to support this hypothesis. It was observed that a sustained elevated level of the immature form of ADAM17 was present following shRNA knock-down of *RHBDF2* in

the cancer cell line, PE/CA-PJ15, but not in the non-cancerous cell line, NOK. It may be that, the sustained levels of immature ADAM17 in the cancer cell line following downregulation of iRhom2 is due to unavailability of the trafficker, iRhom2, to deplete the pool of immature ADAM17. The level therefore remains sustained over time pending gradual depletion. The different observation in NOK cells may simply be related to the timing. The cell lines do not proliferate at the same rate, with PE/CA-PJ15 doubling almost three times faster. There is therefore a longer time interval between overexpression and knock-down of RHBDF2 and harvest of the cells for analysis, and this may be sufficient for the NOK cells to deplete the pool of immature ADAM17 with its reduced levels of iRhom2. This aspect of my work validates available data suggestive of the influence of iRhom2 in the maturation / activation / increased bioavailability of ADAM17. In a study by Yang et al, and using *Uncovered* (hairless) mice to study the role of iRhom2 in hair follicle differentiation, iRhom2 mutation (deletion) was shown to disturb both maturation of ADAM17 and activation of Notch1. This lead to decreased hair proliferation as well as decreased hair shaft differentiation[351].

5.4.2 Effect of iRhom2 on migration.

The expression of iRhom2 and ADAM17 was determined in 6 head and neck cell lines, 4 of which were relatively low passage, and an immortalised normal oral keratinocyte cell line (NOK). Both PE/CA-PJ15 and PE/CA-PJ41 were shown to highly express

iRhom2 and the mature (active) form of ADAM17, while levels were intermediate or low in the low passage cancer and NOK cell lines. Upregulation of iRhom2 in two cancer cell lines and NOKs produced an increased rate of migration, in the form of wound closure, in each of the cancer cell lines that was not as obvious in the NOK cells. This observed increase in rate of migration is not likely due to increased proliferation as cell number assays did previously demonstrate that over-expression of iRhom2 does not alter the rate of change of cell number. Conversely, knock-down of iRhom2 in these over-expressing cell variants reduced migration below the wild-type level. These data implicate activation of the iRhom2-ADAM17 pathway in the pathogenesis of head and neck cancers, and that this system works by influencing or increasing rate of cell migration. Some studies have suggested a proliferative role for iRhom2[349,352], and this would be expected considering its role in EGFR ligand processing, but this is not verified by the current study. Our assay, investigating increased iRhom2 and its effect on cell proliferation did not show a consistent difference in rate of proliferation following upregulation of iRhom2. Brook et al, in their experiment made an attempt to outline a molecular basis for this increased proliferation, with a focus on iRhom2/ADAM17/EGF-family signalling. They used previously immortalised keratinocyte cells obtained from a male and female TOC patients, with already established TOC-associated iRhom2 mutation, and compared these with control keratinocyte cells without the TOC-associated iRhom2 mutation. They were able to demonstrate increased ADAM17 maturation and activity, represented by increased shedding of ADAM17 substrates such as TNFα, Amphiregulin, TGFα and HB-EGF, which were all up-regulated in the TOC keratinocyte cells[349]. The increased shedding was also shown, expectedly, to be abolished

following siRNA knock-down of ADAM17. The mRNA transcript levels of the listed ADAM17 substrates were found to be unaffected following the siRNA knock-down of ADAM17[349], signifying a rather post-translational level of impact, thereby verifying functional changes due to substrate shedding and not from the gene or transcriptional level.

In their experiment with hematopoietic cells, Maretzky et al, demonstrated the essential role of iRhom2 in the activation and substrate selectivity of ADAM17 dependent substrate shedding[352]. They showed that, although the bioavailability of mature ADAM17 remained unaffected following iRhom2 knock-down, the available mature ADAM17 was unable to initiate stimulated shedding of substrates such as HB-EGF and KitL2, but not others such as TGFα and ICAM[352].

5.4.2.1 The mechanism of cell migration

Cell migration is an important multistep cellular activity, vital throughout the lifespan of a cell / tissues. It is important in embryonic morphogenesis, tissue repair and regeneration, and even in disease progression including cancer. Several molecules have been suggested to play key roles in cell migration, ranging from GTPases, kinases, cytoskeleton-modifying proteins and motor proteins[353]. Mechanisms of cell migration are generally known to be highly diverse, with the peculiar mode adopted by a cell / tissues depending on cell type, stage of differentiation and the nature of the microenvironment. The modes / mechanisms are classified as mesenchymal or

amoeboid in form[354,355]. It is equally suggested that cells may adopt a different mode or switch from one mode to another in response to environmental peculiarities and cellular changes[356]. The various mechanisms / modes may share a common basis, considering the fact that Actin, named as an important molecule for migratory activities is implicated in both the mesenchymal and amoeboid mechanisms[357,358]. It is believed that cells, including cancer cells establish specialised protrusive structures which communicate with the extracellular matrix to ensure migration. For this purpose, in cancer cells, EGFR has been shown to play a central role, with its expression shown to correlate with increased chemotactic function[359]. ADAMs, already well documented for their roles in proteolytic activities and indirect involvement in cell adhesion, are also implicated in tumour cell migration. Taking together, with iRhom2 playing a central role in the processing and activities of both proteins, we may be able to suggest a possible explanation to the observed increase in cell migration following over-expression of iRhom2 and ADAM17[360].

Our study does show that indeed iRhom2 is upregulated in HNSCC, and that this upregulation does bring about an increase in the rate of cell migration, but not necessarily proliferation or growth. We have also been able to show that there exist a relationship between iRhom2 and ADAM17. We conclude therefore that, iRhom2 deregulation is implicated in carcinogenesis and suggest that the mechanism has to do with upregulating pathways that are directly or indirectly involved with cell motility. More work is required to completely unravel this, but our evidence is significant enough to provoke additional experiments in this line of questions.

5.4.3 Upregulation of iRhom2 affects cell morphology

Upregulation of iRhom2 was demonstrated to produce obvious phenotypic changes in PE/CA-PJ15 cells, but these changes were not observed in LIV37K or NOK cells. The overexpressing PE/CA-PJ15 variants were found to be slightly more spindle-like in shape. The wild type are typically spindle-like in culture, especially noticeable when less confluent. The spindle-like structures appeared to be more prominent in the upregulated cells.

Cells generally find themselves in multi-signalling microenvironments where several factors and molecules are involved in the control of their shape during migration[361], with cell migration leading to cancer spread[362]. During migration, cells may change shape with outward protrusions towards a stimulus, especially when these are external (extracellular)[363]. The iRhom2-ADAM17 axis has been implicated in Notch signalling, with signalling in the form of cell-to-cell, where ligands from one cell are attracted and bind to transmembrane receptors of neighbouring cells[184]. This will therefore likely require the protrusion of one cell towards another to establish a binding complex between Notch receptors and their ligands.

5.4.4 EGFR signalling and the influence of iRhom2 and ADAM17

EGFR signalling and the role iRhom2 and ADAM17 play has attracted a lot of attention. In this study, we conclude that iRhom2 and ADAM17 are upregulated in head and neck cancers. We propose that upregulation of iRhom2 facilitates intracellular trafficking of ADAM17 thereby increasing its shedding activities on

signalling molecules that may be oncogenic. In cases were upregulation of ADAM17 has not been shown to correlate with upregulation of the mature form of ADAM17, as demonstrated with a number of clinical tissues, the working mechanism of iRhom2 may be via an alternative pathway such as EGFR signalling through direct regulation of EGF.

5.4.4.1 EGFR signalling pathway

In animals, vertebrates and invertebrates alike, epidermal growth factor receptor (EGFR/ErbB) pathway is known to play key roles in cell-cell interactions. Cell fate determination is one of the important roles it plays and in C.elegans and Drosophila, the EGFR pathway has been linked with the formation of compound eye and vulva[364]. Four layered orthologs of the EGFR pathway are known in vertebrates, participating in cell fate determination and cell proliferation. Mutations involving these have also been known to cause human cancers including head and neck cancers[365]. Four members of the ErbB lineage of proteins, namely ErbB1-4 make up the human EGFR family[365]. This group of receptors are generally structured to consist of three main domains, an extracellular glycosylated domain, a transmembrane domain which is hydrophobic, and an intracellular domain. The intracellular domain also consists of a juxtamembrane segment, a protein kinase part and a carboxyterminal tail[365].

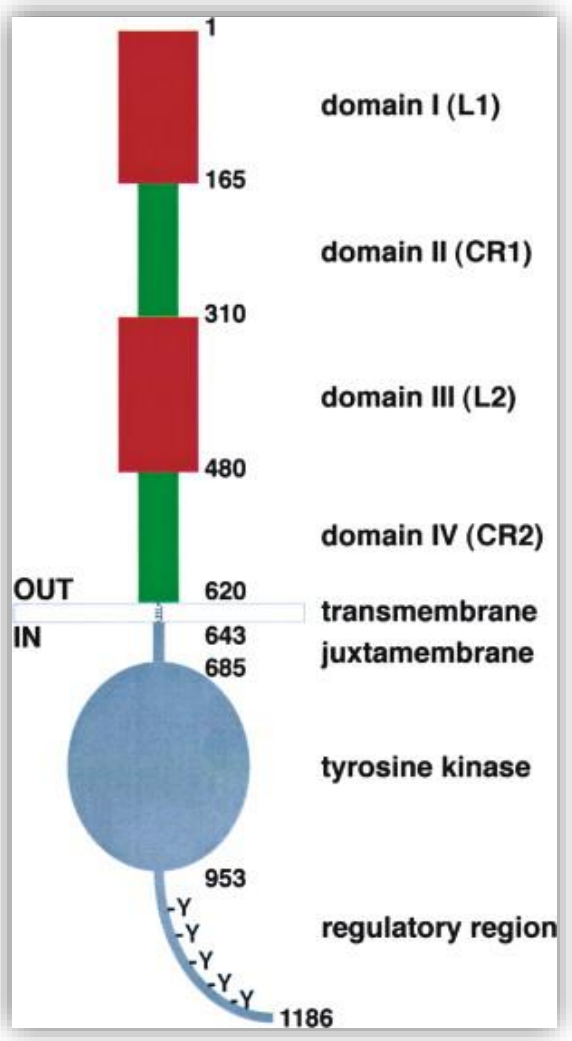

Figure 5.1 Illustration of the domain structure of the typical EGFR[366]

5.4.4.2 EGFR ligands

Seven ligands are known to bind to EGFR, including epidermal growth factor and transforming growth factor α (TGFα). The binding of ligands such as the growth factor to EGFR leads to an extensive conformational change which also involves the exposure of a dimerization arm in its extracellular domain. Following this, its intracellular domain also acquires a conformational change in which an asymmetric

homodimer, similar to that by cyclin and cyclin-dependent kinase, is formed. Subsequent downstream pathways targeted by this ligand-EGFR binding and conformational changes include, the PKB pathway (phosphatidylinositol 3-kinase / AKt), Ras/Raf/MEK/ERK 1/2 pathway and the phospholipase C (PLCy) pathway[365] (**Figure 5.3**).

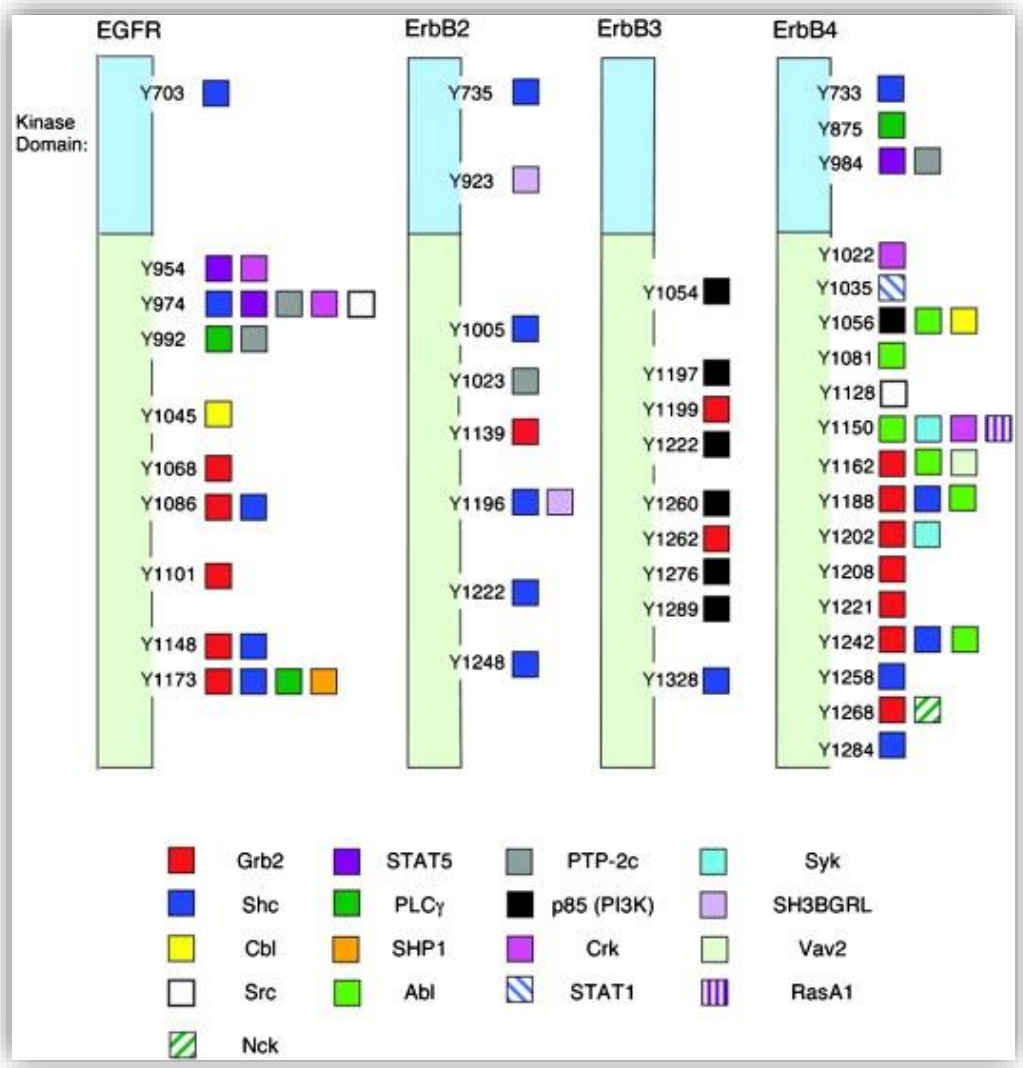

Figure 5.2 Signalling by the ErbB/HER family:

Signalling by the ErbB/HER family. Tyrosyl phosphorylation sites and binding partners are shown. The residue numbers on EGFR correspond to the mature protein, with those of ErbB2/3/4 corresponding to the nascent protein including the signal peptides[365,367].

5.4.4.3 EGFR ligand processing and ADAM17

Associated ligands are single-pass integral membrane proteins. These generally exist in precursor forms and are processed into secreted active forms to enable subsequent binding to their respective corresponding receptors. These ligand precursors are known to be cleaved or shed by the ADAM metalloproteases (ADAM10 and 17)[231] as part of their activation process, a posttranslational switch necessary for the regulation of the activities of such ligands[364] (**Table 5.1**). Apart from ligand processing, the ADAMs also participate in the processing of the membrane receptors.

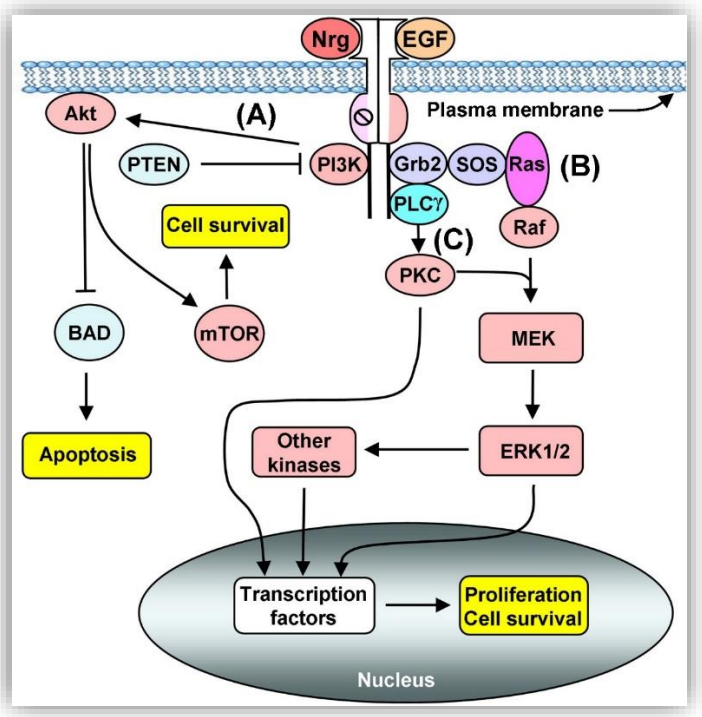

Figure 5.3 Overview of ErbB family signaling:

Overview of ErbB family signaling depicting the main downstream signaling modules. Adopted from Robert Roskoski[365].

5.4.4.4 EGFR signaling and IRhom2

Our study is already based on the theory that the role of iRhom2 in the pathogenesis of head and neck cancer is via the partnership with ADAM17 which likely leads to the increased shedding of notch, with subsequent effect on downstream target genes. In close connection with all this is the EGFR signaling pathway. On the basis of our results, there is a strong argument that the working hypothesis is true. The fact that some of our results from the use of clinical tissues did not exactly follow this trend means we have been forced to imagine that adjuvant and related pathways may exist, in which iRhom2 or iRhom2 and ADAM17 play a significant role, to ultimately drive carcinogenesis. For now, the closest culprit will be the EGFR pathway. The rhomboid family of proteins were discovered in close connection with EGF signaling[283] and as stated earlier, now shown to be key in the activation of EGFR. If indeed certain head and neck cancer tissues do not express significant amount of active ADAM17, in the presence of considerable iRhom2 expression, then the upregulated iRhom2 may be channeled into an alternative pathway independent of ADAM17. We suggest this may be direct interaction between iRhom2 and the EGF. This does not negate the fact that ADAM17 is involved with the shedding of ligands of EGFR, earlier highlighted.

Table 5.1 Ligands for ErbB family and their corresponding sheddases[231,368].

Ligand	Sheddase
Amphiregulin	ADAM17
Betacellulin	ADAM10
EGF	ADAM10
Epigen	ADAM17
Epiregulin	ADAM17
HB-EGF	ADAM17
TGFα	ADAM17
Nrg-1	ADAM17

5.5 Upregulation of iRhom2 is not sufficient to initiate cancer or increase rate of cell migration

Our study has shown that in the absence of underlying cancer, increased levels of iRhom2 may not necessarily confer malignant phenotype. iRhom2 was successfully upregulated in the non-cancer cell lines, NOK, but whereas the upregulation did result in increased rate of migration in the established cell lines, the NOK cells remained unchanged. This is understandable especially when this point is compared with the previous in which cell lines with the higher baseline expression of iRhom2 did not necessarily migrate the fastest. There has to be underlying cancer for the

effect of upregulation of iRhom2 to be felt on rate of migration. This means that certain cells of the body will be safe to have a high expression of the protein and not become cancerous. Indeed, it has been shown that certain cells such as macrophages do have a high baseline expression of iRhom2, and iRhom2 has been shown to be upregulated in secretory cells and pathways. It is therefore likely that the increased iRhom2 is channelled into an already available or constituted pathway in cancer, which is possibly absent or in subnormal levels in normal cells. In addition, already established factors such as loss of cell cycle control and defects in the DNA damage repair mechanism, may not be related to increased iRhom2, and yet important for cancer to be established in cells. Again, this may be towards trafficking of ADAM17 which has already been demonstrated to be upregulated in cancer, or indeed some other pathway such as the EGFR pathway.

5.6 iRhom2 expression in tumour tissues correlates with patient survival.

We were able to demonstrate a correlation between high iRhom2 expression on Western blot analysis and poor patient survival, using the Kaplan-Meier test. Considering data from migration experiments in **section 4.2.6.2,** and the suggestion that increased iRhom2 may be associated with increased migration in cancer cells, the association between poor patient survival and increased iRhom2 expression may therefore have everything to do with migratory regional spread. Oral cancer may not metastasize too frequently but spread to regional sites such as regional lymph nodes

does contribute to poor patient survival. Indeed, the fact that increased iRhom2 has not been associated with increased proliferation, following data in **section 4.2.6.1**, it will be correct to hypothesise that the associated poor patient survival is due to migration to regional sites rather than tumour mass expansion. Apart from correlation with poor patient survival, there was a lack of correlation with other clinicopathological factors that are also often associated with poor survival, such as recurrence, tumour size and extracapsular spread. This again is suggestive that the main morbidity factor might have to do with regional spread rather than tumour size, but this will require further research. A key area will be to consider the iRhom2 protein content of tumours with nodal involvement against those without. A marked difference in levels of iRhom2 expression in both subsets will increase the prospect of improved management of oral cancer cases, with therapy targeted at iRhom2 protein to prevent or slowdown rate of infiltration to regional lymph nodes. From the TMA data no correlations were observed between ADAM17 expression and clinicopathological data. There was no acceptable iRhom2 data from this methodology. It should be appreciated that the antibody used to generate the TMA data does not discriminate between mature (active) or immature (inactive) ADAM17, so we may have been assaying the immature, rather than the functional form.

5.7 Future experiments

Our current data has shown that iRhom2 and ADAM17 are upregulated in HNSCC and that upregulation of iRhom2 correlates with poor patient survival, indicating poor prognosis. We have also been able to show that upregulation of iRhom2 in cancer cell

lines leads to a higher rate of tumour cell migration, which is equally abrogated following downregulation of iRhom2. There is evidence from our study, that upregulation of iRhom2 leads to increased expression of both forms of ADAM17, particularly its mature form.

Moving forward, it is important to carry out several repeats of some of the experiments in this study by way of validating the results obtained. There is also the need to extend the scope of work in an attempt to discover other signalling partners to iRhom2 and alternative pathways that may be involved in sustaining tumorigenesis. A classical alternative pathway is the EGFR pathway. Therefore, for future experiments, analysis of cohort of clinical samples would include probing for iRhom2, ADAM17 and EGF / EGFR. In that case, there would be an attempt to demonstrate increased EGFR signalling where ADAM17 is low, in tumour samples with increased IRhom2 expression. Indeed, the case might also be that there is increased EGFR signalling in the presence or absence of increased ADAM17.

The intracellular distribution of iRhom2 and ADAM17 needs to be studied more, to aid understanding of intracellular movements of both proteins. There is the need to enlarge the cohort of clinical tissues for the part of the study involving analysis of tumour and their paired normal tissues, and the TMA part further optimised for possible positive results for iRhom2 and more specific results for ADAM17. More assays, particularly 3D assays, and co-culture with fibroblasts are required for migration and proliferation work to make them more objective.

5.7.1 TMA experiments

Further optimisation of the TMA experiment is required. Emphasis will be towards being able to correctly detect iRhom2 and ADAM17. Firstly, it will be important to employ samples from the same patients whose tissues are also analysed on western blot. This way, a close correlation between both should be expected and serve as a means of validation of results on both sides (western blot and use of TMA). Also, very key will be the use of highly specific primary antibodies. Antibodies specific enough to select between the two forms of ADAM17 (mature and immature) when used on the TMA cores, and specific enough for iRhom2 (isoform 1 & 2). As earlier highlighted, it is expected that the mature form of ADAM17 will be localised to the cell membrane, while the immature pool remains cytoplasm localised. But again, this may not always be distinctly the case, as the mature form which obtains its maturation in the Golgi apparatus and get trafficked to the cell membrane may also be spotted in some amount in the cytoplasm before it makes its way to the cell membrane. Two sets of identical TMAs, separately stained with highly selective ADAM17 antibodies for the two forms should show different staining patterns to differentiate the two scenarios. For iRhom2, success will greatly depend on the quality of the antibody utilised, specific enough for the correct isoform, and able to detect the rather relatively minutely expressed iRhom2 (isoform2).

5.7.2 Western blot experiments with clinical tissues

The clinical tissues came in varying sizes, and this is understandable as the size of excised tissue will depend on tumour size ab initio, and this will usually undergo further rationing to save portions for other forms of investigations. A good number of the paired normal tissues were particularly small, some too small to be used. Obtaining protein from tissues (unlike cells) for western blot analysis requires a sizeable chunk of about 5mm³, as was the case in this experiment. After initial tissue handling to enable histology, some of the samples were no longer sufficient to have as much as 5mm³ excised from them. Equally, in some cases, the 5mm³ tissue was not sufficient to produce enough total protein to match protein from other samples in terms of total protein concentration. We therefore adopted a different approach enumerated earlier, for normalisation purposes. Moving forward therefore, it will be of great benefit recruiting only tissues big enough to produce enough and highly concentrated protein samples.

The ratio of tumour to normal tissues needs to be as close as possible to make comparison fair enough in terms of frequency. The general sample size may also be increased to about thrice the number used in this experiment to further validate our findings. To make analysis as objective as possible, all protein samples may be extracted from tissues within a very short interval, assembled and analysed on western blot the same day with similar conditions.

A large enough sample size means that there might be the possibility of assessing expression in tissues from a particular tumour site and have data that will be statistically relevant. For instance, if the entire samples size is in the range of 300,

there might be about 100 tongue tumour samples, in which case expression among tongue tissues may be effectively compared. And this will ensure correlation with clinicopathological data is more direct as comparison will be made against expression protein from tissues taken from the same sub-site. This is important, giving that evidence has already shown that tissues express iRhom2 in varying amounts, and that some tissues may not express the protein. For instance, tissues from patients, all with recurrence, but obtained from different sites may show different levels of iRhom2 expression, even if the protein were possibly implicated in recurrence. This is because, the role iRhom2 plays may vary from cell to cell, as well as, the pathogenesis or molecular basis of the same squamous cell carcinoma may vary from site to site in the oral cavity or head and neck region. If therefore tissues from the same site, such as lip are analysed together and compared against clinicopathological data, there is that sense that the baseline expression of the protein in lip tissues are similar ab initio and prior to carcinogenesis. This may be verified to a large extent by the use of the expressing levels in the accompanying paired normal tissues. It will be considered worthy having greater pathological input into tissue selection, for example, if the tumour has infiltrating macrophages. This will help to decipher all the sources of iRhom2 protein following analysis. Laser capture microdissection (LCM) will also be considered to ensure cell specificity and equally aid investigation into source of protein expression.

5.7.3 Expanding experiment with cell lines.

Our results, based on two cancer cell lines and a non-cancer cell line produced results that need to be further verified as the case, in two or three additional cell lines. Recruiting in similar fashion, one with a significant level of baseline expression of iRhom2, one with a moderate expression level, and a non-cancer cell line with any level of iRhom2 expression.

Probing for more partners will also open a window into understanding mechanism by which iRhom2 is involved with tumorigenesis. Suggested earlier, EGF or any of its downstream pathway products may be investigated in line with iRhom2 expression following deregulation of the same.

The use of ADAM17 inhibitors such as KP-457[369] to show whether ADAM17 is required for migration when iRhom2 is overexpressed will be considered.

Proteomic or transcriptomic experiments on the cell lines will be useful to find out what other proteins are affected by upregulation of iRhom2.

If iRhom2 is key for intracellular trafficking of ADAM17, shRNA knock-down of ADAM17 may produce a negative feedback to upregulate iRhom2. shRNA knock-down of ADAM17 may therefore be looked into to further verify a working relationship with the two proteins. Overexpressing ADAM17 may not be of any significance considering the general level of expression of the immature form. It appears to be adequately expressed and there might be the existence of a threshold, above which there may be no significant difference in iRhom2 expression. It will

however be important to verify the level of control on ADAM17 arising from upregulation of iRhom2, whether transcriptional or post-translational.

5.7.4 Migration and proliferation assays, and other functional studies.

Given that some interesting and notable findings have come out of the migration assay of our experiment, it will be important to expand the scope by conducting additional functional assays such as adhesion assay and migration through a membrane or barrier. Examples include transmembrane assays[370] and migration through 3D matrigel[371] to depict invasion through basement membranes by OSCC cells. The migration assay may also be improved upon by enlisting a 3D version. This way, cell migration is multidirectional as the case is in vivo, therefore a more representative approach. Co-culture of the various cell strains with fibroblast will also come as an additional method to evaluate cell growth and migration.

A proposed cell proliferation assay will involve, seeding of cells to achieve discrete colonies of about the same number of cells with each cell variant. That way, a regular count will define a precise rate of growth of cells. An animal tumorigenesis model will also be useful, to investigate possible increase in tumour size with nude mice, following iRhom2 over-expression. A similar model was used by Nicolai et al[372] to investigate expression of αvβ3-integrins in OSCC.

A recent study reemphasised the importance of iRhom2 for ADAM17 trafficking and activation. It was also demonstrated that phosphorylation of iRhom2 is required for

this trafficking / activation function[350]. Therefore for future experiments, phosphorylation or inhibition of phosphorylation of iRhom2 in relation to ADAM17 expression and cell phenotype will be an important aspect to investigate.

5.7.5 RNA analysis

RNA obtained from clinical tissues may be analysed real-time to evaluate levels of expression. This will help to throw more light into whether or not over-expression effect on ADAM17 is due to transcriptional rather than post-translational effect. Like protein expression, data may be used for correlation with clinicopathological data.

5.7.6 Effect of iRhom2 on EGF signalling

It will be important to ascertain if iRhom2 directly controlled the levels and bioavailability of EGF. Just as levels of ADAM17 following up and down-regulation of iRhom2 was investigated, EGF levels could be measured to demonstrate direct effect. In this case, an important arm of the experiment would be to carry out combined deregulation of iRhom2 and ADAM17 to ascertain which might be of more importance in EGF signalling. For instance, if up and down-regulation of both proteins does lead to increased and decreased expression of EGF respectively, to up-regulate one and down regulate the other, vice versa, will likely demonstrate which of ADAM17 or iRhom2 does have the direct effect on EGF signalling.

5.8 Conclusion

In conclusion therefore, we have been able to demonstrate upregulation of iRhom2 and ADAM17 in HNSCC using clinical tissues, with increased iRhom2 expression correlating with poor patient survival. We have also shown that increased expression of iRhom2 provokes subsequent increased expression of ADAM17, particularly its mature form, and the resultant increased expression of iRhom2 or iRhom2 and ADAM17 does lead to increased cancer cell migration, independent of increased rate of cell proliferation. On the basis of these data, we have been able to validate the initial hypothesis that iRhom2 plays a role in the pathogenesis of head and neck squamous cell carcinomas and that this role is in partnership with ADAM17. The need for further experiments to reaffirm our findings has also been emphasised.

References

1. The experimental study of tumor progression: A review. *Cancer Res*. 1954;14(5):327-339.

2. Hanahan D, Weinberg RA. Hallmarks of cancer: The next generation. *Cell*. 2011;144(5):646-674.

3. Kliewer A, Reinscheid RK, Schulz S. Emerging paradigms of G protein-coupled receptor dephosphorylation. *Trends in Pharmacological Sciences*. 2017;38(7):621-636. doi: https://doi-org.liverpool.idm.oclc.org/10.1016/j.tips.2017.04.002.

4. Roggiani F, Mezzanzanica D, Rea K, Tomassetti A. Guidance of signaling activations by cadherins and integrins in epithelial ovarian cancer cells. *International Journal of Molecular Sciences*. 2016;17(9):1-17.

5. Multhaupt HAB, Leitinger B, Gullberg D, Couchman JR. Extracellular matrix component signaling in cancer. *Adv Drug Deliv Rev*. 2016;97(1):28-40.

6. Zhang Q, Lao X, Huang J, et al. Soluble production and function of vascular endothelial growth factor/basic fibroblast growth factor complex peptide. *Biotechnol Prog*. 2015;31(1):194-203.

7. Lappano R, De Marco P, De Francesco EM, Chimento A, Pezzi V, Maggiolini M. Cross-talk between GPER and growth factor signaling. *J Steroid Biochem Mol Biol*. 2013;137(1):50-56.

8. Martinelli E, Morgillo F, Troiani T, Ciardiello F. Cancer resistance to therapies against the EGFR-RAS-RAF pathway: The role of MEK. *Cancer Treat Rev*. 2017;53(1):61-69.

9. A HIF-1 alpha-dependent autocrine feedback loop promotes survival of serum-deprived prostate cancer cells. *Prostate*. 2009;69(3):263-275.

10. Dreesen O, Brivanlou A. Signaling pathways in cancer and embryonic stem cells. *Stem Cell Reviews and Reports*. 2007;3(1):7-17.

11. Biphasic calcium response of platelet-derived growth factor stimulated glioblastoma cells is a function of cell confluence. *Cytometry Part A*. 2005;67A(2):172-179.

12. Nickerson NK, Mohammad KS, Gilmore JL, et al. Decreased autocrine EGFR signaling in metastatic breast cancer cells inhibits tumor growth in bone and mammary fat pad. *PLoS One*. 2012;7(1):1-13.

13. Sjöström S, Andersson U, Liu Y, et al. Genetic variations in EGF and EGFR and glioblastoma outcome. *Neuro-oncology*. 2010;12(8):815-821.

14. Slamon D, Clark G, Wong S, Levin W, Ullrich A, McGuire W. Human breast cancer: Correlation of relapse and survival with amplification of the HER-2/neu oncogene. *Science*. 1987;235(4785):177-182.

15. Nicholson RI, Gee JMW, Harper ME. EGFR and cancer prognosis. *European Journal of Cancer*. 2001;37(Supplement 4):9-15. doi: https://doi.org/10.1016/S0959-8049(01)00231-3.

16. Forbes SA, Bindal N, Bamford S, et al. COSMIC: Mining complete cancer genomes in the catalogue of somatic mutations in cancer. *Nucleic Acids Res*. 2011;39(Database i):D945-D950.

17. Amin ARMR, Karpowicz PA, Carey TE, et al. Evasion of anti-growth signaling: A key step in tumorigenesis and potential target for treatment and prophylaxis by natural compounds. *Seminars in Cancer Biology*. 2015;35(Supplement):S55-S77. doi: https://doi-org.liverpool.idm.oclc.org/10.1016/j.semcancer.2015.02.005.

18. Kastan MB, Bartek J. Cell-cycle checkpoints and cancer. *Nature*. 2004;432(7015):316-323.

19. Weinberg RA. The retinoblastoma protein and cell cycle control. *Cell*. 1995;81(3):323-330. doi: https://doi.org/10.1016/0092-8674(95)90385-2 ".

20. Cobrinik D. Pocket proteins and cell cycle control. *Oncogene*. 2005;24(17):2796-2809.

21. Kerr JFR, Wyllie AH, Currie AR. Apoptosis: A basic biological phenomenon with wideranging implications in tissue kinetics. *Br J Cancer*. 1972;26(4):239-257.

22. Apoptosis in cancer: From pathogenesis to treatment. *Journal of Experimental & Clinical Cancer Research (17569966)*. 2011;30(1):87-100.

23. Novaleski CK, Carter BD, Sivasankar MP, Ridner SH, Dietrich MS, Rousseau B. Apoptosis and vocal fold disease: Clinically relevant implications of epithelial cell death. *Journal of Speech, Language & Hearing Research*. 2017;60(5):1264-1272.

24. Wu HJ, Pu JL, Krafft PR, Zhang JM, Chen S. The molecular mechanisms between autophagy and apoptosis: Potential role in central nervous system disorders. *Cell Mol Neurobiol*. 2015;35(1):85-99.

25. Elmore S. Apoptosis: A review of programmed cell death. *Toxicol Pathol*. 2007;35(4):495-516.

26. McIlwain DR, Berger T, Mak TW. Caspase functions in cell death and disease. *Cold Spring Harbor Perspectives in Biology*. 2013;5(4):1-28.

27. Ishizaki Y, Cheng L, Mudge AW, Raff MC. Programmed cell death by default in embryonic cells, fibroblasts, and cancer cells. *Mol Biol Cell*. 1995;6(11):1443-1458.

28. Giancotti FG, Ruoslahti E. Integrin signaling. *Science*. 1999;285(5430):1028-1032.

29. Zhang X, Li D, Wang H, Wu Y, Wen F. Elevated plasma cytochrome c levels in patients with chronic obstructive pulmonary disease. *Curr Sci*. 2016;110(8):1532-1535.

30. Scorrano L, Korsmeyer SJ. Mechanisms of cytochrome c release by proapoptotic BCL-2 family members. *Biochem Biophys Res Commun*. 2003;304(3):437-444.

31. Powell E, Piwnica-Worms D, Piwnica-Worms H. Contribution of p53 to metastasis. *Cancer Discovery*. 2014;4(4):405-14.

32. Fernald K, Kurokawa M. Evading apoptosis in cancer. *Trends Cell Biol*. 2013;23(12):620-633.

33. Pitti RM, Marsters SA, Lawrence DA, et al. Genomic amplification of a decoy receptor for fas ligand in lung and colon cancer. *Nature*. 1998;396(6712):699-703.

34. Judith Campisi, Ladislas Robert. Cell senescence, role in aging and age-related diseases. . 2014.

35. Blagoev KB. Cell proliferation in the presence of telomerase. *PLoS One*. 2009;4(2):e4622.

36. Cellular senescence and cancer. *J Pathol*. 1999;187(1):100-111.

37. Mortality and immortality at the cellular level. A review. *Biochemistry (Moscow) = Biokhimiia*. 1997;62(11):1180-1190.

38. Wegwitz F, Kluth MA, Mänz C, et al. Tumorigenic WAP-T mouse mammary carcinoma cells: A model for a self-reproducing homeostatic cancer cell system. *PLoS One*. 2010;5(8):1-22.

39. Counter CM, Avilion AA, LeFeuvre CE, et al. Telomere shortening associated with chromosome instability is arrested in immortal cells which express telomerase activity. *EMBO J*. 1992;11(5):1921-1929.

40. Klement K, Goodarzi AA. DNA double strand break responses and chromatin alterations within the aging cell. *Experimental Cell Research*. 2014;329(1):42-52. doi: https://doi-org.liverpool.idm.oclc.org/10.1016/j.yexcr.2014.09.003.

41. Jafri MA, Ansari SA, Alqahtani MH, Shay JW. Roles of telomeres and telomerase in cancer, and advances in telomerase-targeted therapies. *Genome medicine : Medicine in the post-genomic era*. 2016;8(1):1-18.

42. Wang Z, Dabrosin C, Yin X, et al. Broad targeting of angiogenesis for cancer prevention and therapy. *Seminars in Cancer Biology*. 2015;35(Supplement):S224-S243. doi: https://doi.org/10.1016/j.semcancer.2015.01.001.

43. Yihai Cao, Arbiser J, D'Amato RJ, et al. Forty-year journey of angiogenesis translational research. *Science Translational Medicine*. 2011;3(114):1.

44. Guo H, Vander Kooi CW. Neuropilin functions as an essential cell surface receptor. *The Journal of Biological Chemistry*. 2015;290(49):29120-29126.

45. Roskoski R. Vascular endothelial growth factor (VEGF) and VEGF receptor inhibitors in the treatment of renal cell carcinomas. *Pharmacological Research*. 2017;120(Supplement C):116-132. doi: https://doi-org.liverpool.idm.oclc.org/10.1016/j.phrs.2017.03.010.

46. Ferrara N. Timeline: VEGF and the quest for tumour angiogenesis factors. *Nature Reviews Cancer*. 2002;2(10):795-803.

47. Bull HA, Brickell PM, Dowd PM. Src-related protein tyrosine kinases are physically associated with the surface antigen CD36 in human dermal microvascular endothelial cells. *FEBS letters (Elsevier)*. 1994;351(1):41-44.

48. Wu M, Wu L, Chou C. The anticancer potential of thrombospondin-1 by inhibiting angiogenesis and stroma reaction during cervical carcinogenesis. *Gynecology and Minimally Invasive Therapy*. 2016;5(2):48-53. doi: https://doi-org.liverpool.idm.oclc.org/10.1016/j.gmit.2015.09.001.

49. Zhang X, Lawler J. Thrombospondin-based antiangiogenic therapy. *Microvascular Research*. 2007;74(2):90-99. doi: https://doi-org.liverpool.idm.oclc.org/10.1016/j.mvr.2007.04.007.

50. Santagiuliana R, Ferrari M, Schrefler BA. Simulation of angiogenesis in a multiphase tumor growth model. *Comput Methods Appl Mech Eng*. 2016;304(1):197-216.

51. Ribatti D, Crivellato E. Mast cells, angiogenesis, and tumour growth. *Biochimica et Biophysica Acta (BBA) - Molecular Basis of Disease*. 2012;1822(1):2-8. doi: https://doi.org/10.1016/j.bbadis.2010.11.010.

52. Stefanatos RKA, Vidal M. Tumor invasion and metastasis in drosophila: A bold past, a bright future. *Journal of Genetics and Genomics*. 2011;38(10):431-438.

53. van Zijl F, Krupitza G, Mikulits W. Initial steps of metastasis: Cell invasion and endothelial transmigration. *Mutation Research/Reviews in Mutation Research*. 2011;728(1–2):23-34.

54. Podsypanina K, Du YN, Jechlinger M, Beverly LJ, Hambardzumyan D, Varmus H. Seeding and propagation of untransformed mouse mammary cells in the lung. *Science*. 2008;321(5897):1841-1844.

55. Coghlin C, Murray GI. Current and emerging concepts in tumour metastasis. *J Pathol*. 2010;222(1):1-15.

56. Wells A, Grahovac J, Wheeler S, Ma B, Lauffenburger D. Targeting tumor cell motility as a strategy against invasion and metastasis. *Trends in Pharmacological Sciences*. 2013;34(5):283-289. doi: https://doi-org.liverpool.idm.oclc.org/10.1016/j.tips.2013.03.001.

57. Clark AG, Vignjevic DM. Modes of cancer cell invasion and the role of the microenvironment. *Current Opinion in Cell Biology*. 2015;36(Supplement C):13-22. doi: https://doi-org.liverpool.idm.oclc.org/10.1016/j.ceb.2015.06.004.

58. Nguyen DX, Massagué J. Genetic determinants of cancer metastasis. *Nature Reviews Genetics*. 2007;8(5):341-352.

59. E AA, A H, K AS, L JR. Signal transduction and signal modulation by cell adhesion receptors: The role of integrins, cadherins, immunoglobulin-cell adhesion molecules, and selectins. *Pharmacol Rev*. 1998;50(2):197-263.

60. Gill KS, Fernandes P, O'Donovan TR, et al. Glycolysis inhibition as a cancer treatment and its role in an anti-tumour immune response. *Biochimica et Biophysica Acta (BBA) - Reviews on Cancer*. 2016;1866(1):87-105. doi: https://doi-org.liverpool.idm.oclc.org/10.1016/j.bbcan.2016.06.005.

61. Adeva-Andany M, López-Ojén M, Funcasta-Calderón R, et al. Comprehensive review on lactate metabolism in human health. *Mitochondrion*. 2014;17(Supplement C):76-100. doi: https://doi-org.liverpool.idm.oclc.org/10.1016/j.mito.2014.05.007.

62. Jiang B. Aerobic glycolysis and high level of lactate in cancer metabolism and microenvironment. *Genes & Diseases*. 2017;4(1):25-27. doi: https://doi-org.liverpool.idm.oclc.org/10.1016/j.gendis.2017.02.003.

63. The metabolism of tumours: Investigations from the kaiser wilhelm institute for biology, berlin-dahlem. . 1930.

64. Jones RG, Thompson CB. Tumor suppressors and cell metabolism: A recipe for cancer growth. *Genes Dev*. 2009;23(5):537-548.

65. DeBerardinis RJ, Lum JJ, Hatzivassiliou G, Thompson CB. The biology of cancer: Metabolic reprogramming fuels cell growth and proliferation. *Cell Metabolism*. 2008;7(1):11-20. doi: https://doi-org.liverpool.idm.oclc.org/10.1016/j.cmet.2007.10.002.

66. Semenza GL. HIF-1: Upstream and downstream of cancer metabolism. *Current Opinion in Genetics & Development*. 2010;20(1):51-56. doi: https://doi-org.liverpool.idm.oclc.org/10.1016/j.gde.2009.10.009.

67. Vander Heiden MG, Cantley LC, Thompson CB. Understanding the warburg effect: The metabolic requirements of cell proliferation. *Science*. 2009;324(5930):1029-1033.

68. Kennedy KM, Dewhirst MW. Tumor metabolism of lactate: The influence and therapeutic potential for MCT and CD147 regulation. *Future Oncology*. 2010;6(1):127-148.

69. Vajdic CM, van Leeuwen MT. Cancer incidence and risk factors after solid organ transplantation. *International Journal of Cancer*. 2009;125(8):1747-1754.

70. Teng MWL, Swann JB, Koebel CM, Schreiber RD, Smyth MJ. Immune-mediated dormancy: An equilibrium with cancer. *J Leukoc Biol*. 2008;84(4):988-993.

71. Smyth MJ, Dunn GP, Schreiber RD. Cancer immunosurveillance and immunoediting: The roles of immunity in suppressing tumor development and shaping tumor immunogenicity. *Advances in Immunology*. 2006;90(Supplement C):1-50. doi: https://doi.org/10.1016/S0065-2776(06)90001-7.

72. Pagès F, Galon J, Dieu-Nosjean MC, Tartour E, Sautès-Fridman C, Fridman WH. Immune infiltration in human tumors: A prognostic factor that should not be ignored. *Oncogene*. 2010;29(8):1093-102.

73. Strauss DC, Thomas JM. Transmission of donor melanoma by organ transplantation. *The Lancet Oncology*. 2010;11(8):790-796. doi: https://doi-org.liverpool.idm.oclc.org/10.1016/S1470-2045(10)70024-3.

74. Loeb LA, Loeb KR, Anderson JP. Multiple mutations and cancer. *Proceedings of the National Academy of Sciences of the United States of America (PNAS)*. 2003;100(3):776-781.

75. Review: Histone methylation and the DNA damage response. *Mutation Research/Reviews in Mutation Research*. 2017.

76. Cartwright EJ. *Transgenesis techniques [electronic book] : Principles and protocols.* New York : Humana Press, 2009; 3rd ed. / edited by Elizabeth J. Cartwright; 2009. http://search.ebscohost.com.ezproxy.liv.ac.uk/login.aspx?direct=true&db=cat00003a&AN=lvp.b2588170&site=eds-live&scope=site; http://ezproxy.liv.ac.uk/login?url=http://dx.doi.org/10.1007/978-1-60327-019-9; http://ezproxy.liv.ac.uk/login?url=http://www.springerprotocols.com/doiresolver?genre=book&pid=10.1007/978-1-60327-019-9.

77. Kuhmann C, Li C, Kloor M, et al. Altered regulation of DNA ligase IV activity by aberrant promoter DNA methylation and gene amplification in colorectal cancer. *Hum Mol Genet*. 2014;23(8):2043-54.

78. LEVINE A. p53, the cellular gatekeeper for growth and division. *Cell*. 1997;88(3):323-31.

79. Deben C, Deschoolmeester V, Lardon F, Rolfo C, Pauwels P. TP53 and MDM2 genetic alterations in non-small cell lung cancer: Evaluating their prognostic and predictive value. *Critical Reviews in Oncology/Hematology*. 2016;99(Supplement C):63-73. doi: https://doi-org.liverpool.idm.oclc.org/10.1016/j.critrevonc.2015.11.019.

80. DeNardo DG, Andreu P, Coussens LM. Interactions between lymphocytes and myeloid cells regulate pro- versus anti-tumor immunity. *Cancer Metastasis Rev*. 2010;29(2):309-316.

81. Qian B, Pollard JW. Macrophage diversity enhances tumor progression and metastasis. *Cell*. 2010;141(1):39-51. doi: https://doi-org.liverpool.idm.oclc.org/10.1016/j.cell.2010.03.014.

82. Grivennikov SI, Greten FR, Karin M. Immunity, inflammation, and cancer. *Cell*. 2010;140(6):883-899. doi: https://doi-org.liverpool.idm.oclc.org/10.1016/j.cell.2010.01.025.

83. Ernani V, Saba NF. Oral cavity cancer: Risk factors, pathology, and management. *Oncology*. 2015;89(4):187-195.

84. Lee AWM, Lin JC, Ng WT. Current management of nasopharyngeal cancer. *Seminars in Radiation Oncology*. 2012;22(3):233-244. doi: https://doi-org.liverpool.idm.oclc.org/10.1016/j.semradonc.2012.03.008.

85. Babak Jahan-Parwar. Lip and perioral region anatomy. http://emedicine.medscape.com/article/835209-overview#a2. Updated 2013. Accessed 01/08, 2017.

86. Apostolos Christopoulos. Mouth anatomy. http://emedicine.medscape.com/article/1899122-overview. Updated 2015. Accessed 09/27, 2017.

87. Anatomy and physiology of the oral cavity. http://www.cancer.ca/en/cancer-information/cancer-type/oral/oral-cancer/the-mouth/?region=on. Accessed 09/27, 2017.

88. Eelam Aalia Adil. Tongue anatomy. http://emedicine.medscape.com/article/1899434-overview#a4. Updated 2016. Accessed 01/08, 2017.

89. Neil S. Norton, Frank H. Netter. Oral cavity, boundaries of the oral cavity. In: *Netter`s head and neck anatomy for dentistry.* 2nd ed. Elsevier Saunders; 2011:332-333-336, 374.

90. Tumuluri V, Thomas GA, Fraser IS. Analysis of the ki-67 antigen at the invasive tumour front of human oral squamous cell carcinoma. *Journal of Oral Pathology & Medicine*. 2002;31(10):598-604.

91. Jerjes W, Upile T, Petrie A, et al. Clinicopathological parameters, recurrence, locoregional and distant metastasis in 115 T1-T2 oral squamous cell carcinoma patients. *Head and Neck Oncology*. 2010;2(1):1.

92. RIVERA C, VENEGAS B. Histological and molecular aspects of oral squamous cell carcinoma. *Oncology Letters*. 2014;8(1):7-11.

93. Release C2. Head and neck cancer incidence by sex and UK. http://www.cancerresearchuk.org/health-professional/cancer-statistics/statistics-by-cancer-type/oral-cancer/incidence#heading-Zero. Updated 2016. Accessed January / 11, 2017.

94. Chi AC, Day TA, Neville BW. Oral cavity and oropharyngeal squamous cell carcinoma--an update. *CA - A Cancer Journal for Clinicians*. 2015;65(5):401-21.

95. Chaturvedi AK, Anderson WF, Lortet-Tieulent J, et al. Worldwide trends in incidence rates for oral cavity and oropharyngeal cancers. *Journal of Clinical Oncology: official journal of the American Society of Clinical Oncology*. 2013;31(36):4550-4559.

96. Buckley L, Gupta R, Ashford B, Jabbour J, Clark JR. Oropharyngeal cancer and human papilloma virus: Evolving diagnostic and management paradigms. *ANZ J Surg*. 2016;86(6):442-447.

97. Chang K, Chang Y, Wang LH, Tsai H, Huang W, Su I. Pathogenesis of virus-associated human cancers: Epstein–Barr virus and hepatitis B virus as two examples. *Journal of the Formosan Medical Association*. 2014;113(9):581-590. doi: https://doi-org.liverpool.idm.oclc.org/10.1016/j.jfma.2013.09.001.

98. Kim KY, Le Q, Yom SS, et al. Current state of PCR-based epstein-barr virus DNA testing for nasopharyngeal cancer. *Journal of the National Cancer Institute: JNCI*. 2017;109(4).

99. Sarwar N, Stebbing J, Bower M. Translational review of AIDS-related kaposi's sarcoma. *Update on cancer therapeutics*. 2007;2(1):53-60.

100. Tilakaratne WM, Klinikowski MF, Saku T, Peters TJ, Warnakulasuriya S. Oral submucous fibrosis: Review on aetiology and pathogenesis. *Oral Oncology*. 2006;42(6):561-568. doi: https://doi.org/10.1016/j.oraloncology.2005.08.005.

101. D'AGULHAM A,Clara Duszczak, CHAIBEN CL, de LIMA A,Adilson Soares, TORRES-PEREIRA C, MACHADO MÂN. Fanconi anemia: Main oral manifestations. *RGO: Revista Gaúcha de Odontologia*. 2014;62(3):281-287.

102. Prime SS, Thakker NS, Pring M, Guest PG, Paterson IC. A review of inherited cancer syndromes and their relevance to oral squamous cell carcinoma. *Oral Oncology*. 2001;37(1):1-16. doi: https://doi-org.liverpool.idm.oclc.org/10.1016/S1368-8375(00)00055-5.

103. Ellis A, Risk JM, Maruthappu T, Kelsell DP. Tylosis with oesophageal cancer: Diagnosis, management and molecular mechanisms. *Orphanet journal of rare diseases*. 2015;10(1):1-6.

104. Ali J, Sabiha B, Jan HU, Haider SA, Khan AA, Ali SS. Genetic etiology of oral cancer. *Oral Oncol*. 2017;70(1):23-28.

105. Mouth cancer. http://www.macmillan.org.uk/information-and-support/head-and-neck-cancers/mouth-cancer. Updated 2016. Accessed 09/04, 2017.

106. Leemans CR, Braakhuis BJ, Brakenhoff RH. The molecular biology of head and neck cancer. *Nature Reviews Cancer*. 2011;11(1):9-22.

107. Quinlan-Davidson SR, Mohamed ASR, Myers JN, et al. Outcomes of oral cavity cancer patients treated with surgery followed by postoperative intensity modulated radiation therapy. *Oral Oncology*. 2017;72(Supplement C):90-97. doi: https://doi-org.liverpool.idm.oclc.org/10.1016/j.oraloncology.2017.07.002.

108. Spiotto MT, Jefferson G, Wenig B, Markiewicz M, Weichselbaum RR, Koshy M. Differences in survival with surgery and postoperative radiotherapy compared with definitive chemoradiotherapy for oral cavity cancer: A national cancer database analysis. *JAMA Otolaryngology - Head & Neck Surgery*. 2017;143(7):691-699.

109. Jesinghaus M, Boxberg M, Konukiewitz B, et al. A novel grading system based on tumor budding and cell nest size is a strong predictor of patient outcome in esophageal squamous cell carcinoma : *Am J Surg Pathol*. 2017;41(8):1112-1120.

110. Huang S, O'Sullivan B. Overview of the 8th edition TNM classification for head and neck cancer. *Current Treatment Options in Oncology*. 2017;18(7):1-13.

111. Treatment options for oral cavity and oropharyngeal cancer by stage. https://www.cancer.org/cancer/oral-cavity-and-oropharyngeal-cancer/treating/by-stage.html. Updated 2017. Accessed 09/28, 2017.

112. Rivera CA, Droguett DA, Kemmerling U, Venegas BA. Chronic restraint stress in oral squamous cell carcinoma. *J Dent Res*. 2011;90(6):799-803.

113. Oliveira LR, Ribeiro-Silva A, Costa JPO, Simões AL, Matteo, Miguel Angel Sala Di, Zucoloto S. Prognostic factors and survival analysis in a sample of oral squamous cell carcinoma patients. *Oral Surgery, Oral Medicine, Oral Pathology, Oral Radiology, and Endodontology*. 2008;106(5):685-695.

114. Amin MB, Greene FL, Edge SB, et al. The eighth edition AJCC cancer staging manual: Continuing to build a bridge from a population-based to a more "personalized" approach to cancer staging. *CA - A Cancer Journal for Clinicians*. 2017;67(2):93-99.

115. Rosenberg PS, Alter BP, Ebell W. Cancer risks in fanconi anemia: Findings from the german fanconi anemia registry. *Haematologica*. 2008;93(4):511-517.

116. S RP, H GM, P AB. Cancer incidence in persons with fanconi anemia. *Blood*. 2003;101(3):822-6.

117. I KD, Bhuvanesh S, Jaya S, et al. A 20-year perspective on the international fanconi anemia registry (IFAR). *Blood*. 2003;101(4):1249-1256.

118. Tanaka A, Weinel S, Nagy N, et al. Germline mutation in ATRin autosomal-dominant oropharyngeal cancer syndrome. *Am J Hum Genet*. 2012;90(3):511-517.

119. Papadimitrakopoulou VA. Chemoprevention of head and neck cancer: An update : *Curr Opin Oncol*. 2002;14(3):310-7.

120. Oropharyngeal cancer. http://www.macmillan.org.uk/information-and-support/head-and-neck-cancers/oropharnygeal-cancer. Updated 2016. Accessed 09/04, 2017.

121. Hinni ML, Nagel T, Howard B. Oropharyngeal cancer treatment : The role of transoral surgery. *Current Opinion in Otolaryngology & Head & Neck Surgery*. 2015;23(2):132-138.

122. Bisase B, Kerawala C, Skilbeck C, Spencer C. Current practice in management of the neck after chemoradiotherapy for patients with locally advanced oropharyngeal squamous cell carcinoma. *British Journal of Oral and Maxillofacial Surgery*. 2013;51(1):14-18. doi: https://doi-org.liverpool.idm.oclc.org/10.1016/j.bjoms.2012.02.017.

123. Head and neck cancer. https://www.nhs.uk/conditions/cancer-of-the-head-and-neck/Pages/Definition.aspx. Updated 2015. Accessed 10/29, 2017.

124. Umar B, Ahmed R. Nasopharyngeal carcinoma, an analysis of histological subtypes and their association with EBV, a study of 100 cases of pakistani population. *Asian Journal of Medical Sciences*. 2014;5(4):16-20.

125. Stevens SJC, Verkuijlen, Sandra A. W. M., Hariwiyanto B, et al. Diagnostic value of measuring epstein-barr virus (EBV) DNA load and carcinoma-specific viral mRNA in relation to anti-EBV immunoglobulin A (IgA) and IgG antibody levels in blood of nasopharyngeal carcinoma patients from indonesia. *J Clin Microbiol*. 2005;43(7):3066-3073.

126. Nasopharyngeal cancer. http://www.macmillan.org.uk/information-and-support/head-and-neck-cancers/nasopharnygeal-cancer. Updated 2016. Accessed 09/04, 2017.

127. Lee AW, Ma BB, Ng WT, Chan AT. Management of nasopharyngeal carcinoma: Current practice and future perspective. *Journal of Clinical Oncology: official journal of the American Society of Clinical Oncology*. 2015;33(29):3356-3364.

128. Lewis JS Jr. Not your usual cancer case: Variants of laryngeal squamous cell carcinoma. *Head & Neck Pathology*. 2011;5(1):23-30.

129. Larynx cancer. http://www.macmillan.org.uk/information-and-support/larynx-cancer/understanding-cancer/types.html. Updated 2016. Accessed 09/04, 2017.

130. Salvador-Coloma C, Cohen E. Multidisciplinary care of laryngeal cancer. *Journal of Oncology Practice*. 2016;12(8):717-724.

131. Greco A, Rizzo M, Virgilio A, et al. Cancer stem cells in laryngeal cancer: What we know. *European Archives of Oto-Rhino-Laryngology*. 2016;273(11):3487-3495.

132. Kinshuck AJ, Shenoy A, Jones TM. Voice outcomes for early laryngeal cancer : *Current Opinion in Otolaryngology & Head & Neck Surgery*. 2017;25(3):211-216.

133. Bakhoum SF, Compton DA. Chromosomal instability and cancer: A complex relationship with therapeutic potential. *J Clin Invest*. 2012;122(4):1138-43.

134. Riaz N, Morris LG, Lee W, Chan TA. Unraveling the molecular genetics of head and neck cancer through genome-wide approaches. *Genes & Diseases*. 2014;1(Preprints):75-86.

135. Sato H, Uzawa N, Takahashi K, Myo K, Ohyama Y, Amagasa T. Prognostic utility of chromosomal instability detected by fluorescence in situ hybridization in fine-needle aspirates from oral squamous cell carcinomas. *BMC Cancer*. 2010;10(1):182-182.

136. Mechanisms of nuclear size regulation in model systems and cancer. *Adv Exp Med Biol*. 2014;773:537-69.

137. Is DNA ploidy related to smoking? *Journal of Oral Pathology & Medicine*. 2017.

138. Zargoun IM, Bingle L, Speight PM. DNAploidy and cell cycle protein expression in oral squamous cell carcinomas with and without lymph node metastases. *Journal of Oral Pathology & Medicine*. 2017;46(9):738-743.

139. Vargas PA, Soubhia AMP, Miyahara G, et al. High incidences of DNA ploidy abnormalities in tongue squamous cell carcinoma of young patients: An international collaborative study. *Histopathology*. 2011;58(7):1127-1135.

140. Sharma AK, Eils R, König R. Copy number alterations in enzyme-coding and cancer-causing genes reprogram tumor metabolism. *Cancer Res*. 2016;76(14):4058-4067.

141. Yoshioka S, Tsukamoto Y, Hijiya N, et al. Genomic profiling of oral squamous cell carcinoma by array-based comparative genomic hybridization. *PLoS One*. 2013;8(2):e56165.

142. Chen Y, Chen C. DNA copy number variation and loss of heterozygosity in relation to recurrence of and survival from head and neck squamous cell carcinoma: A review. *Head Neck*. 2008;30(10):1361-1383.

143. Use of allelic loss to predict malignant risk for low-grade oral epithelial dysplasia. *Clinical Cancer Research*. 2000;6(2):357-362.

144. Chen C, Zhang Y, Loomis MM, et al. Genome-wide loss of heterozygosity and DNA copy number aberration in HPV-negative oral squamous cell carcinoma and their associations with disease-specific survival. *PLoS One*. 2015;10(8):1-23.

145. Huang M-, Chang Y-, Liao P-, Huang T-, Tsay C-, Chou M-. Loss of heterozygosity of p53 gene of oral cancer detected by exfoliative cytology. *Oral Oncol*. 1999;35(3):296-301.

146. TNM classification of carcinomas of the oral cavity. http://screening.iarc.fr/atlasoralclassiftnm.php. Accessed 10/18, 2017.

147. Signatures of mutational processes in human cancer. *Mutagenesis*. 2014;29(6):499-499.

148. The cancer genome atlas. https://cancergenome.nih.gov/. Updated 2017. Accessed 10/24, 2017.

149. Therapeutic targeting of p53: All mutants are equal, but some mutants are more equal than others. *Nature Reviews Clinical Oncology*. 2017.

150. The incidence of p53 mutations increases with progression of head and neck cancer. *Cancer Res*. 1993;53(19):4477-4480.

151. Braakhuis BJM, Leemans CR, Brakenhoff RH. A genetic progression model of oral cancer: Current evidence and clinical implications. *Journal of Oral Pathology & Medicine*. 2004;33(6):317-322.

152. Olivier M, Hollstein M, Hainaut P. TP53 mutations in human cancers: Origins, consequences, and clinical use. *Cold Spring Harbor Perspectives in Biology*. 2010;2(1):a001008.

153. Rothenberg SM, Ellisen LW. The molecular pathogenesis of head and neck squamous cell carcinoma. *J Clin Invest*. 2012;122(6):1951-7.

154. Merkel O, Taylor N, Prutsch N, et al. When the guardian sleeps: Reactivation of the p53 pathway in cancer. *Mutation Research/Reviews in Mutation Research*. 2017;773(Supplement C):1-13. doi: https://doi-org.liverpool.idm.oclc.org/10.1016/j.mrrev.2017.02.003.

155. Poeta ML, Manola J, Goldwasser MA, et al. TP53 mutations and survival in squamous-cell carcinoma of the head and neck. *N Engl J Med*. 2007;357(25):2552-2561.

156. Mizuarai S, Machida T, Kobayashi T, Komatani H, Itadani H, Kotani H. Expression ratio of CCND1 to CDKN2A mRNA predicts RB1 status of cultured cancer cell lines and clinical tumor samples. *Molecular Cancer*. 2011;10(1):31.

157. Frequent loss of chromosome 9p21-22 early in head and neck cancer progression. *Cancer Res*. 1994;54(5):1156-8.

158. p16(INK4a)/CDKN2 expression and its relationship with oral squamous cell carcinoma is our current knowledge enough? *Cancer Lett*. 2011;306(2):134-141.

159. Growth inhibition of human MDA-MB-231 breast cancer cells by δ-tocotrienol is associated with loss of cyclin D1/CDK4 expression and accompanying changes in the state of phosphorylation of the retinoblastoma tumor suppressor gene product. *Anticancer Research: International Journal of Cancer Research and Treatment*. 2008;28(5 A):2641-2647.

160. Gelbert LM, Cai S, Lin X, et al. Preclinical characterization of the CDK4/6 inhibitor LY2835219: In-vivo cell cycle-dependent/independent anti-tumor activities alone/in combination with gemcitabine. *Invest New Drugs*. 2014;32(5):825-37.

161. Schmitz S, Ang KK, Vermorken J, et al. Targeted therapies for squamous cell carcinoma of the head and neck: Current knowledge and future directions. *Cancer Treat Rev*. 2014;40(3):390-404.

162. Tripathi Bhar A, Banerjee S, Chunder N, et al. Differential alterations of the genes in the CDKN2A-CCND1-CDK4-RB1 pathway are associated with the

development of head and neck squamous cell carcinoma in indian patients. *J Cancer Res Clin Oncol*. 2003;129(11):642-650.

163. Wang L, Hu H, Pan Y, et al. PIK3CA mutations frequently coexist with EGFR/KRAS mutations in non-small cell lung cancer and suggest poor prognosis in EGFR/KRAS wildtype subgroup. *PLoS One*. 2014;9(2):1-10.

164. Kandoth C, McLellan MD, Vandin F, et al. Mutational landscape and significance across 12 major cancer types. *Nature*. 2013;502(7471):333-352.

165. Engelman JA. Targeting PI3K signalling in cancer: Opportunities, challenges and limitations. *Nature Reviews Cancer*. 2009;9(8):550-562.

166. Al-Amri A, Vatte C, Cyrus C, et al. Novel mutations of PIK3CA gene in head and neck squamous cell carcinoma. *Cancer Biomarkers*. 2016;16(3):377-383.

167. Murugan AK, Munirajan AK, Tsuchida N. Genetic deregulation of the PIK3CA oncogene in oral cancer. *Cancer Letters*. 2013;338(2):193-203. doi: https://doi-org.liverpool.idm.oclc.org/10.1016/j.canlet.2013.04.005.

168. Zhang Y, Koneva LA, Virani S, et al. Subtypes of HPV-positive head and neck cancers are associated with HPV characteristics, copy number alterations, PIK3CA mutation, and pathway signatures. *Clinical Cancer Research*. 2016;22(18):4735-4745.

169. Nichols AC, Palma DA, Chow W, et al. High frequency of activating PIK3CA mutations in human papillomavirus-positive oropharyngeal cancer. *JAMA Otolaryngology - Head & Neck Surgery*. 2013;139(6):617-622.

170. Hynes NE, Lane HA. ERBB receptors and cancer: The complexity of targeted inhibitors. *Nature Reviews Cancer*. 2005;5(5):341-54.

171. Keren S, Shoude Z, Lu Z, Beibei Y. Role of EGFR as a prognostic factor for survival in head and neck cancer: A meta-analysis. *Tumour Biol*. 2014;35(3):2285-2295.

172. Molinolo AA, Hewitt SM, Amornphimoltham P, et al. Dissecting the akt/mammalian target of rapamycin signaling network: Emerging results from the head and neck cancer tissue array initiative. *Clinical Cancer Research*. 2007;13(17):4964-4973.

173. Elevated levels of transforming growth factor alpha and epidermal growth factor receptor messenger RNA are early markers of carcinogenesis in head and neck cancer. *Cancer Res*. 1993;53(15):3579-84.

174. Temam S, Kawaguchi H, El-Naggar AK, et al. Epidermal growth factor receptor copy number alterations correlate with poor clinical outcome in patients with head and neck squamous cancer. *Journal of Clinical Oncology: official journal of the American Society of Clinical Oncology*. 2007;25(16):2164-2170.

175. Impact of epidermal growth factor receptor expression on survival and pattern of relapse in patients with advanced head and neck carcinoma. *Cancer Res*. 2002;62(24):7350-7356.

176. Hansen AR, Siu LL. Epidermal growth factor receptor targeting in head and neck cancer: Have we been just skimming the surface? *Journal of Clinical Oncology: official journal of the American Society of Clinical Oncology*. 2013;31(11):1381-1383.

177. Butko E, Pouget C, Traver D. Complex regulation of HSC emergence by the notch signaling pathway. *Developmental Biology*. 2016;409(1):129-138. doi: https://doi-org.liverpool.idm.oclc.org/10.1016/j.ydbio.2015.11.008.

178. Vinson KE, George DC, Fender AW, Bertrand FE, Sigounas G. The notch pathway in colorectal cancer. *International Journal of Cancer*. 2016;138(8):1835-1842.

179. Takebe N, Nguyen D, Yang SX. Targeting notch signaling pathway in cancer: Clinical development advances and challenges. *Pharmacol Ther*. 2014;141(2):140-9.

180. Dunwoodie SL, Henrique D, Harrison SM, Beddington RS. Mouse Dll3: A novel divergent delta gene which may complement the function of other delta homologues during early pattern formation in the mouse embryo. *Development*. 1997;124(16):3065.

181. LINDSELL C, Lindsell CE, Shawber CJ, Boulter J, Weinmaster G. Jagged: A mammalian ligand that activates notch1. *Cell*. 1995;80(6):909.

182. Shawber C, Boulter J, Lindsell CE, et al. Jagged2: A serrate-like gene expressed during rat embryogenesis. *Developmental Biology: An official journal of the Society for Developmental Biology*. 1996;180(1):370.

183. Takebe N, Miele L, Harris PJ, et al. Targeting notch, hedgehog, and wnt pathways in cancer stem cells: Clinical update. *Nature Reviews Clinical Oncology*. 2015;12(8):445-464.

184. Sjöqvist M, Andersson ER. Do as I say, not(ch) as I do: Lateral control of cell fate. *Developmental Biology*. 2017. doi: https://doi.org/10.1016/j.ydbio.2017.09.032.

185. Mumm JS, Kopan R, Mumm JS, Kopan R. Notch signaling: From the outside in. *Dev Biol*. 2000;228(2):151.

186. Sanalkumar R, Indulekha CL, Divya TS, et al. ATF2 maintains a subset of neural progenitors through CBF1/notch independent hes-1 expression and synergistically activates the expression of hes-1 in notch-dependent neural progenitors. *J Neurochem*. 2010;113(4):807-818.

187. Perdigoto CN, Bardin AJ. Sending the right signal: Notch and stem cells. *Biochimica et Biophysica Acta (BBA) - General Subjects*. 2013;1830(2):2307-2322. doi: https://doi-org.liverpool.idm.oclc.org/10.1016/j.bbagen.2012.08.009.

188. Amsen D, Helbig C, Backer RA. Notch in T cell differentiation: All things considered. *Trends Immunol*. 2015;36(12):802-814.

189. Kiernan AE. Notch signaling during cell fate determination in the inner ear. *Semin Cell Dev Biol*. 2013;24(5):470-479.

190. Drevon C, Jaffredo T. Cell interactions and cell signaling during hematopoietic development. *Experimental Cell Research*. 2014;329(2):200-206. doi: https://doi-org.liverpool.idm.oclc.org/10.1016/j.yexcr.2014.10.009.

191. Wael H, Yoshida R, Kudoh S, Hasegawa K, Niimori-Kita K, Ito T. Notch1 signaling controls cell proliferation, apoptosis and differentiation in lung carcinoma. *Lung Cancer*. 2014;85(2):131-140. doi: https://doi.org/10.1016/j.lungcan.2014.05.001.

192. Guo S, Liu M, Gonzalez-Perez RR. Role of notch and its oncogenic signaling crosstalk in breast cancer. *Biochimica et Biophysica Acta (BBA) - Reviews on Cancer*. 2011;1815(2):197-213.

193. Jithesh J. The epigenetic landscape of oral cancer. .

194. Sun W, Gaykalova DA, Ochs MF, et al. Activation of the NOTCH pathway in head and neck cancer. *Cancer Res*. 2014;74(4):1091.

195. Aoyama K, Ota Y, Kajiwara K, Hirayama N, Kimura M. Frequent mutations in NOTCH1 ligand-binding regions in japanese oral squamous cell carcinoma. *Biochem Biophys Res Commun*. 2014;452(4):980-985.

196. Agrawal N, Frederick MJ, Pickering CR, et al. Exome sequencing of head and neck squamous cell carcinoma reveals inactivating mutations in NOTCH1. *Science*. 2011;333(6046):1154-1157.

197. Sun W, Gaykalova DA, Ochs MF, et al. Activation of the NOTCH pathway in head and neck cancer. *Cancer Res*. 2014;74(4):1091.

198. Frederick AN. Exome sequencing of head and neck squamous cell carcinoma reveals inactivating mutations in NOTCH1. *Science*. 2011;333(6046):1154-1157.

199. Rettig EM, Chung CH, Bishop JA, et al. Cleaved NOTCH1 expression pattern in head and neck squamous cell carcinoma is associated with NOTCH1 mutation, HPV status, and high-risk features. *Cancer Prevention Research*. 2015;8(4):287-295.

200. Weaver AN, Burch MB, Cooper TS, et al. Notch signaling activation is associated with patient mortality and increased FGF1-mediated invasion in squamous cell carcinoma of the oral cavity. *Molecular Cancer Research*. 2016;14(9):883-891.

201. Kopan R, Ilagan MXG. The canonical notch signaling pathway: Unfolding the activation mechanism. *Cell*. 2009;137(2):216-233.

202. Notch pathway activation is essential for maintenance of stem-like cells in early tongue cancer. *Oncotarget*. 2016;7(31):50437-50449.

203. Fu,. Expression of Stat3 and Notch1 is associated with cisplatin resistance in head and neck squamous cell carcinoma. *Oncol Rep*. 2010;23(3):671-676.

204. Baumgart A, Mazur PK, Anton M, et al. Opposing role of Notch1 and Notch2 in a KrasG12D-driven murine non-small cell lung cancer model. *Oncogene*. 2015;34(5):578.

205. Functional role of notch signaling in the developing and postnatal heart. *J Mol Cell Cardiol*. 2008;45(4):495-504.

206. Dotto GP. Notch tumor suppressor function. *Oncogene*. 2008;27(38):5115-23.

207. Mohammed TA, Holen KD, Jaskula-Sztul R, et al. A pilot phase II study of valproic acid for treatment of low-grade neuroendocrine carcinoma. *Oncologist*. 2011;16(6):835.

208. Nicolas M, Wolfer A, Raj K, et al. Notch1 functions as a tumor suppressor in mouse skin. *Nat Genet*. 2003;33(3):416.

209. Sriuranpong V, Borges MW, Ravi RK, Arnold DR, Nelkin BD, Baylin SB et al. Notch signaling induces cell cycle arrest in small cell lung cancer cells. *Cancer Res 61: 3200–3205*. 2001.

210. Janes PW, Saha N, Barton WA, et al. Adam meets eph: An ADAM substrate recognition module acts as a molecular switch for ephrin cleavage in trans. *Cell*. 2005;123(2):291.

211. Brou C, Logeat F, Gupta N, et al. A novel proteolytic cleavage involved in notch signaling. *Mol Cell*. 2000;5(2):207.

212. Guo Z, Jin X, Jia H. Inhibition of ADAM-17 more effectively down-regulates the notch pathway than that of γ-secretase in renal carcinoma. *Journal of Experimental & Clinical Cancer Research (17569966)*. 2013;32(1):1-9.

213. Mizuno S, Yoda M, Shimoda M, et al. A disintegrin and metalloprotease 10 (ADAM10) is indispensable for maintenance of the muscle satellite cell pool. *The Journal of Biological Chemistry*. 2015;290(47):28456-28464.

214. HUNTER T. Oncoprotein networks. *Cell*. 1997;88(3):333-346.

215. Hanahan D, Weinberg RA. The hallmarks of cancer. *Cell*. 2000;100(1):57-70.

216. Blaydon D, Etheridge S, Risk J, et al. RHBDF2 mutations are associated with tylosis, a familial esophageal cancer syndrome. *The American Journal of Human Genetics*. 2012;90(2):340.

217. Zou H, Thomas SM, Yan Z, Grandis JR, Vogt A, Li L. Human rhomboid family-1 gene RHBDF1 participates in GPCR-mediated transactivation of EGFR growth signals in head and neck squamous cancer cells. *The FASEB journal : Official Publication of the Federation of American Societies for Experimental Biology*. 2009;23(2):425-432.

218. Chromosome 17q25 genes, RHBDF2 and CYGB, inovarian cancer. *Int J Oncol*. 2012;40(6):1865-1880.

219. Adrain C, Zettl M, Christova Y, et al. Tumor necrosis factor signaling requires iRhom2 to promote trafficking and activation of TACE. *Science*. 2012;335(6065):225.

220. Nakagawa T, Guichard A, Castro CP, et al. Characterization of a human rhomboid homolog, p100hRho/RHBDF1, which interacts with TGF-α family ligands. *Developmental dynamics*. 2005;233(4):1315-1331.

221. Dylan E. Review: The ADAM metalloproteinases. *Mol Aspects Med*. 2008;29(5):258.

222. Dreymueller D, Uhlig S, Ludwig A, Dreymueller D, Uhlig S, Ludwig A. ADAM-family metalloproteinases in lung inflammation: Potential therapeutic targets. *American Journal of Physiology: Lung Cellular and Molecular Physiology*. 2015;308(4):L325.

223. Clark P, Clark P, Clark P, Clark P. Protease-mediated ectodomain shedding: Figure 1. *Thorax*. 2014;69(7):682.

224. Atapattu L, Lackmann M, Janes PW, et al. The role of proteases in regulating eph/ephrin signaling. *Cell Adhesion & Migration*. 2014;8(4):294.

225. Khokha R, Murthy A, Weiss A. Metalloproteinases and their natural inhibitors in inflammation and immunity. *Nat Rev Immunol*. 2013;13(9):649-665.

226. Lorenzen I, Lokau J, Korpys Y, et al. Control of ADAM17 activity by regulation of its cellular localisation. *Scientific Reports (Nature Publisher Group)*. 2016;6(1):35067.

227. Lorenzen I, Lokau J, Korpys Y, et al. Control of ADAM17 activity by regulation of its cellular localisation. *Scientific Reports (Nature Publisher Group)*. 2016;6(1):35067.

228. Endres K, Anders A, Kojro E, Gilbert S, Fahrenholz F, Postina R. Tumor necrosis factor-alpha converting enzyme is processed by proprotein-convertases to its mature form which is degraded upon phorbol ester stimulation. *European Journal of Biochemistry*. 2003;270(11):2386-2393.

229. Doedens JR, Black RA. Stimulation-induced down-regulation of tumor necrosis factor-alpha converting enzyme. *The Journal of Biological Chemistry*. 2000;275(19):14598-14607.

230. Klein T, Bischoff R, Klein T, Bischoff R. Active metalloproteases of the A disintegrin and metalloprotease (ADAM) family: Biological function and structure. *Journal of proteome research*. 2011;10(1):17.

231. Blobel CP. ADAMs: Key components in egfr signalling and development. *Nature Reviews Molecular Cell Biology*. 2005;6(1):32-43.

232. Tousseyn T, Jorissen E, Reiss K, et al. (Make) stick and cut loose—Disintegrin metalloproteases in development and disease. *Birth Defects Research Part C Embryo Today Reviews*. 2006;78(1):24.

233. Loechel F, Fox JW, Murphy G, et al. ADAM 12-S cleaves IGFBP-3 and IGFBP-5 and is inhibited by TIMP-3. *Biochem Biophys Res Commun*. 2000;278(3):511.

234. Schlöndorff, J. (1,2), Blobel CP(1), Becherer JD(3). Intracellular maturation and localization of the tumour necrosis factor a convertase (TACE). *Biochem J*. 2000;347(1):131-138.

235. Lum L, Reid MS, Blobel CP, Lum L, Reid MS, Blobel CP. Intracellular maturation of the mouse metalloprotease disintegrin MDC15. *The Journal of Biological Chemistry*. 1998;273(40):26236.

236. Edwards DR, Handsley MM, Pennington CJ, EDWARDS D, HANDSLEY M, PENNINGTON C. The ADAM metalloproteinases. *Mol Aspects Med*. 2008;29(5):258.

237. Gooz M. ADAM-17: The enzyme that does it all. *Crit Rev Biochem Mol Biol*. 2010;45(2):146-169.

238. White J, White J, White JM. ADAMs: Modulators of cell–cell and cell–matrix interactions. *Curr Opin Cell Biol*. 2003;15(5):598.

239. Bax DV, Messent AJ, Tart J, et al. Integrin alpha5beta1 and ADAM-17 interact in vitro and co-localize in migrating HeLa cells. *The Journal of Biological Chemistry*. 2004;279(21):22377-22386.

240. Zheng Y, Schlondorff J, Blobel CP, Zheng Y. Evidence for regulation of the tumor necrosis factor alpha -convertase (TACE) by protein-tyrosine phosphatase PTPH1. *The Journal of Biological Chemistry*. 2002;277(45):42463.

241. Duffy MJ. The role of ADAMs in disease pathophysiology. .

242. Matthews AL, Noy PJ, Reyat JS, Tomlinson MG. Regulation of A disintegrin and metalloproteinase (ADAM) family sheddases ADAM10 and ADAM17: The emerging role of tetraspanins and rhomboids. *Platelets*. 2017;28(4):333-341.

243. Cho C. Testicular and epididymal ADAMs: Expression and function during fertilization. *Nature Reviews Urology*. 2012;9(10):550-60.

244. Cho C, Primakoff P, White JM, Myles DG. Chromosomal assignment of four testis-expressed mouse genes from a new family of transmembrane proteins (ADAMs) involved in Cell–Cell adhesion and fusion. *Genomics*. 1996;34(3):413-417.

245. Mishra HK, Ma J, Walcheck B. Ectodomain shedding by ADAM17: Its role in neutrophil recruitment and the impairment of this process during sepsis. *Frontiers in Cellular and Infection Microbiology*. 2017;7:138.

246. Simabuco FM, Kawahara R, Yokoo S, et al. ADAM17 mediates OSCC development in an orthotopic murine model. *MOLECULAR CANCER*. 2014;13.

247. Klessner JL, Desai BV, Amargo EV, Getsios S, Green KJ. EGFR and ADAMs cooperate to regulate shedding and endocytic trafficking of the desmosomal cadherin desmoglein 2. *Mol Biol Cell*. 2009;20(1):328-337.

248. Murphy G, Murphy G, Murphy G, Murphy G, Murphy G. The ADAMs: Signalling scissors in the tumour microenvironment. *Nature Reviews.Cancer*. 2008;8(12):932.

249. Staberg M, Michaelsen SR, Olsen LS, et al. Combined EGFR- and notch inhibition display additive inhibitory effect on glioblastoma cell viability and glioblastoma-induced endothelial cell sprouting in vitro. *Cancer Cell International*. 2016;16(1):1-10.

250. Normanno N, De Luca A, Bianco C, et al. Epidermal growth factor receptor (EGFR) signaling in cancer. *Gene*. 2006;366(1):2.

251. Sheu JJ-, Hua C-, Wan L, et al. Functional genomic analysis identified epidermal growth factor receptor activation as the most common genetic event in oral squamous cell carcinoma. *Cancer Res*. 2009;69(6):2568.

252. Andrade,Ana Luiza Dias Leite de, Ferreira SJ, Ferreira SMS, Ribeiro CMB, Freitas RdA, Galvão HC. Immunoexpression of EGFR and EMMPRIN in a series of cases of head and neck squamous cell carcinoma. *Pathology - Research and Practice*. 2015;211(10):776-781. doi: https://doi-org.liverpool.idm.oclc.org/10.1016/j.prp.2015.07.005.

253. Fung C, Zhou P, Joyce S, et al. Identification of epidermal growth factor receptor (EGFR) genetic variants that modify risk for head and neck squamous cell carcinoma. *Cancer Letters*. 2015;357(2):549-556. doi: https://doi-org.liverpool.idm.oclc.org/10.1016/j.canlet.2014.12.008.

254. Hsu J, Chang J, Chang K, Chang W, Chen B. Epidermal growth factor–induced pyruvate dehydrogenase kinase 1 expression enhances head and neck squamous cell carcinoma metastasis viaup-regulation of fibronectin. *The FASEB journal : Official Publication of the Federation of American Societies for Experimental Biology*. 2017;31(10):4265-4276.

255. Vatte C, Al Amri AM, Cyrus C, et al. Tyrosine kinase domain mutations of EGFR gene in head and neck squamous cell carcinoma. *OncoTargets and therapy*. 2017;10:1527-1533.

256. Nagalakshmi, K. (1,2), Jamil K(1), Pingali U(2), Reddy MV(3), Attili SSV(4). Epidermal growth factor receptor (EGFR) mutations as biomarker for head and neck squamous cell carcinomas (HNSCC). *Biomarkers*. 2014;19(3):198-206.

257. Alterio D, Marvaso G, Maffini F, et al. Role of EGFR as prognostic factor in head and neck cancer patients treated with surgery and postoperative radiotherapy: Proposal of a new approach behind the EGFR overexpression. *Medical Oncology*. 2017;34(6):1-10.

258. POLANSKA H, RAUDENSKA M, HUDCOVÁ K, et al. Evaluation of EGFR as a prognostic and diagnostic marker for head and neck squamous cell carcinoma patients. *Oncology Letters*. 2016;12(3):2127-2132.

259. Koi L, Löck S, Linge A, et al. EGFR-amplification plus gene expression profiling predicts response to combined radiotherapy with EGFR-inhibition: A preclinical trial in 10 HNSCC-tumour-xenograft models. *Radiotherapy and Oncology*. 2017;124(3):496-503. doi: https://doi-org.liverpool.idm.oclc.org/10.1016/j.radonc.2017.07.009.

260. Prognostic and predictive value of EGFR in head and neck squamous cell carcinoma. *Oncotarget*. 2016;7(45):74362-74379.

261. Lin C, Lu W, Ren Z, et al. Elevated RET expression enhances EGFR activation and mediates EGFR inhibitor resistance in head and neck squamous cell carcinoma. *Cancer Letters*. 2016;377(1):1-10. doi: https://doi-org.liverpool.idm.oclc.org/10.1016/j.canlet.2016.04.023.

262. Gonzales CB, De La Chapa JJ, Saikumar P, et al. Co-targeting ALK and EGFR parallel signaling in oral squamous cell carcinoma. *Oral Oncology*. 2016;59(Supplement C):12-19. doi: https://doi-org.liverpool.idm.oclc.org/10.1016/j.oraloncology.2016.05.007.

263. Argiris A. EGFR inhibition for recurrent or metastatic HNSCC. *Lancet Oncology*. 2015;16(5):488-489.

264. Liebig H, Günther G, Kolb M, et al. Reduced proliferation and colony formation of head and neck squamous cell carcinoma (HNSCC) after dual targeting of EGFR and hedgehog pathways. *Cancer Chemother Pharmacol*. 2017;79(2):411-420.

265. XIAOHONG LV, YANG LI, MING QIAN, et al. ADAM17 silencing suppresses the migration and invasion of non-small cell lung cancer. *Molecular Medicine Reports*. 2014;9(5):1935-1940.

266. Shou Z, Jin X, Zhao Z. Upregulated expression of ADAM17 is a prognostic marker for patients with gastric cancer : *Ann Surg*. 2012;256(6):1014-1022.

267. Wang HP, Wang X, Gong LF, et al. Nox1 promotes colon cancer cell metastasis via activation of the ADAM17 pathway. *Eur Rev Med Pharmacol Sci*. 2016;20(21):4474-4481.

268. Narita D, Ilina R, Cireap N, Lazar E, Nicola T, Anghel A. Tumor growth factor alpha converting enzyme expression in malignant and benign breast tumors. *Annals of the Romanian Society for Cell Biology*. 2010;15(2):147-155.

269. Pasqualon T, Pruessmeyer J, Weidenfeld S, et al. A transmembrane C-terminal fragment of syndecan-1 is generated by the metalloproteinase ADAM17 and promotes lung epithelial tumor cell migration and lung metastasis formation. *Cellular and Molecular Life Sciences*. 2015;72(19):3783-3801.

270. Differential surface expression of ADAM10 and ADAM17 on human T lymphocytes and tumor cells. *PLoS One*. 2013;8(10).

271. McGowan PM. ADAM-17 predicts adverse outcome in patients with breast cancer. .

272. Duffy MJ. The role of ADAMs in disease pathophysiology. .

273. Simabuco FM, Kawahara R, Yokoo S, et al. ADAM17 mediates OSCC development in an orthotopic murine model. *Molecular Cancer*. 2014;13(1):24.

274. Franovic A. Multiple acquired renal carcinoma tumor capabilities abolished upon silencing of ADAM17. *Cancer Res*. 2006;66(16):8083.

275. McGowan PM, Ryan BM, Hill ADK, McDermott E, O'Higgins N, Duffy MJ. ADAM-17 expression in breast cancer correlates with variables of tumor progression. *Clinical Cancer Research*. 2007;13(8):2335-2343.

276. Kenny PA, Bissell MJ. Targeting TACE-dependent EGFR ligand shedding in breast cancer. *J Clin Invest*. 2007;117(2):337-345.

277. Shou Z, Jin X, Zhao Z. Upregulated expression of ADAM17 is a prognostic marker for patients with gastric cancer : *Ann Surg*. 2012;256(6):1014.

278. Greten FR, Eckmann L, Greten TF, et al. IKKβ links inflammation and tumorigenesis in a mouse model of colitis-associated cancer. *Cell*. 2004;118(3):285-296.

279. Das S, Czarnek M, Bzowska M, et al. ADAM17 silencing in mouse colon carcinoma cells: The effect on tumoricidal cytokines and angiogenesis. *PLoS One*. 2012;7(12):1-13.

280. Buchanan PC, Boylan KLM, Walcheck B, et al. Ectodomain shedding of the cell adhesion molecule nectin-4 in ovarian cancer is mediated by ADAM10 and ADAM17. *The Journal of Biological Chemistry*. 2017;292(15):6339-6351.

281. Chalaris A, Adam N, Sina C, et al. Critical role of the disintegrin metalloprotease ADAM17 for intestinal inflammation and regeneration in mice. *J Exp Med*. 2010;207(8):1617-24.

282. Role of ADAM17 in invasion and migration of CD133-expressing liver cancer stem cells after irradiation. *Oncotarget*. 2016;7(17):23482-23497.

283. Shilo B. Signaling by the drosophila epidermal growth factor receptor pathway during development. *Exp Cell Res*. 2003;284(1):140-149.

284. Golembo M, Raz E, Shilo BZ. The drosophila embryonic midline is the site of spitz processing, and induces activation of the EGF receptor in the ventral ectoderm. *Development*. 1996;122(11):3363-3370.

285. Bang AG, Kintner C. Rhomboid and star facilitate presentation and processing of the drosophila TGF-alpha homolog spitz. *Genes Dev*. 2000;14(2):177-186.

286. Wasserman JD, Urban S, Freeman M. A family of rhomboid-like genes: Drosophila rhomboid-1 and roughoid/rhomboid-3 cooperate to activate EGF receptor signaling. *Genes Dev*. 2000;14(13):1651-1663.

287. Grieve AG, Xu H, Künzel U, Bambrough P, Sieber B, Freeman M. Phosphorylation of iRhom2 at the plasma membrane controls mammalian TACE-dependent inflammatory and growth factor signalling. *eLife*. 2017;6.

288. Jeyaraju DV, Sood A, Laforce-Lavoie A, Pellegrini L. Rhomboid proteases in mitochondria and plastids: Keeping organelles in shape. *Biochimica et Biophysica Acta (BBA) - Molecular Cell Research*. 2013;1833(2):371-380.

289. Strisovsky K, Sharpe HJ, Freeman M. Sequence-specific intramembrane proteolysis: Identification of a recognition motif in rhomboid substrates. *Mol Cell*. 2009;36(6):1048-1059.

290. Dickey SW, Baker RP, Cho S, Urban S, a. Proteolysis inside the membrane is a rate-governed reaction not driven by substrate affinity. *Cell*. 2013;155(6):1270-81.

291. Fleig L, Bergbold N, Sahasrabudhe P, Geiger B, Kaltak L, Lemberg MK. Ubiquitin-dependent intramembrane rhomboid protease promotes ERAD of membrane proteins. *Mol Cell*. 2012;47(4):558-569.

292. Lemberg MK, Freeman M, Lemberg MK, Freeman M. Functional and evolutionary implications of enhanced genomic analysis of rhomboid intramembrane proteases. *Genome Res*. 2007;17(11):1634.

293. Yongcheng Wang, Yingjiu Zhang, Ya Ha. Crystal structure of a rhomboid family intramembrane protease. *Nature*. 2006;444(7116):179-183.

294. Lemberg MK, Menendez J, Misik A, Garcia M, Koth CM, Freeman M. Mechanism of intramembrane proteolysis investigated with purified rhomboid proteases. *EMBO J*. 2005;24(3):464-472.

295. Bondar A. Biophysical mechanism of rhomboid proteolysis: Setting a foundation for therapeutics. *Semin Cell Dev Biol*. 2016;60(1):46-51.

296. Brooks CL, Lemieux MJ. Untangling structure–function relationships in the rhomboid family of intramembrane proteases. *Biochimica et Biophysica Acta (BBA) - Biomembranes*. 2013;1828(12):2862-2872.

297. Strisovsky K. Rhomboid protease inhibitors: Emerging tools and future therapeutics. *Semin Cell Dev Biol*. 2016;60(1):52-62.

298. Baker RP, Urban S. Architectural and thermodynamic principles underlying intramembrane protease function. *Nature chemical biology*. 2012;8(9):759-768.

299. McQuibban GA, Saurya S, Freeman M. Mitochondrial membrane remodelling regulated by a conserved rhomboid protease. *Nature*. 2003;423(6939):537-41.

300. Tsai YC, Weissman AM. A ubiquitin-binding rhomboid protease aimed at ERADication. *Developmental Cell*. 2012;23(3):454-6.

301. Greenblatt EJ, Olzmann JA, Kopito RR. Making the cut: Intramembrane cleavage by a rhomboid protease promotes ERAD. *Nature Structural and Molecular Biology*. 2012;19(10):979-981.

302. Lee M, Nam K, Choi K. iRhoms; its functions and essential roles. *Biomolecules & Therapeutics*. 2016;24(2):109-114.

303. Breshears LM, Gillman AN, Stach CS, Schlievert PM, Peterson ML. Local epidermal growth factor receptor signaling mediates the systemic pathogenic effects of staphylococcus aureus toxic shock syndrome. *PLoS One*. 2016;11(7):1-15.

304. RHBDL2 is a critical membrane protease for anoikis resistance in human malignant epithelial cells. *The Scientific World Journal*. 2014.

305. Cheng T, Wu Y, Lin H, et al. Functions of rhomboid family protease RHBDL2 and thrombomodulin in wound healing. *J Invest Dermatol*. 2011;131(12):2486-2494.

306. Lohi O, Urban S, Freeman M. Diverse substrate recognition mechanisms for rhomboids: Thrombomodulin is cleaved by mammalian rhomboids. *Current Biology*. 2004;14(3):236-241.

307. JUNYI HAN, JUNCHAO BAI, YAO YANG, et al. Lentivirus-mediated knockdown of rhomboid domain containing 1 inhibits colorectal cancer cell growth. *Molecular Medicine Reports*. 2015;12(1):377-381.

308. Song W, Liu W, Zhao H, et al. Rhomboid domain containing 1 promotes colorectal cancer growth through activation of the EGFR signalling pathway. *Nature Communications*. 2015;6(8):8022.

309. Düsterhöft S, Künzel U, Freeman M. Rhomboid proteases in human disease: Mechanisms and future prospects. *Biochimica et Biophysica Acta (BBA) - Molecular Cell Research*. 2017(Preprints).

310. Wei X, Lv T, Chen D, Guan J. Lentiviral vector mediated delivery of RHBDD1 shRNA down regulated the proliferation of human glioblastoma cells. *Technology in Cancer Research & Treatment*. 2014;13(1):87-93.

311. Bergbold N, Lemberg MK. Emerging role of rhomboid family proteins in mammalian biology and disease. *Biochimica et Biophysica Acta (BBA) - Biomembranes*. 2013;1828(12):2840-2848.

312. Adrain C, Freeman M. New lives for old: Evolution of pseudoenzyme function illustrated by iRhoms. *Nature Reviews.Molecular Cell Biology*. 2012;13(8):489-498.

313. Adrain C, Freeman M. New lives for old: Evolution of pseudoenzyme function illustrated by iRhoms. *Nature Reviews.Molecular Cell Biology*. 2012;13(8):489-498.

314. Roghani M, Becherer JD, Moss ML, et al. Metalloprotease-disintegrin MDC9: Intracellular maturation and catalytic activity. *J Biol Chem*. 1999;274(6):3531.

315. Etheridge S, Brooke M, Kelsell D, et al. Rhomboid proteins: A role in keratinocyte proliferation and cancer. *Cell Tissue Res*. 2013;351(2):301.

316. Zettl M, Adrain C, Strisovsky K, Lastun V, Freeman M. Rhomboid family pseudoproteases use the ER quality control machinery to regulate intercellular signaling. *Cell*. 2011;145(1):79-91.

317. Adrain C, Strisovsky K, Zettl M, Hu L, Lemberg MK, Freeman M. Mammalian EGF receptor activation by the rhomboid protease RHBDL2. *EMBO Rep*. 2011;12(5):421-427.

318. Alanazi IO, Khan Z. Understanding EGFR signaling in breast cancer and breast cancer stem cells: Overexpression and therapeutic implications. *Asian Pacific Journal of Cancer Prevention*. 2016;17(2):445.

319. Dinglin X, Ding L, Li Q, Liu Y, Zhang J, Yao H. RYBP inhibits progression and metastasis of lung cancer by suppressing EGFR signaling and epithelial-mesenchymal transition. *Translational Oncology*. 2017;10(2):280-287.

320. Oliveira-Cunha M, Newman WG, Siriwardena AK. Epidermal growth factor receptor in pancreatic cancer. *Cancers*. 2011;3(2):1513-1526.

321. Chang KY, Tsai SY, Chen SH, et al. Dissecting the EGFR-PI3K-AKT pathway in oral cancer highlights the role of the EGFR variant III and its clinical relevance. *J Biomed Sci*. 2013;20(1):1-10.

322. Blaydon D, Etheridge S, Risk J, et al. RHBDF2 mutations are associated with tylosis, a familial esophageal cancer syndrome. *The American Journal of Human Genetics*. 2012;90(2):340-346.

323. Varela AB, Blanco Rodríguez MM, Boullosa PE, Silva JG. Tylosis A with squamous cell carcinoma of the oesophagus ina spanish family : *Eur J Gastroenterol Hepatol*. 2011;23(3):286-288.

324. Sun W, Gaykalova DA, Ochs MF, et al. Activation of the NOTCH pathway in head and neck cancer. *Cancer Res*. 2014;74(4):1091-1104.

325. Blaydon D, Etheridge S, Risk J, et al. RHBDF2 mutations are associated with tylosis, a familial esophageal cancer syndrome. *The American Journal of Human Genetics*. 2012;90(2):340-346.

326. Dhanda J, Triantafyllou A, Liloglou T, et al. SERPINE1 and SMA expression at the invasive front predict extracapsular spread and survival in oral squamous cell carcinoma. *Br J Cancer*. 2014;111(11):2114-21.

327. pIRESneo vector information. http://www.biofeng.com/zaiti/buru/pIRESneo.html. Updated 2015. Accessed 09/03, 2017.

328. Christova Y, Adrain C, Bambrough P, Ibrahim A, Freeman M. Mammalian iRhoms have distinct physiological functions including an essential role in TACE regulation. *EMBO Rep*. 2013;14(10):884-890.

329. Rudland PS, Platt-Higgins AM, Davies LM, et al. Significance of the fanconi anemia FANCD2 protein in sporadic and metastatic human breast cancer. *The American Journal of Pathology*. 2010;176(6):2935-2947.

330. Hosur V, Johnson KR, Burzenski LM, Stearns TM, Maser RS, Shultz LD. Rhbdf2 mutations increase its protein stability and drive EGFR hyperactivation through enhanced secretion of amphiregulin. *Proceedings of the National Academy of Sciences of the United States of America (PNAS)*. 2014;111(21):E2200.

331. Mullooly M, McGowan PM, Crown J, Duffy MJ. The ADAMs family of proteases as targets for the treatment of cancer. *Cancer Biology & Therapy*. 2016;17(8):870-880.

332. Kenny PA. TACE: A new target in epidermal growth factor receptor dependent tumors. *Differentiation*. 2007;75(9):800-808.

333. iRhom2: A novel regulator of wound healing and cancer. *Br J Dermatol*. 2015;172(5):E39.

334. Leilei Y, Bing L, Yang L, et al. iRhom2 mutation leads to aberrant hair follicle differentiation in mice. *PLoS One*. 2014;9(12):1-18.

335. Sanderson RJ, Ironside JAD, Martin E. Squamous cell carcinomas of the head and neck. *BMJ (British Medical Journal)*. 2002;325(7368):822.

336. Christova Y, Adrain C, Bambrough P, Ibrahim A, Freeman M. Mammalian iRhoms have distinct physiological functions including an essential role in TACE regulation. *EMBO Rep*. 2013;14(10):884-890.

337. Etheridge S. *iRhom2 in skin disease and oesophageal cancer.* [PhD]. Queen Mary, University Of London; 2015.

338. Maney SK, McIlwain DR, Polz R, et al. Deletions in the cytoplasmic domain of iRhom1 and iRhom2 promote shedding of the TNF receptor by the protease ADAM17. *Science Signaling*. 2015;8(401):1.

339. Inactive rhomboid protein 2. http://www.uniprot.org/uniprot/Q6PJF5. Updated 2008. Accessed March 26, 2018.

340. iRhom2: A novel regulator of wound healing and cancer. *Br J Dermatol*. 2015;172(5):E39.

341. Li X, Maretzky T, Weskamp G, et al. iRhoms 1 and 2 are essential upstream regulators of ADAM17-dependent EGFR signaling. *Proceedings of the National Academy of Sciences of the United States of America (PNAS)*. 2015;112(19):6080-6085.

342. iRhoms; its functions and essential roles. *Biomolecules*. 2016;24(2):109.

343. Siggs OM, Grieve A, Xu H, Bambrough P, Christova Y, Freeman M. Genetic interaction implicates iRhom2 in the regulation of EGF receptor signalling in mice. *Biology Open*. 2014;3(12):1151-1157.

344. Braunholz D, Saki M, Niehr F, et al. Spheroid culture of head and neck cancer cells reveals an important role of EGFR signalling in anchorage independent survival. *PLoS One*. 2016;11(9):1-14.

345. YUICHI OHNISHI, HIROKI YASUI, KENJI KAKUDO, MASAMI NOZAKI. Regulation of cell migration via the EGFR signaling pathway in oral squamous cell carcinoma cells. *Oncology Letters*. 2017;13(2):930-936.

346. iRhom2 controls the substrate selectivity of stimulated ADAM17-dependent ectodomain shedding. *Proceedings of the National Academy of Sciences of the United States of America (PNAS)*. 2013.

347. Takamune Y, Ikebe T, Nagano O, et al. ADAM-17 associated with CD44 cleavage and metastasis in oral squamous cell carcinoma. *Virchows Archiv*. 2007;450(2):169-177.

348. Pascall JC, Brown KD. Intramembrane cleavage of ephrinB3 by the human rhomboid family protease, RHBDL2. *Biochem Biophys Res Commun*. 2004;317(1):244-252.

349. Brooke MA, Etheridge SL, Kaplan N, et al. iRHOM2-dependent regulation of ADAM17 in cutaneous disease and epidermal barrier function. *Hum Mol Genet*. 2014;23(15):4064-4076.

350. Cavadas M, Oikonomidi I, Gaspar CJ, et al. Phosphorylation of iRhom2 controls stimulated proteolytic shedding by the metalloprotease ADAM17/TACE. *Cell Reports*. 2017;21(3):745-757.

351. Leilei Y, Yang L, Shaoxia W, et al. iRhom2 mutation leads to aberrant hair follicle differentiation in mice. *PLOS ONE*. 2014;9(12).

352. Maretzky T, McIlwain DR, Issuree PDA, et al. iRhom2 controls the substrate selectivity of stimulated ADAM17-dependent ectodomain shedding. *Proceedings of the National Academy of Sciences of the United States of America (PNAS)*. 2013;110(28):11433.

353. Erik S. Welf, Jason M. Haugh. Signaling pathways that control cell migration: Models and analysis. *March, 2011*. 2011.

354. Dubrez L, Rajalingam K. IAPs and cell migration. *Semin Cell Dev Biol*. 2015;39(1):124-131.

355. Callan-Jones AC, Voituriez R. Actin flows in cell migration: From locomotion and polarity to trajectories. *Current Opinion in Cell Biology*. 2016;38(Supplement C):12-17. doi: https://doi-org.liverpool.idm.oclc.org/10.1016/j.ceb.2016.01.003.

356. Liu Y, Le Berre M, Lautenschlaeger F, et al. Confinement and low adhesion induce fast amoeboid migration of slow mesenchymal cells. *Cell*. 2015;160(4):659-672.

357. Lämmermann T, Sixt M. Mechanical modes of 'amoeboid' cell migration. *Current Opinion in Cell Biology*. 2009;21(5):636-644. doi: https://doi-org.liverpool.idm.oclc.org/10.1016/j.ceb.2009.05.003.

358. Hawkins R, Poincloux R, Bénichou O, Piel M, Chavrier P, Voituriez R. Spontaneous contractility-mediated cortical flow generates cell migration in three-dimensional environments. *Biophysical Journal*. 2011;101(5):1041-1045. doi: https://doi-org.liverpool.idm.oclc.org/10.1016/j.bpj.2011.07.038.

359. Yamaguchi H, Wyckoff J, Condeelis J. Cell migration in tumors. *Current Opinion in Cell Biology*. 2005;17(5):559-564. doi: https://doi-org.liverpool.idm.oclc.org/10.1016/j.ceb.2005.08.002.

360. Arribas J, Bech-Serra J, Santiago-Josefat B. ADAMs, cell migration and cancer. *Cancer Metastasis Rev*. 2006;25(1):57-68.

361. Hamdy Doweidar M, Jamaleddin Mousavi S, Hamdy Doweidar M. Three-dimensional numerical model of cell morphology during migration in multi-signaling substrates. *PLOS ONE*. 2015;10(3).

362. Ramis-Conde I, Drasdo D, Anderson ARA, Chaplain MAJ. Modeling the influence of the E-cadherin-β-catenin pathway in cancer cell invasion: A multiscale approach. *Biophys J*. 2008;95(1):155-165.

363. Tanos B, Rodriguez-Boulan E. The epithelial polarity program: Machineries involved and their hijacking by cancer. *Oncogene*. 2008;27(55):6939.

364. Yarden Y, Shilo B. SnapShot: EGFR signaling pathway. *Cell*. 2007;131(5):1018.e1.

365. Roskoski R. The ErbB/HER family of protein-tyrosine kinases and cancer. *Pharmacological Research*. 2014;79(1):34-74.

366. Burgess AW, Cho H, Eigenbrot C, et al. An open-and-shut case? recent insights into the activation of EGF/ErbB receptors. *Molecular Cell*. 2003;12(3):541-552. doi: http://dx.doi.org.liverpool.idm.oclc.org/10.1016/S1097-2765(03)00350-2.

367. Wilson KJ, Gilmore JL, Foley J, Lemmon MA, Riese DJ. Functional selectivity of EGF family peptide growth factors: Implications for cancer. *Pharmacol Ther*. 2009;122(1):1-8.

368. Rocks N, Paulissen G, El Hour M, et al. Emerging roles of ADAM and ADAMTS metalloproteinases in cancer. *Biochimie*. 2008;90(2):369-379.

369. Hirata S, Murata T, Suzuki D, et al. Selective inhibition of ADAM17 efficiently mediates glycoprotein ibα retention during ex vivo generation of human induced pluripotent stem cell-derived platelets. *Stem Cells Translational Medicine*. 2017;6(3):720-730.

370. Hulkower KI, Herber RL. Cell migration and invasion assays as tools for drug discovery. *Pharmaceutics pharmaceutics*. 2011;3(1):107-124.

371. Chandrasekaran S, Deng H, Fang Y. PTEN deletion potentiates invasion of colorectal cancer spheroidal cells through 3D matrigel. *Integrative Biology (RSC)*. 2015;7(3):324-334.

372. Purcz N, Tiwari S, Will O, et al. Op093. *Oral Oncol*. 2013;49(5):S41.

6 APPENDIX 1

Table showing a collection of all tissue samples available for the study and their histology. The “use?” column indicates whether or not a sample was deemed suitable for the study, based on the type, size and especially tumour cell load. Of the 127 tissue samples assessed, 95 (68 tumour and 27 normal) samples were deemed suitable for the study, with the remaining 28 rejected, based on their tumour cell population, unusable tissue type or size (too little).

sample no.	T/N	Pt. No.	path 1st section	path last section	Use?	comments	Additional sections
5041	T	3400	50% tumour	50% tumour	y	`+ inflammatory response	
5042	N	3400	no tumour	no tumour	y	salivary gland/small sections	
5047	T	3401	40% tumour	30% tumour	n	inflammation + gland	
5048	N	3401	10% tumour	no tumour	y	keratinised tissue/ small sections	
5059	T	3408	50% tumour	60% tumour	y		
5060	N	3408	microinvasive tumour (40%)	no tumour	y	`+ conenctive tissue	
5083	T	3412	>60% Cis?	>60% Cis?	y		
5084	N	3412	mild dysplasia	mild dysplasia	y	80% connective tissue	
5089	T	3413	60% tumour	50% tumour	y		
5090	N	3413	epithelium	mild dysplasia	y	80% connective tissue	
5099	T	3415	salivary gland	salivary gland	n	v. small	
5100	N	3415	5% tumour	no tumour	y		
5300	T	3421	artefactual probably 90% tumo	90% tumour	y	small sections	
5301	N	3421	no tumour	no tumour	y	v. small	
5316	T	3425	30% tumour	40% tumour	n	`+ inflammation	
5317	N	3425	muscle	muscle	y		
5332	T	3429	30% tumour	30% tumour	n		
5333	N	3429	no tumour	no tumour	y	keratinised	
5351			no tissue	no tumour		? 5356	
5355	T	3440	80% tumour	80% tumour	y		
5359	T	3441	80% tumour	70% tumour	y		
5360	N	3441	muscle	muscle	y	dysplastic epithelium	
5363	T	3442	90% tumour	90% tumour	y		
5364	N	3442	dysplasia	dyspalsia	y		
5367	T	3443	80% tumour	90% tumour	y		
5368	N	3443	no tumour	no tumour	n	fat	
5401	N	3451	no tumour	no tumour	y		
5405	N	3452	no tumour (muslce)	no tumour (muscle)	y		
5425	N	3449	some dysplasia; no tumour	some dysplasia; no tumour	y		
5451	T	3458	30% tumour	50% tumour	n		
5452	N	3458	no tumour	no tumour	y		
5455	T	3459	40% tumour	40% tumour	n		
5456	N	3459	normal gland	normal gland	y		
5505	T	3462	90% tumour	80% tumour	y		
5506	N	3462	no tumour	no tumour	y	small sections	
5514	N	3464	hyperplasia; no tumour	no tumour	y		
5603	N	3477	no tumour	no tumour	y		
5610	T	3479	30% tumour	40% tumour	n		
5611	N	3479	hyperplasia; no tumour	hyperplasia; no tumour	y		
5623	N	3482	dysplasia; no tumour	no tumour	y		
5635	N	3485	no tissue	no tissue	n		
5638	T	3486	40% tumour	70% tumour	y		
5639	N	3486	no tumour	no tumour	y		
5654	T	3495	80% tumour	100% tumour	y	small sections	

5662	T	3497	10% dysplasia	10% dysplasia	n	`+ salivary gland/small sections					
5670	T	3499	80% tumour	80% tumour	y						
5674	T	3500	90% tumour	85% tum	y						
5678	T	3501	40% tumour	60% tumour	y						
5694	T	3505	90% tumour	100% tumour	y						
5698	T	3506	60% tumour	55% tumour	y						
5706	T	3508	70% tumour	70% tumour	y						
5710	T	3509	50% tumour	60% tumour	y	`+ inflammation					
5714	T	3510	100% tumour	100% tumour	y						
5718	T	3449	30% tumour	20% tumour	n	`+ inflammation					
5840	T	3531	hyperplasia	hyperplasia	n	small sections					
5844	T	3534	20% tumour	15% tumour	n	`+ inflammation					
5856	T	3535	95% tumour	95% tumour	y						
5864	T	3537	40% tumour	40% tumour	n	50% muscle					
5876	T	3540	100% tumour	100% tumour	y						
5880	T	3541	90% tumour	90% tumour	y						
5884	T	3542	80% tumour	70% tumour	y						
5892	T	3544	90% tumour	90% tumour	y						
5904	T	3547	50% tumour	60% tumour	y						
5908	T	3548	100% tumour	90% tumour	y	40% highly keratinised					
5940	T	3550	50% tumour (keratinized)	50% tumour	y	small sections					
5972	T	3558	no tumour	10% tumour (mainly keratin	n	v small					
10002	T	3566	80% tumour	70% tumour	y						
10010	T	3568	70% tumour	80% tumour	y						
10014	T	3569	mainly keratinized	>90% tumour	y	v small					
10022	T	3571	no tumour	no tumour	n	small sections					
10026	T	3572	50% tumour	50% tumour	y	freezing artefacts in tissue, but OK					
10030	T	3573	60% tumour	dysplasia & invasive carcinon	y		do not use any further sections from this tissue				
10034	T	3574	70% tumour	70% tumour	y						
10058	T	3580	80% tumour	80% tumour	y	small sections					
10062	T	3581	v little tumour, 25%	>30% tumour	N	small sections	slice off ~10 sections and recut 1 section for H&E				
10066	T	3582	50% tumour	35% tumour	Y	small sections	do not use any further sections from this tissue				
10078	T	3585	50% tumour (dyscohesive)	50% tumour	y	small sections					
10126	T	3630	60% tumour	70% tumour	y	small sections					
10130	T	3631	90% tumour	80% tumour	y						
10134	T	3632	30% tumour	20% tumour	n						
			no tissue	60% cancer	y (2nd set)	v small	slice off ~10 sections and recut 1 section for H&E				
10138	T	3633	30% tumour	70% tumour	y						
10142	T	3634	40% tumour	no tumour	n	v small					
10154	T	3637	25% tumour	80% tumour	y	small sections					
10158	T	3638	100% tumour	100% tumour	Y						
10166	T	3640	10% tumour (mixed)	10% tumour (mixed)	N						
10170	T	3641	40% tumour	>60% tumour	Y						
10178	T	3643	<10% tumour	<10%^ tumour	N	small sections					
10182	T	3644	80% tumour	80% tumour	Y	small sections					
10190	T	3646	<10% dysplasia only	mostly severere dysplasia	N	small sections					
10194	T	3647	few cells only	30% tumour (mixed)	N	small sections					
10206	T	3650	>60% tumour	100% tumour	Y						
10682	T	3661	30% tumour	100% tumour	Y						
10686	T	3662	>90% tumour	>90% tumour	Y						
10698	T	3665	60% tumour	60% tumour	y						
10722	T	3671	100% tumour	100% tumour	y	50% highly keratinised/small sections					
10742	T	3676	no tumour	no tumour	n	skin					
10778	T	3685	~30% tumour	30% tumour	n	freezing artefacts make assessment difficult					
10790	T	3688	no tumour	no tumour	n	v. small					
10794	T	3689	no tumour	no tumour	n	small sections					

10861	T	3721	60% tumour	60% tumour	y	`+ salivary gland		
11001	T	3701	80% tumour	60% tumour	y	`+ inflammation		
11065	T	3717	50% tumour	65% tumour	y			
11069	T	3718	~20% tumour	30% tumour	n	salivary gland		
11073	T	3719	80% tumour	80% tumour	y	`+ dysplastic surface epithelium		
11115	T	3723	100% tumour	80% tumour	y			
11123	T	3725	90% tumour	100% tumour	y			
11127	T	3726	100% tumour	90% tumour	y	extensive keratinisation		
11131	T	3727	100% tumour	100% tumour	y			
11135	T	3728	too small	>80% tumour	y			
11136	N	3728	no tumour	no tumour	y			
11139	T	3729	60% tumour	70% tumour	y	basaloid		
11140	N	3729	no tumour	no tumour	y			
11143	T	3730	40% tumour	>85% tumour	y			
11144	N	3730	dysplasia	dysplasia	y			
11155	T	3415	>95% tumour	>95% tumour	y			
11156	N	3415	no tumour	dysplastic	y			
11167	T	3736	blood	<20%	N			
11168	N	3736	no tumour	no tumour	y			
11179	T	3739	70% tumour	70% tumour	y	fully keratinised		
11180	N	3739	no tumour	no tumour	y			
12475	T	3785	too small	25% dysplasis	N			
12476	N	3785	no tumour	no tumour	y			
12479	T	3786	artefactual - can't score	<10% tumour	N			
12480	N	3786	no tumour	no section provided	y	muscle & salivary gland		
12487	T	3788	70% tumour	80% tumour	y			
12488	N	3788	no tumour	no tumour	y			
12491	T	3789	no tissue	60% tumour	y	basaloid		
12493	N	3789	no tumour	no tumour	y			
12504	T	3792	>70% tumour	>70% tumour	y	basaloid		
12505	N	3792	dysplastia only	dysplasia	be normal tissue - no marking on slide			
12508	T	3793	<5% tumour	<5% tumour	N			
12509	N	3793	no tumour	no tumour	y			
12512	T	3794	70% tumour	<40% tumour	y			
12513	N	3794	no tumour (muslce)	no tumour	y			
12517	T	3801	>70% tumour	40% tumour	y			
12518	N	3801	no tumour	no tumour	y	salivary gland		
12525	T	3803	70% tumour	70% tumour	y			
12526	N	3803	no tumour (muscle)	no section provided	y			

7 APPENDIX 2

Buffers and solutions

Components of resolving gel (sufficient for two gels) – 10% SDS

Component	Volume / Mass	Remark
Water	35 ml	Double Distilled
0.5 M Tris (8.8)	20 ml	Stored in fridge (Fisher Scientific)
30% Acrylamide	23 ml	Stored in fridge (Fisher Scientific)
10% SDS	900 µl	Storage – room temperature (Fisher Scientific)
10% APS	500 µl	Prepared fresh from powder (Sigma)
TEMED	120 µl	Stored in fridge (Sigma)

Components of stacking gel (sufficient for two gels) – 10% SDS

Component	Volume / Mass	Remark
Water	15 ml	Double Distilled
1.5 M Tris (6.8)	6.6 ml	Stored in fridge (Fisher Scientific)
30% Acrylamide	3.3 ml	Stored in fridge (Fisher Scientific)
10% SDS	250 µl	Storage – room temperature (Fisher Scientific)
10% APS	150 µl	Prepared fresh from powder (Sigma)
TEMED	60 µl	Stored in fridge (Sigma)

Electrophoresis running buffer

Component	Volume / Mass (per volume of buffer)	Remarks
Tris Base	3g	Room temperature storage (Fisher Scientific)
Glycine	14.4g	Room temperature storage (Fisher Scientific)
10% SDS	10ml	Room temperature storage (Fisher Scientific)

Western blotting transfer buffer

Component	Volume / Mass (per volume of buffer)	Remarks
Tris Base	3g	Room temperature storage (Fisher Scientific)
Glycine	14.4g	Room temperature storage (Fisher Scientific)
Methanol	200ml	Room temperature storage (Fisher Scientific)

8 APPENDIX 3

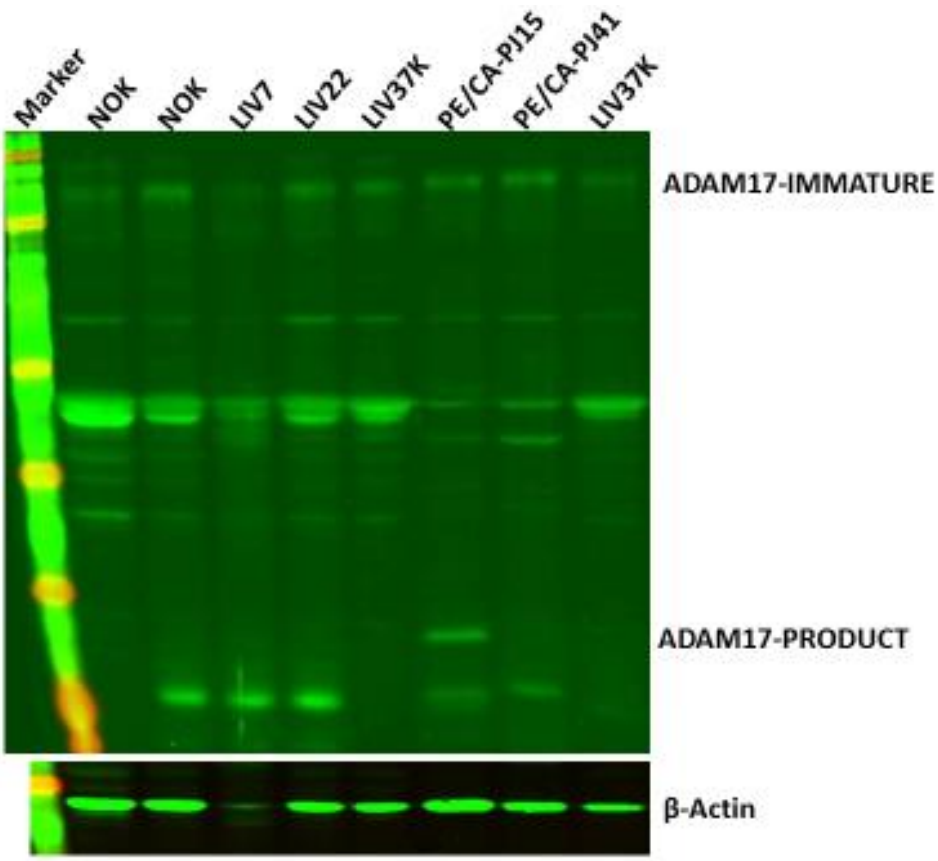

Profiling of cell lines – ADAM17 expression (N-Terminal). Variable levels of ADAM17 expression with detection of the cleaved-off low molecular weight fragment detected in PJ15 cell lines, but undetected in the other cell lines used.